With suppression according to individual cylinders, the number of control increments is the same as the number of cylinders. Because this limited number of control stages is still inadequate for a (as an example) four-cylinder engine, a supplementary strategy is employed: this is referred to as alternating injection suppression. It consists of varying the number of active cylinders by one after every two crankshaft rotations to produce a mean torque lying between the torques produced at the two cylinder stages. This method doubles the number of control stages to achieve an acceptable level of driving comfort, while complementary reductions in ignition advance can be employed to provide additional incremental adjustments.

In cases where the excess torque is substantial, injection suppression can be supplemented by short-term ignition cutout to provide extremely rapid output reductions. Figure 16.12 shows the design of the system. In addition to the modest expense, this system also offers vehicle manufacturers an additional advantage in the form of space savings (no additional space required) and simplicity (limited amount of extra wiring).

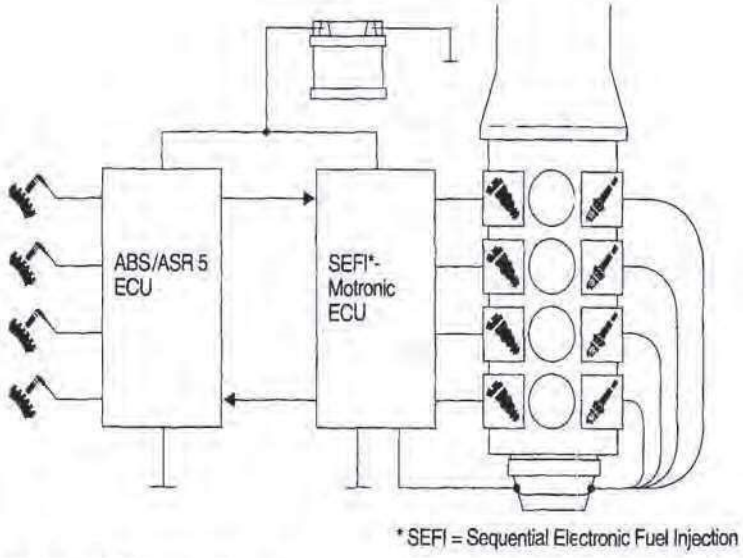


FIGURE 16.12 ASR EZ system.

16.6 APPLICATIONS ON HEAVY COMMERCIAL VEHICLES

Heavy commercial vehicles are used in a highly variegated range of applications. In principle, the ASR installed on these vehicles employs the same control strategies used for passenger cars: engine-output control and braking intervention.

Differences in vehicle application can make it necessary to employ ASR systems in various levels of complexity (for instance, relying on braking control or engine output control exclusively). The control unit recognizes the design stage and carries out its control functions accordingly. This makes it possible to employ the most economical ASR system for each vehicle type and particular application.

Figure 16.13 features a schematic diagram showing a typical 4×2 vehicle equipped with a top-of-the-line ABS/ASR system. During acceleration on μ-split surfaces, the brake-force regulator limits slip between the drive wheels. The ASR valve (4) is activated on the side with the spinning wheel, while the ABS pressure-control valve (3) allows graduated increases in pressure at the wheel cylinder.

If both drive wheels start to spin on a road surface affording equal traction on both sides, the engine-output controller responds by reducing the drive slip to optimum values. In this example, the electric performance control (EPC) (10) assumes the role of final-control ele-

IPR2023-01234
Petitioner - Ex. 2017 - Page 371

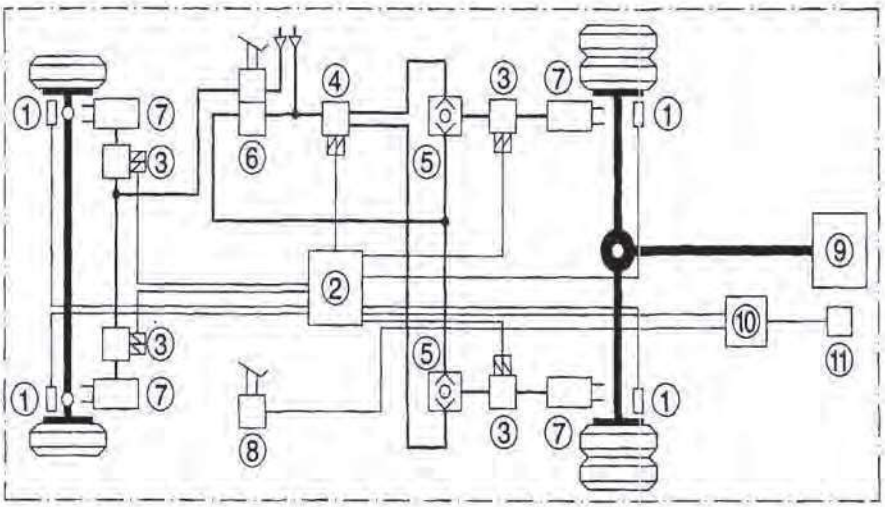


FIGURE 16.13 Four-circuit ABS/ASR, 4 x 2 vehicle.

ment. The ABS/ASR control unit (2) transmits the desired increment of reduction to the EPC control unit via interface, and also controls the electric motor at the injection pump.

16.7 FUTURE TRENDS

Ensuring driving stability is the most important task of ASR with rear-wheel-drive cars. This task can be achieved by a fast engine torque control or a combination of throttle control and a fast brake control.

ASR systems with a fast engine torque control (ignition and injection intervention) and brake control without stored energy will be widely used.

Although the application of controllable differential locks also offers efficient ASR control, the higher costs of this system will prevent wide usage.

The predominant demand on ASR systems for front-wheel-drive cars is that of traction optimization. Therefore, an ASR system with brake torque control is needed. The combination of brake torque control and engine torque control results in a complex, efficient system.

In the future, only ASR systems with brake torque control will be widely used with front-wheel-drive cars. Especially the combination of brake torque control and engine torque control with ignition and injection intervention will be widely used.

GLOSSARY

ABS return pump A piston pump that draws back brake fluid to the master cylinder.

Alternating injection suppression A variation of the number of active cylinders by one after every two crankshaft rotations in order to modulate the engine torque.

IPR2023-01234
Petitioner - Ex. 2017 - Page 372

ASR deactivation switch A device to switch off ASR on sand and loose gravel in order to achieve maximum traction on these surfaces.

Automatic throttle valve actuator A simple actuator for automatic throttle angle reduction in case of excessive acceleration slip.

Braking intervention Automatic brake application at drive wheels in case of excessive acceleration slip.

D controller A controller with differentiating characteristics.

Electronic performance control Electronic accelerator control.

Engine torque control An actuator to modulate engine torque in case of excessive acceleration slip.

PI controller Controller with proportional and integral characteristics.

Slip threshold switch Switch to increase desired slip threshold on sand and loose gravel.

Switchover valve A valve to switch hydraulic performance from normal braking to ASR performance.

Throttle valve control ASR actuator to modulate the throttle angle.

3/3 ABS valve A valve with three connections and three positions for ABS wheel pressure modulation.

BIBLIOGRAPHY

Maisch, Wolfgang, Jonner Wolf-Dieter, and Alfred Sigl, "Traction control—a logical addition to ABS," *SAE International Congress and Exposition,* Detroit, Feb. 23–27, 1987.

Kolberg, Gerhard, "Elektronische Motorsteuerung für Kraftfahrzeuge," *Motortechnische Zeitschrift,* Germany, 1985.

Demel, H., and A. Czinczel, "ABS-task, design, and function," *I Mech E Conference,* London, 1988-6, pp. 89–94.

Buschmann, G., N. Ocvirk, and P. Volz, "Integrated traction control function—the consequent extension of highly sophisticated anti-lock systems," *I Mech E Conference,* 1988-6, pp. 103–112.

Klein, Hans-Christof, "PkW-ABV-Bremssysteme mit weiteren integrierten Funktionen," *Automobilindustrie,* May 1989, pp. 659–673.

Kupper, R., and N. Hover, "Anti-slip-control system with high safety and comfort," *I Mech E,* C382/113, 1989, pp. 523–531.

Sigl, A., and H. Demel, "ASR-traction control, state of the art and some prospects," SAE 900.24.

Sigl, A., and A. Czinczel, "ABS/ASR5—the new ABS/ASR system for passenger cars," *I Mech E Conference,* London, 1993, pp. 81–87.

ABOUT THE AUTHOR

Dipl. Ing. Armin Czinczel received a degree in mechanical engineering at the Technical University in Hanover, Germany. He started his professional career with development work on navigation systems. He joined Bosch in 1968, working on ABS development until his retirement in 1994.

IPR2023-01234
Petitioner - Ex. 2017 - Page 373

CHAPTER 17
SUSPENSION CONTROL

Akatsu Yohsuke
Manager, Vehicle Research Laboratory
Nissan Motor Co., Ltd.

The function of a suspension system in an automobile is to improve ride comfort and stability. An important consideration in suspension design is how to obtain both improved ride comfort and stability, since they are normally in conflict. Advances in electronic control technology, applied to the automobile, can resolve this conflict.

17.1 SHOCK ABSORBER CONTROL SYSTEM

During the past 20 years, many different damping control systems have been studied. The main purpose of all these systems is to select the optimum damping force for various driving conditions. The first function of a shock absorber is to control vehicle movement against inertial forces, such as roll when the vehicle turns and pitch when the vehicle is braked. The second function is to prevent vehicle vibration caused by road surface inputs. To satisfy both functions it is necessary to control damping forces.

There are three basic parts of a damping control system: a damping control device (actuator), sensors, and software (control strategy). Optimum damping forces should be set for various running conditions in order to improve ride comfort and handling stability.

17.1.1 System Configuration

One of the damping control system configurations is shown in Fig. 17.1. This system uses five sensors, including a supersonic road sensor, to detect running conditions. Control signals are sent to adjust the damping force of the variable shock absorbers to optimum values. A main advantage to this type of system is that, through the use of a road sensor, it can provide optimum control in accordance with the actual road conditions. This system incorporates three discrete damper characteristics. Sensors used are: a vehicle speed sensor, a steering angle sensor, an acceleration and deceleration sensor, a brake sensor, and a supersonic sensor to detect road conditions.

One system uses four piezo sensors and four piezo actuators on each wheel in order to change the damping forces as quickly as possible. This system incorporates two discrete damper characteristics. Sensors used are: four piezo sensors on each wheel, a stop lamp switch, a steering sensor, and a vehicle speed sensor.

IPR2023-01234
Petitioner - Ex. 2017 - Page 375

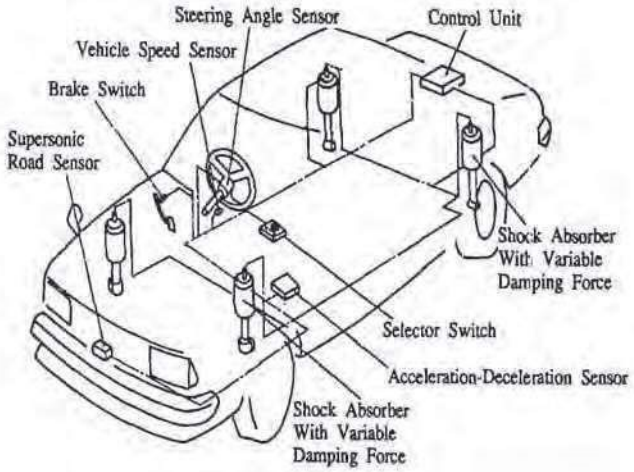


FIGURE 17.1 Principal components of a damping control system.

17.1.2 Actuator and Sensor

Actuator. Discrete damping control actuators often use a built-in motor to change the damping force. This motor turns a rotary valve to select the orifice diameter for three different damping levels: soft, medium, and hard. The stopping position of the rotary valve is controlled by encoder signals.

Another actuator is a piezo actuator consisting of 88 piezo elements, and it is installed in the piston rod of a shock absorber. When a high voltage (500 V) is applied to the piezo actuator, it expands about 50 μm with reverse piezoelectric effect. Elongation in the piezo actuator causes the plunger pin to be pushed out through the displacement hydraulic coupling unit. As a result, the plunger pin moves down to open the bypass of the damping force switching valve. The result is a soft damping force. Figure 17.2 shows this valve.

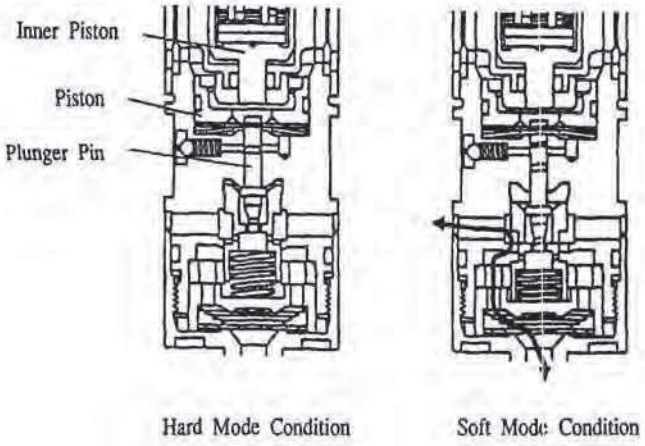


FIGURE 17.2 Damping force switching valve.

Sensor. A sensor using a supersonic wave to detect the road surface is shown in Fig. 17.3. The vehicle height from road to body is calculated on the basis of reflection time T. Judgment of the road condition is made by analyzing the pattern of change in vehicle height.

A sensor using the piezoelectric effect is shown in Fig. 17.4. Installed in the piston rod of a shock absorber, the sensor generates an electric charge in accordance with axial force from the road surface.

IPR2023-01234
Petitioner - Ex. 2017 - Page 376

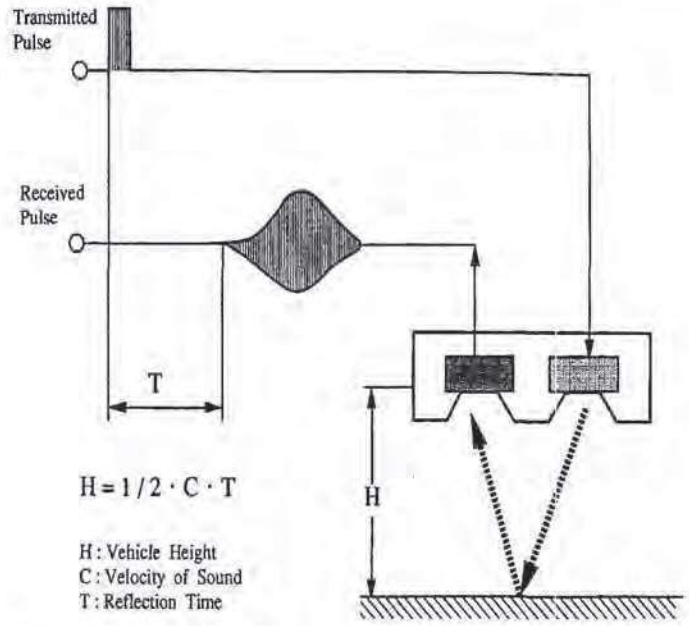


FIGURE 17.3 Supersonic sensor.

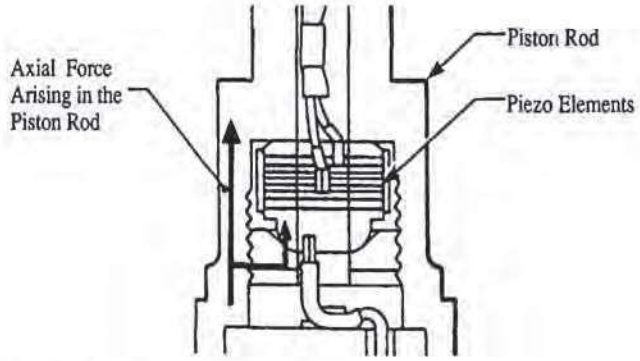


FIGURE 17.4 Piezoelectric sensor.

17.1.3 Control System

The control system of Fig. 17.1 is shown in Table 17.1. The occurrence of roll and pitch can be predicted from various sensors. Single bumps or dips are detected from changes in vehicle height. The outline of the road surface judgment logic is shown in Table 17.2.

The block diagram of the system using four piezo sensors and four piezo actuators is shown in Fig. 17.5. The damping force arising in an absorber increases instantaneously as the tire or wheel goes up or down in accordance with unevenness of the road surface. Each piezo sensor outputs to the electronic control unit continuous signals indicating damping force differential. If the value of damping force differential exceeds a predetermined level, the system switches from firm mode to soft mode. The system is designed so that the firm mode reengages immediately after the vibrations due to poor road surface cease.

Many of the limitations and disadvantages of the conventional shock absorber can be eliminated by the damping control systems. They include semiactive suspension systems which are capable of providing both ride comfort and good handling.

IPR2023-01234
Petitioner - Ex. 2017 - Page 377

TABLE 17.1 Damping Force Control System

Control objectives		Sensors used					Damping force Front / Rear
		Vehicle speed	Steering angle	Accel/ decel	Brake	Road condition	
Roll	Roll reduction for quick steering operation	○	○				Hard / Hard
Pitch	Reduction of nose diving by braking				○	○	Hard / Hard
	Reduction of pitching when accelerating and decelerating	○		○			Medium / Medium
Bouncing	Reduction of light, bouncy vibrations in bottoming	○				○	Medium / Medium
	Reduction of light, bouncy vibrations in bouncing on a heaving road	○				○	Medium / Medium
Road holding performance	Road holding performance improvement when running on rough roads	○				○	Medium / Medium
Others	Stability improvement at high speed	○					Medium / Soft
	Prevention of shaking when stopping and rocking when passengers exit or enter	○					Hard / Hard

TABLE 17.2 Road Condition Judgment Logic

High-frequency components	Low-frequency components	
	Small	Large
Small	Smooth road	Heaving road
Large	damping force control *unnecessary*	Rough road

17.2 HYDROPNEUMATIC SUSPENSION CONTROL SYSTEM

A hermetically sealed quantity of gas is used in the hydropneumatic suspension control system. The gas and hydraulic oil are separated by a rubber diaphragm, as shown in Fig. 17.6*a*. The mechanical springs are replaced by gas. The shock absorber damping mechanism is achieved by the orifice fitted with valves.

17.2.1 System Configuration

As shown in Fig. 17.6*b*, by adding an additional sphere to the hydropneumatic system, a controllable hydropneumatic system can be realized. If the regulator is closed, the system is in a firm mode. If the regulator is open, the spring constant of the suspension system becomes lower by increasing the total volume of the sphere, and the total damping force is reduced.

IPR2023-01234
Petitioner - Ex. 2017 - Page 378

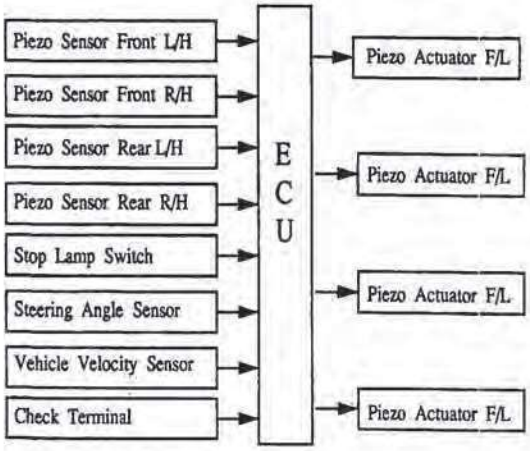


FIGURE 17.5 Block diagram of damping control system.

Depending on the sensors used, which detect vehicle driving and road surface conditions, this system can change the regulator characteristics in order to achieve both good ride comfort and handling stability.

17.3 ELECTRONIC LEVELING CONTROL SYSTEM

In a pneumatic and hydropneumatic suspension, the vehicle body can be maintained at a constant height from the road surface, keeping a low spring constant. The advantages of an electronic control system are:

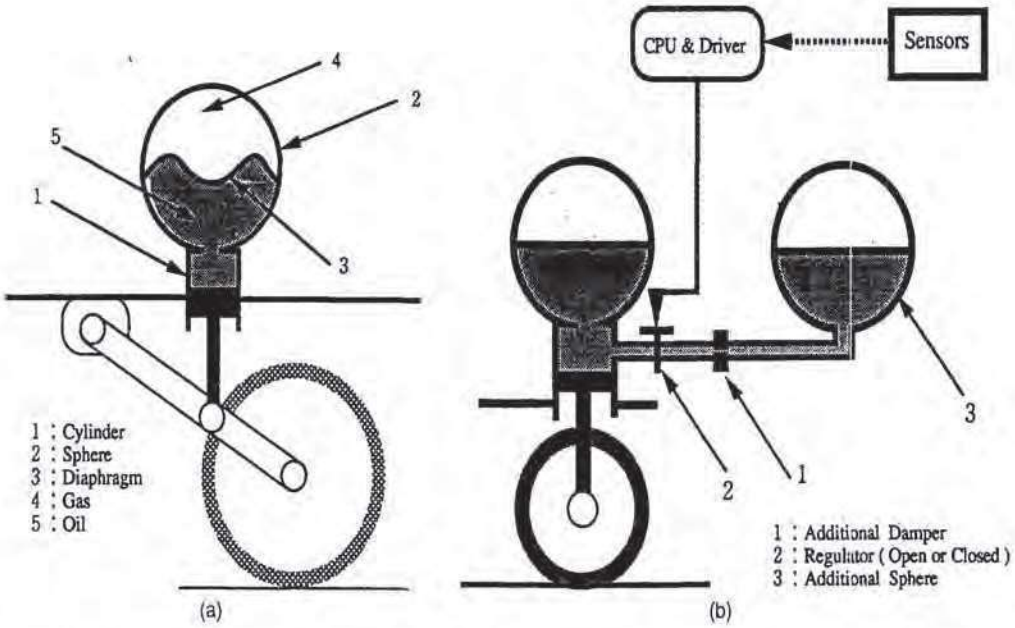


FIGURE 17.6 (*a*) Hydropneumatic suspension system; (*b*) Controllable hydropneumatic suspension system.

IPR2023-01234
Petitioner - Ex. 2017 - Page 379

- Keeping a low spring rate to achieve good ride comfort independent of load conditions
- Increase in vehicle body height on rough road surfaces
- Changing spring rate and damping force in accordance with driving conditions and road surfaces

17.3.1 System Configuration

The system is shown in Fig. 17.7. It consists of eight sensors, a mode select switch, air spring/shock absorber units on four wheels, actuators to operate the changing valves in the unit, a compressor unit and five height control valves for air springs, and an electronic control unit (ECU). The system configuration is shown in Fig. 17.8.

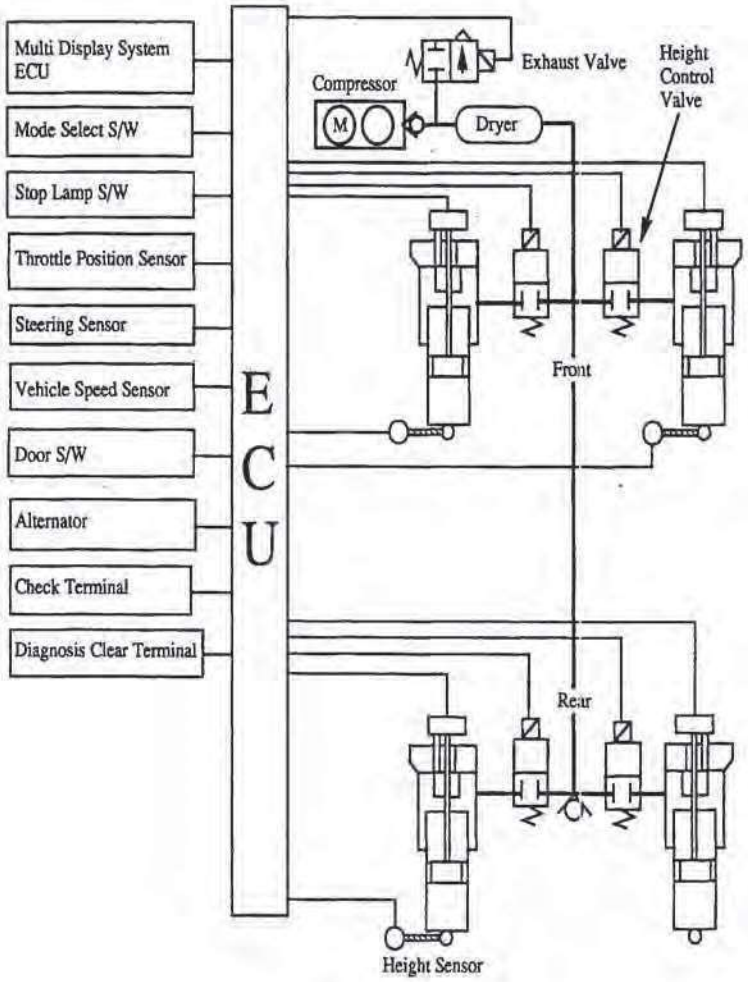


FIGURE 17.7 Principal components of an air suspension system.

17.3.2 Components

The structure of the air suspension unit consists of a shock absorber, a pneumatic piston surrounding the shock absorber, main and sub-air chambers, a rolling diaphragm, and valves which change the suspension stroke.

The actuator uses a dc motor, which has two shafts to operate the valves for the air spring and the shock absorber. The rotation of the motor is reduced by the sector gear and operates

IPR2023-01234
Petitioner - Ex. 2017 - Page 380

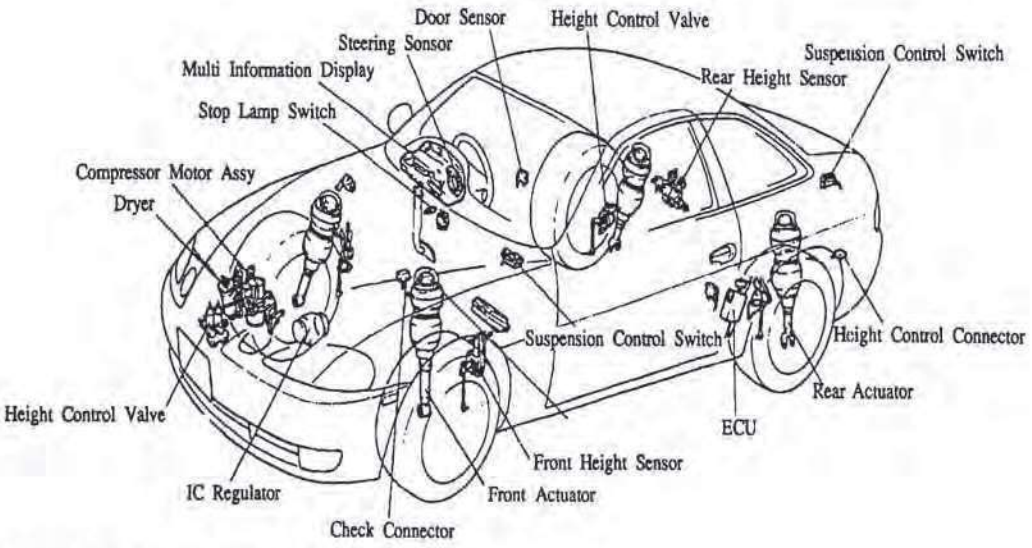


FIGURE 17.8 Configuration of an air suspension system.

the rotary valve to change the damping force. At the same time, another gear engaged with the sector gear operates the air valve to change the spring rate.

17.3.3 Control System

This system can change the spring rate and the damping force into three levels and vehicle height levels of low, normal, or high can be selected. One of the control logics is shown in Table 17.3. This is a control which changes the suspension characteristics in response to vehicle speed and road conditions. The spring rate/damping force and the vehicle height are controlled independently according to each control logic.

Electronic leveling control systems do not need much energy to control vehicle height. They control both spring rate and damping force. As a result of keeping the low spring rate, electronic leveling control systems can provide both good ride comfort and handling stability.

TABLE 17.3 Basic Control Logic of Air Suspension System

		Spring rate, damping force					
		Soft mode			Medium mode		
Function	Operating condition	Soft	Medium	Firm	Soft	Medium	Firm
Antiroll	Rapid steering	○		→ ○		○	→ ○
Antidive	Braking at V* > 60 km/h	○		→ ○		○	→ ○
Antisquat	Rapid starting at V < 20 km/h	○		→ ○		○	→ ○

* V: Vehicle speed.

IPR2023-01234
Petitioner - Ex. 2017 - Page 381

17.4 ACTIVE SUSPENSION

Suspension control systems for passenger cars have evolved through several stages over the years. Work in the field began with the air suspension for controlling vehicle height and then progressed to the hydropneumatic suspension and suspensions with variable damping force and spring rate control. Now efforts are underway to develop an active suspension. It is defined as one that has the following features:

- Energy is constantly supplied to the suspension and the force generated by that energy is continuously controlled
- The suspension incorporates various types of sensors and a unit for processing their signals that generates forces that are a function of the signal outputs

17.4.1 System Configurations

Basic Configuration. Hydraulic active suspension can be divided into two large systems: the hydraulic system and the control system, as shown in Fig. 17.9. The hydraulic pressure of each of the actuators located on each wheel is controlled in accordance with the output values from the G sensors to suppress changes in vehicle body position (bounce, pitch, roll) and reduce vibration from the road surface.

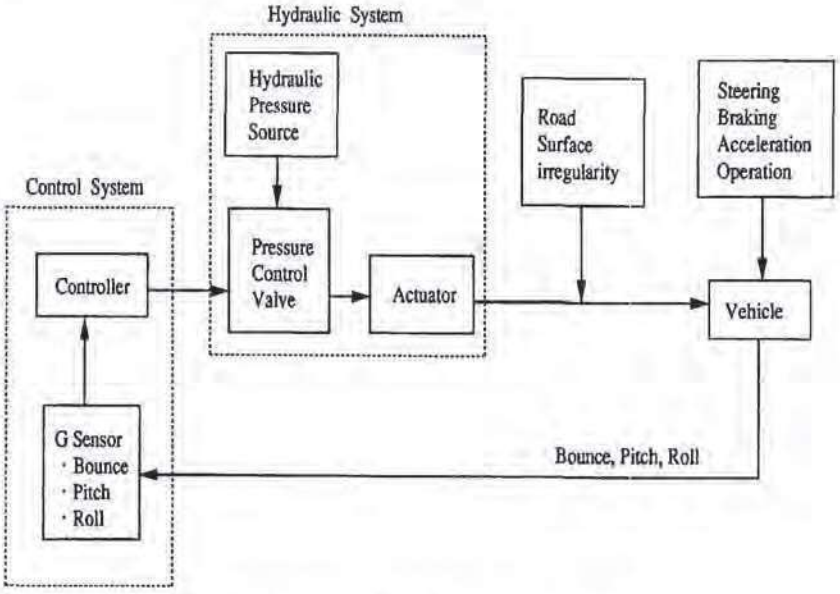


FIGURE 17.9 Hydraulic and control systems for an active suspension.

Hydraulic and Control System Configuration. A basic overview of the system is shown in Fig. 17.10. The functions of the main units of the hydraulic system are shown in Table 17.4.

As shown in Fig. 17.11, the control system contains the controller and all of the sensors including the vertical G sensors, lateral G sensors, fore and aft G sensors, and vehicle height sensors.

17.4.2 Components

Oil Pump. The oil pump has seven cylinders arranged around the circumference and can output a maximum oil flow of 12 liters per minute. The pump is connected in tandem with the power steering vane pump.

IPR2023-01234
Petitioner - Ex. 2017 - Page 382

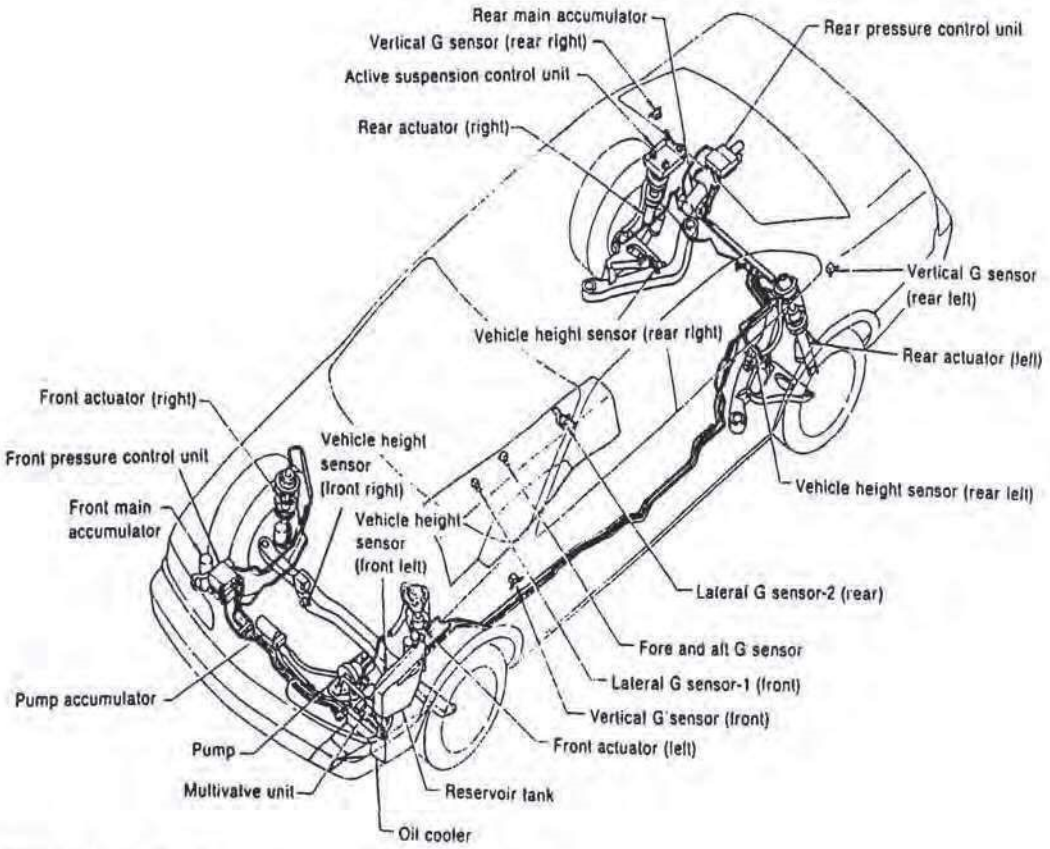


FIGURE 17.10 Principal components of an active suspension system.

Pump Accumulator. To dampen pulsating hydraulic pressure generated by the oil pump, pump accumulators are installed in the hydraulic supply unit, including one on the side of the oil pump. To dampen the high-frequency pulsations, a metal-bellows-type accumulator is used.

Multivalve Unit. As shown in Fig. 17.12, the multivalve unit contains valves for many different functions. The main purpose of the multivalve unit is the basic control of hydraulic pressure for the whole system. The function of the multivalve unit is shown in Table 17.5.

Main Accumulator. The main accumulator is positioned at both the front and rear axles. The main accumulator has two principal functions: it stores oil from the multivalve unit and provides extra flow to the actuators when necessary, and it preserves vehicle height when the engine is turned off.

TABLE 17.4 The Functions of Main Units of the Hydraulic Systems

	Main basic function
Oil pump	Supplies the necessary oil for system operation (power supply)
Pump accumulator	Removes the pulsating action from pressurized oil supplied by the oil pump
Multivalve unit	Controls the supply of pressurized oil, failsafe function, etc.
Main accumulator	Maintains oil pressure, compensates when large amount of flow is required and preserves vehicle body height
Pressure control unit	Controls the hydraulics for the actuators on each wheel according to signals received from the control unit
Actuator	Controls vehicle attitude and absorbs external forces from the road surface

IPR2023-01234
Petitioner - Ex. 2017 - Page 383

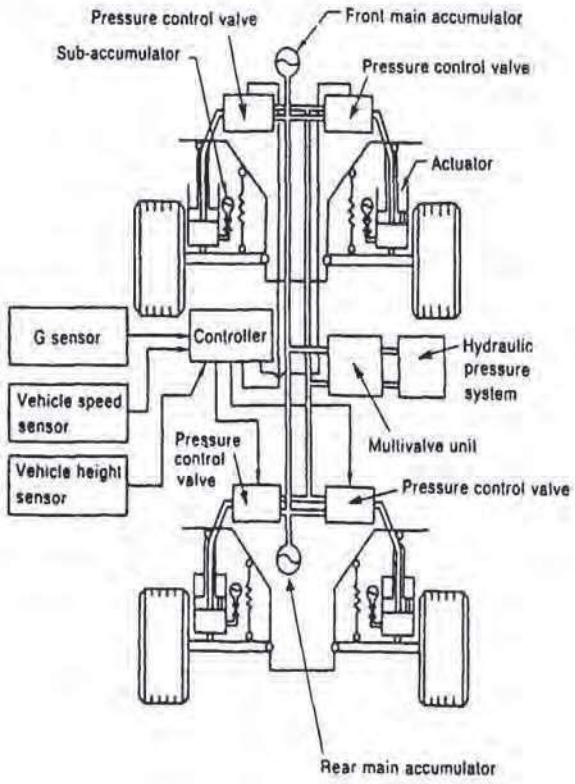


FIGURE 17.11 Controls for an active suspension system.

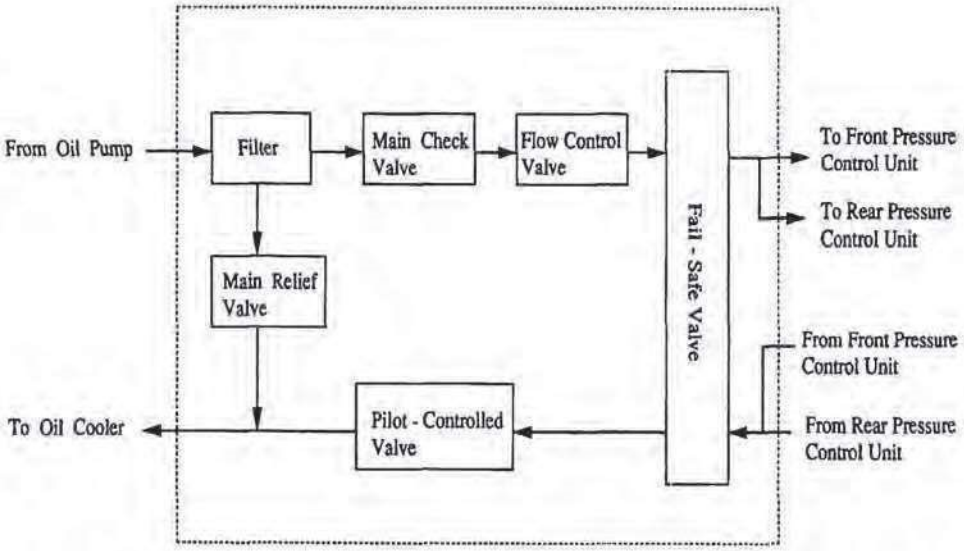


FIGURE 17.12 Multivalve unit configuration.

Pressure Control Unit. As shown in Fig. 17.13, the pressure control unit controls the hydraulic movement of the actuator of each wheel in accordance with instructions received from the control unit. Table 17.6 shows the valve's construction and operating principle.

The electrohydraulic pressure control system consists of a pressure actuator and a pressure control valve. The actuator is of the single acting type and is provided with a damping valve and an accumulator below the cylinder. The pressure control valve is built with three ports

IPR2023-01234
Petitioner - Ex. 2017 - Page 384

TABLE 17.5 Multivalve Unit Functions

Function	Valve	Outline
Pressure supply management function	Main relief valve	When the oil pressure exceeds a constant value, the main relief valve will return some of the oil flow. This keeps the oil supply pressure at a constant pressure.
Vehicle height maintenance function	Main check valve Pilot-controlled check valve	The main check valve is a nonreturn valve that controls the flow from the line filter and directs it to the flow control valve. The pilot controlled check valve is a supply-pressure-reaction-type open/closed valve. When the hydraulic pressure exceeds a constant value, the valve opens and when the hydraulic pressure falls below that level, it closes. In addition, it maintains the hydraulic pressure at a constant level when the engine is turned off.
Vehicle height control function	Flow control valve	When the engine is turned off, the flow control valve closes the main passage and directs the flow through the bypass passage orifice, slowly increasing the hydraulic pressure, after which the main passage is opened. This prevents any sudden changes in vehicle height when starting the engine.
Failsafe function	Failsafe valve	When any irregularities occur in the electronic system, it changes the hydraulic passage, preventing any sudden changes in vehicle height.

and employs a pilot type proportional electromagnetic control valve. This pressure control valve has two main functions:

- It controls the pressure of the actuator according to the control input. This is accomplished by driving the solenoid so that it adjusts the pilot valve, causing the spool to move.
- Feedback control is applied to move the spool in response to fluctuations in actuator pressure caused by road surface inputs; the action of the spool works to keep the actuator pressure at a certain fixed level.

Actuator. As shown in Fig. 17.14, the actuator consists of the hydraulic power cylinder, subaccumulator, damping valve, etc. Auxiliary coil springs are also employed to reduce the pressure necessary for the overall system and to reduce the amount of horsepower expended. The subaccumulator and damping valve at the bottom of the hydraulic power cylinder absorb and damp the high-frequency vibration from the road surface.

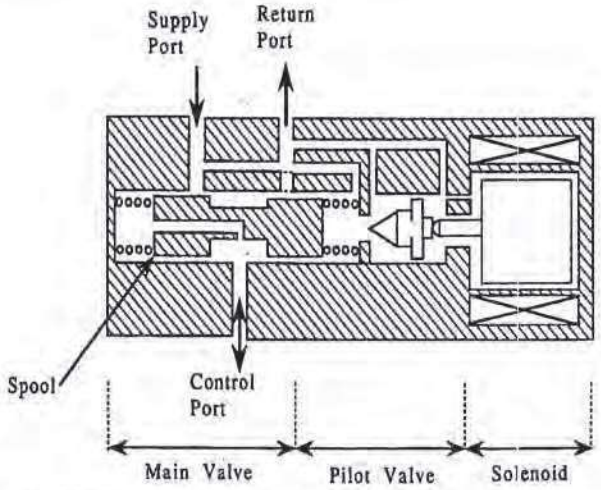


FIGURE 17.13 Pressure control valve construction.

IPR2023-01234
Petitioner - Ex. 2017 - Page 385

TABLE 17.6 Pressure Control Valve Functions

Active control function	The pressure in the control port (actuator) is controlled in response to the electric current applied to the solenoid, thus controlling the vehicle attitude.
Passive damping function	When various pressure levels are caused in the interior of the actuator by road surface forces, this pressure passes through the control port, causing feedback on the spool and the generation of appropriate damping forces.

Controller. As shown in Fig. 17.15, the controller is constructed using two 16-bit microcomputers, MCU1 and MCU2.

MCU1 processes signals from the G sensors and then sends attitude control signals to the pressure control valve solenoid drive circuit. MCU2 processes signals from the vehicle height sensors and then sends attitude control signals to the solenoid drive circuit.

MCU1 and MCU2 normally perform mutual transmission, but should an irregularity occur, the signal will be sent to the failsafe circuit, causing the failsafe valve to operate and thus guarantee a high degree of safety.

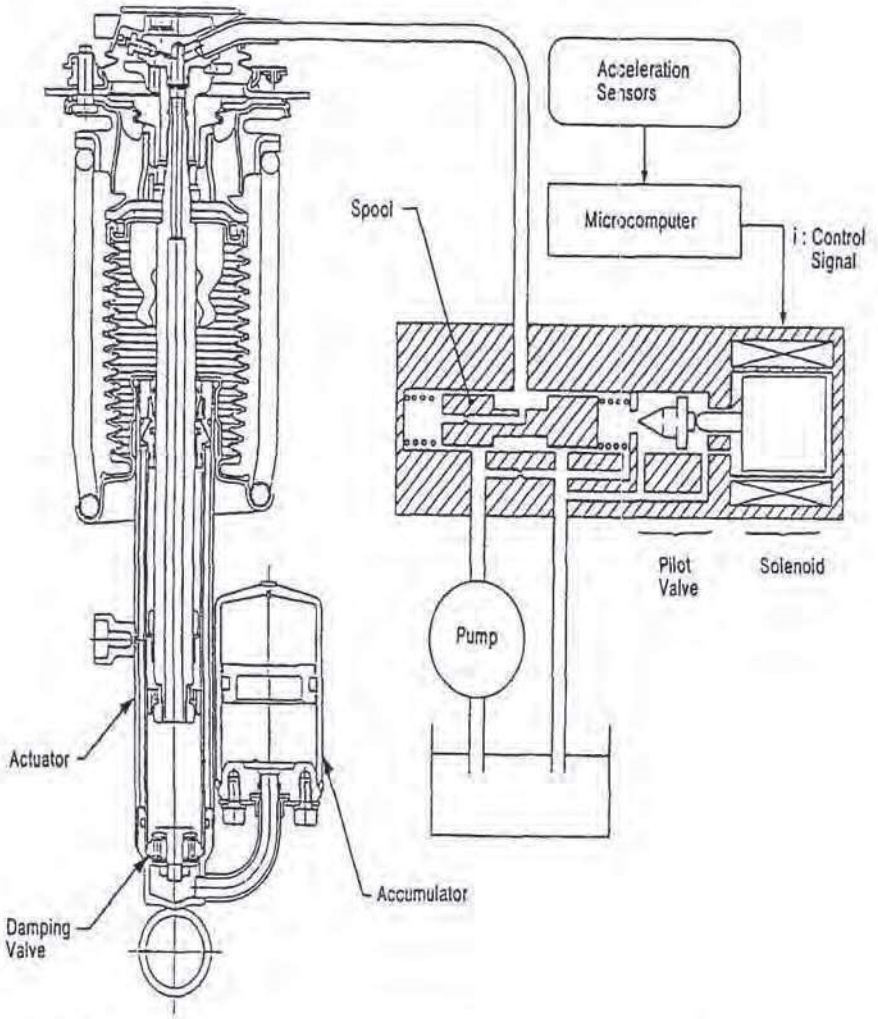


FIGURE 17.14 Schematic diagram of electrohydraulic pressure control system.

IPR2023-01234
Petitioner - Ex. 2017 - Page 386

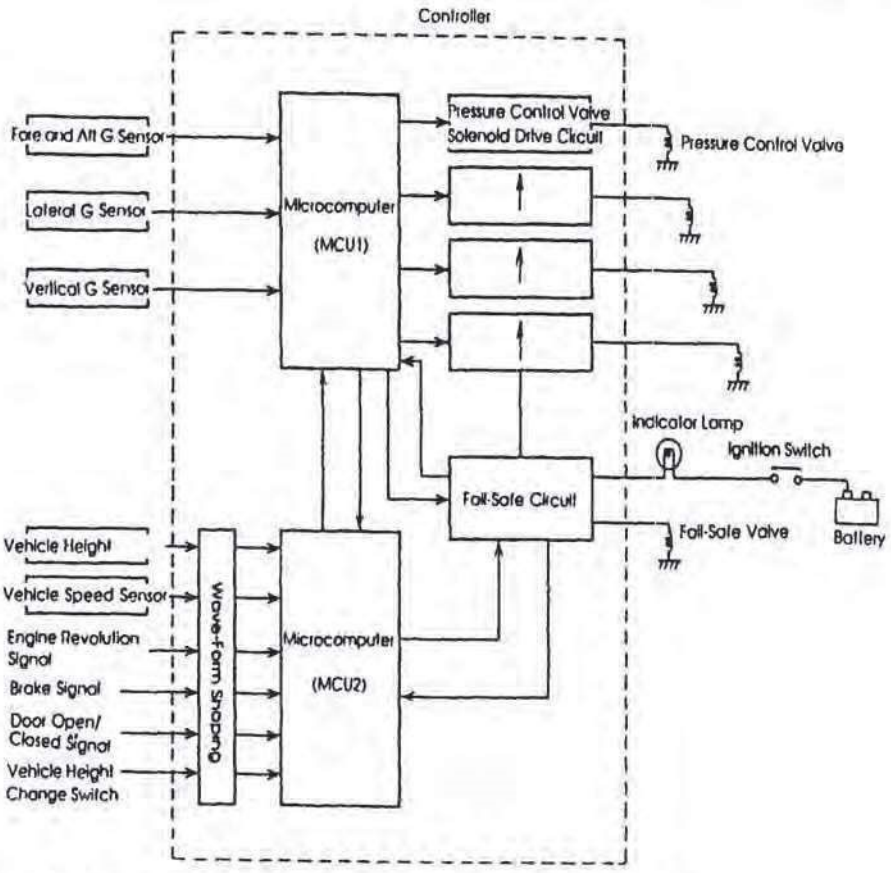


FIGURE 17.15 Interior construction of the electrohydraulic pressure controller.

G Sensors. The G sensors are ball position detection type sensors. They detect changes in the magnetic field caused by the position change of a steel ball as the result of acceleration.

17.4.3 Control System

Roll Control. The inertia force, which causes the car to roll, is detected by the lateral G sensor. Roll control is initiated by increasing the control pressure on the wheels on the outside of the turn and by decreasing the control pressure for the wheels on the inside of the turn. Figure 17.16 shows this operating principle.

The relation between the lateral G and the force generated by the actuator is:

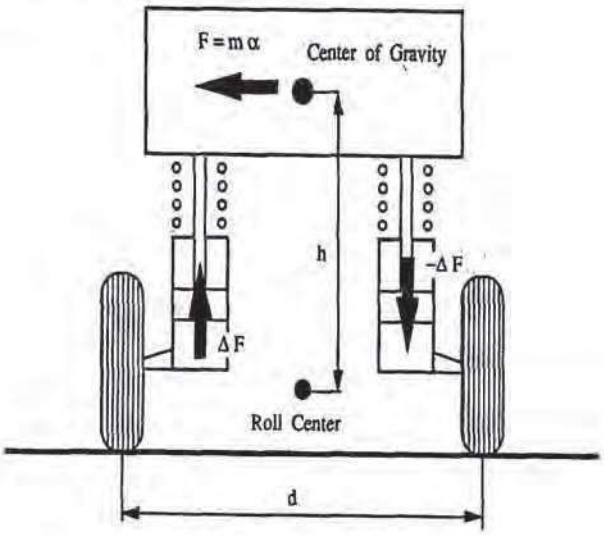
$$F = m\alpha \tag{17.1}$$

$$Fh = \Delta Fd$$

$$\Delta F = \frac{Fh}{d} = \frac{m\alpha h}{d}$$

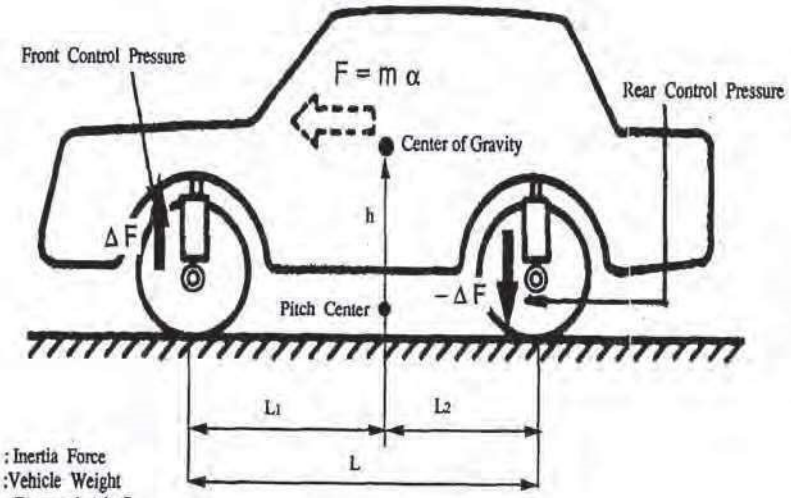
Pitch Control. During braking, inertia is generated at the vehicle's center of gravity and causes pitching. The longitudinal G sensor detects this inertia and cancels it to suppress nose dive by increasing the control pressure to the front and decreasing control pressure to the rear, as shown in Fig. 17.17. The relationship between longitudinal G and the actuator generated force is:

IPR2023-01234
Petitioner - Ex. 2017 - Page 387



α : Lateral G
F : Inertia
ΔF : Actuator Generated Force
d : Tread

FIGURE 17.16 Operating principle for roll control.



F : Inertia Force
m : Vehicle Weight
α : Fore and Aft G
ΔF : Actuator - Generated Force
L : Wheel Base

FIGURE 17.17 Pitch control parameters.

$$Fh = \Delta F (L_1 + L_2)$$

$$\Delta F = \frac{Fh}{(L_1 + L_2)} = \frac{m\alpha h}{L} \tag{17.2}$$

Bounce Control. The vertical G sensor attached to the vehicle body detects the value for vehicle body acceleration. By integration of the acceleration, the absolute velocity of the body is calculated. A force proportional to the absolute velocity is generated by the pressure control valve.

IPR2023-01234
Petitioner - Ex. 2017 - Page 388

This control method, called skyhook damper control, is adapted. It dampens the motion of the car body regardless of any input from the road surface.

In the case of a passive damper, the vertical motion of the body relative to the road surface inputs can be given as:

$$\frac{X_2}{X_1} = \frac{2j\omega_2\xi_2\omega + \omega_2^2}{-\omega^2 + 2j\omega_2\xi_2\omega + \omega_2^2} \tag{17.3}$$

The vibration transmission rate at the resonant point is:

$$\left|\frac{X_2}{X_1}\right|_{\omega=\omega_2} = \sqrt{1 + \frac{1}{4\xi_2^2}} \tag{17.4}$$

and always has a value greater than one.

By contrast, the vibration characteristics of the skyhook damper are given as:

$$\frac{X_2}{X_1} = \frac{2j\omega_2\xi_2\omega + \omega_2^2}{-\omega^2 + 2j\omega_2(\xi_2 + \xi_s)\omega + \omega_2^2} \tag{17.5}$$

The vibration transmission ratio at the resonant point is:

$$\left|\frac{X_2}{X_1}\right|_{\omega=\omega_2} = \frac{\sqrt{4\xi_2^2 + 1}}{2(\xi_2 + \xi_s)} \tag{17.6}$$

hence,

$$\xi_s \geq \sqrt{\xi_2^2 + \frac{1}{4}} - \xi_2 \tag{17.7}$$

and it is possible to reduce the ratio to less than one.

The effects of the hydraulic active suspension are organized in Table 17.7 according to those related to the vehicle.

17.4.4 Effectiveness

Figure 17.18 shows the lateral G and angle of roll during cornering. Figure 17.19 shows the fore and aft G force, angle of nose dive, and squat angle during starts and stops. In either case, the car with the hydraulic active suspension outperformed the other cars with conventional suspensions.

TABLE 17.7 Effect of Active Suspension Control

Control	Vehicle-related effects
Roll control	During transient control of wheel loading, as when changing lanes, the steering characteristics of the vehicle can be optimally controlled. The tires are used to their utmost performance ability because there is minimal roll, minimal change in the camber of the tires to the ground, and because the tires are continually kept in square contact with the road.
Pitch control	Nose dive and tail lift are minimized during braking. Squats are minimized during starts and rapid acceleration.
Bounce control	Vertical vibration of the vehicle is reduced and continuity is improved. Vertical load fluctuation is minimal, and the contact of the tires with the road is greatly improved.

IPR2023-01234
Petitioner - Ex. 2017 - Page 389

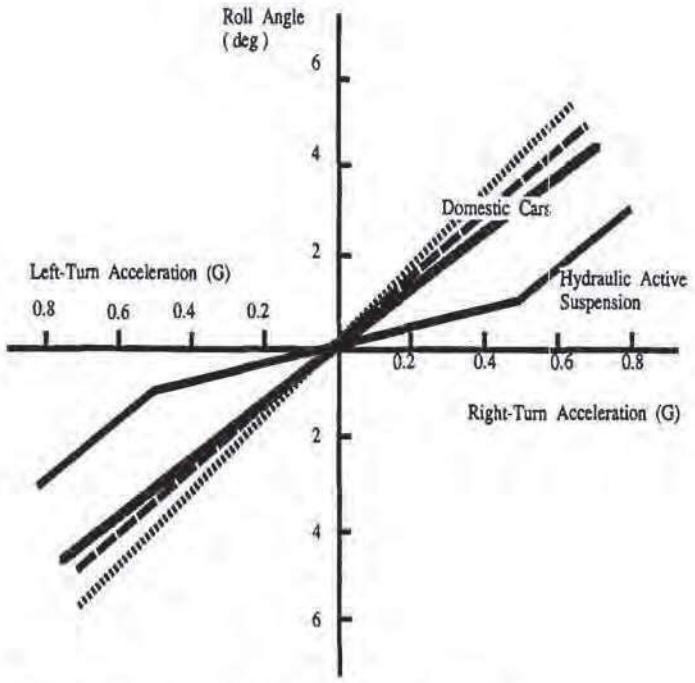


FIGURE 17.18 Comparison of roll angles during cornering.

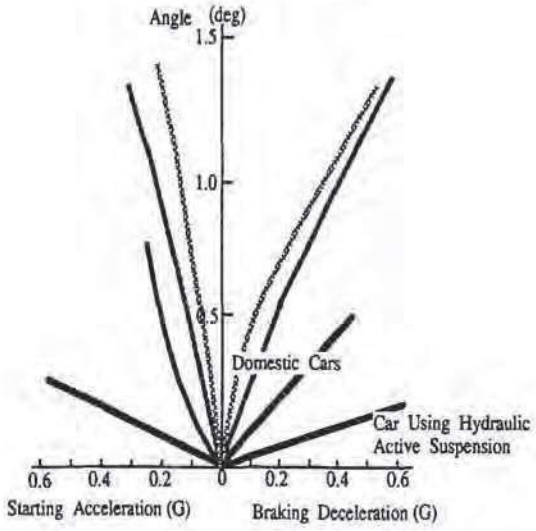


FIGURE 17.19 Comparison of nose dive and squat angles.

Figure 17.20 shows the effects of bounce control for the skyhook damper. Compared with cars using conventional suspension systems, the car with the hydraulic active suspension system exhibited superior performance and low vibration levels.

Figure 17.21 shows the ride characteristics and roll rate for various cars with some suspension systems. As the results clearly demonstrated, the hydraulic active suspension system, through advanced roll control and bounce control, provides a ride and a level of control far superior to that of other suspension systems.

IPR2023-01234
Petitioner - Ex. 2017 - Page 390

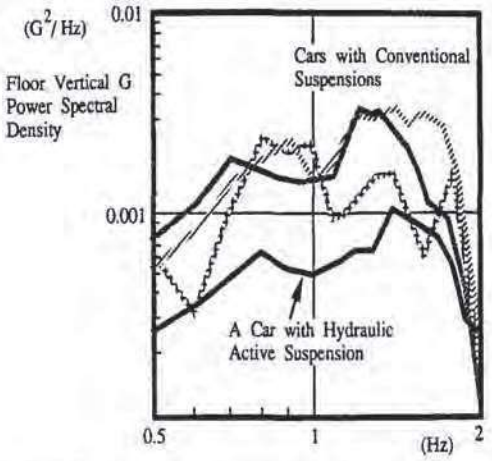


FIGURE 17.20 Comparison of vertical vibrations.

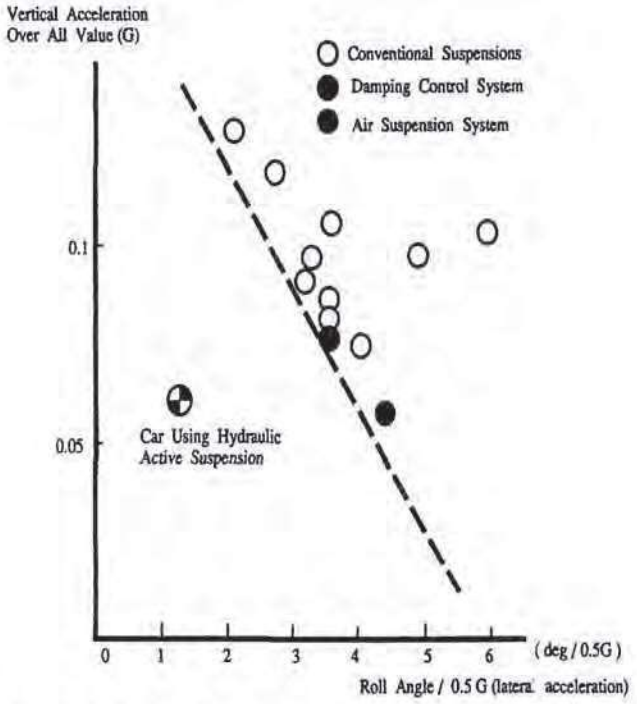


FIGURE 17.21 Ride characteristics and roll rate for various cars with different suspension systems.

17.5 CONCLUSION

The active suspension system provides outstanding levels of performance which are unobtainable with other suspension control systems and conventional passive suspensions. Evaluations made with actual vehicles confirmed the effectiveness of the active suspension system in improving ride comfort and handling properties.

IPR2023-01234
Petitioner - Ex. 2017 - Page 391

GLOSSARY

Hydropneumatic suspension A suspension system using oil or air to support the car body.

Skyhook damper control The control law applied to control the vehicle as if it were fixed within absolute space suspended from the sky.

Supersonic sensor A sensor used to measure the distance between a car body and the road surface using supersonic waves.

NOMENCLATURE

C_2: passive damping coefficient
C_s: active damping coefficient
K_1: tire stiffness
K_2: spring stiffness
M_1: unsprung mass
M_2: sprung mass
$\omega_1 = (K_1/M_1)^{1/2}$ natural frequency of unsprung mass
$\omega_2 = (K_2/M_2)^{1/2}$ natural frequency of sprung mass
$\xi_2 = (C_2/2)\,(M_2K_2)^{1/2}$ active damping ratio
$\xi_S = (C_S/2)\,(M_2/K_2)^{1/2}$ passive damping ratio

BIBLIOGRAPHY

Decker, H., and W. Scramm, "An optimized approach to suspension control," SAE Paper 900661, 1990.

Decker, H., W. Scramm, and R. Kallenbach, "A modular concept for suspension control," *XXIII Fisita Congress,* Torino, Italy, 1990, 905124.

Decker, H., W. Scramm, and R. Kallenbach, "A practical approach toward advanced suspension systems," *Proc. IMechE International Conference on Advanced Suspensions,* London, 1988, S. 93–99.

Doi, S., E. Yasuda, and Y. Hayashi, "An experimental study of optimal vibration adjustment using adaptive control methods," *Proceedings of the Institution of Mechanical Engineers,* London, Oct. 24–25, 1988.

Guy, Y., M. B. Lizell, and M. W. Kerastas, "A solenoid-actuated pilot valve in a semi-active damping system," SAE Paper 881139, Aug. 1988.

Haget, K. H., et al., "Continuous adjustable shock absorbers for rapid-acting ride control systems (RCS)," *XXIII Fisita Congress,* Torino, Italy, 1990, 905125.

Hennecke, D., P. Baier, B. Jordan, and E. Walek, "EDCIII—the new variable damper system for BMW's top models—a further development of our adaptive, frequency-dependent damper control," SAE Paper 900662.

Hennecke, D., P. Baier, B. Jordan, and E. Walek, "Further market-oriented development of adaptive damper force control," *XXIII Fisita Congress,* Torino, Italy, 1990, 905143.

Hennecke, D., B. Jordan, and U. Ochner, "Electronic damper control—a fully automatic adaptive system for damping force adjustment on the BMW 635 CSi," *ATZ 89,* 9, 1987, pp. 471–479.

Hrovat, D., D. L. Margolis, and M. Hubbard, "An approach toward the optimal semi-active suspension," *Transactions of the ASME,* 288, vol. 110, Sept. 1988.

IPR2023-01234
Petitioner - Ex. 2017 - Page 392

Karnop, D., and D. L. Margolis, "Adaptive suspension concepts for road vehicles," *Vehicle System Dynamics,* 13, 1984, pp. 145–160.

Karnop, D., M. J. Crosby, and R. A. Harwood, "Vibration control using semi-active force generators," *ASME Journal of Engineering for Industry Transactions of the ASME,* No. 96, 1974, S. 613–626.

Margolis, D. L., "Semi-active control of wheel hop in ground vehicles," *Vehicle System Dynamics,* 12, 1983, pp. 317–330.

Sharp, R. S., and S. A. Hassan, "Performance and design considerations for dissipative semi-active suspension systems for automobiles," *Proceedings Institution of Mechanical Engineers,* vol. 201, no. D2, pp. 149–153.

Sugasawa, F., et al., "Electronically controlled shock absorber system used as a road sensor which utilizes super sonic waves," SAE Paper 851652, 1985.

Tsutsumi, Y., H. Sato, H. Kawaguchi, and M. Hirose, "Development of Piezo TEMS (Toyota Electronic Modulated Suspension)," SAE Paper 901745, 1990.

Yokota, Y., K. Asami, and T. Hajima, "Toyota electronic modulated suspension system for the 1983 Soarer," SAE Paper 840341, 1984.

Hydropneumatic Suspension

Akatsu, Y., N. Fukushima, K. Takahashi, M. Satoh, and Y. Kawarazaki, "An active suspension employing an electrohydraulic pressure control system," *XXIII Fisita Congress,* Torino, Italy, 1990, 905123.

Carbonaro, O., "Hydractive suspension electronic control system," *XXIII Fisita Congress,* Torino, Italy, 1990, 905101.

Dominy, J., and D. N. Bulman, "An active suspension for a Formula One Grand Prix racing car," *Transactions ASME, Journal Dynamic Systems Measurement Control,* vol. 107, 1, 1985, pp. 73–78.

Hedrick, J. K., "Railway vehicle active suspensions," *Vehicle System Dynamics* **10**, 1981, pp. 267–283.

Henning, H., "Citroen SM V6," *ATZ 92,* 1990, pp. 23–27.

Hrovat, D., "Optimal active suspension structures for quarter-car vehicle models," *Automatica,* vol. 26, 5, 1990, pp. 845–860.

Karnop, D., "Active damping in road vehicle suspension systems," *Vehicle System Dynamics* **12**, 1983, pp. 291–316.

Sharp, R. S., and S. A. Hassan, "An evaluation of passive automotive suspension systems with variable stiffness and damping parameters," *Vehicle System Dynamics,* **15**(6):1986, pp. 335–350.

Tanahashi, H., K. Shindo, T. Nogami, and T. Oonuma, "Toyota electronic modulated air suspension for the 1986 Soarer," SAE Paper 870541, 1987.

Thompson, A. G., "An active suspension with optimal linear state feedback," *Vehicle System Dynamics* **5**, 1976, pp. 187–203.

Tobata, H., N. Fukushima, K. Fukuyama, and T. Kimura, "Advanced control method of active suspension," *Avec92,* Yokohama, Japan, 1992, 923023.

Wright, P., "The application of active suspension to high performance road vehicle," *I MechE,* C239/84, 1984.

ABOUT THE AUTHOR

Akatsu Yohsuke has been Vehicle Research Manager for Nissan Motor Co., Ltd., since 1980. He was awarded the B.E. degree from the Tokyo Institute of Technology in 1978 and the M.E. degree from there in 1980.

IPR2023-01234
Petitioner - Ex. 2017 - Page 393

CHAPTER 18
STEERING CONTROL

Makoto Sato
Honda R&D Co., Ltd.

The application of electronic control technology to vehicle steering systems is still in the development stage. The structure and functioning of such systems are not yet clearly defined. Accordingly, the material that follows is intended primarily to introduce systems which have already been published, and it is devoted entirely to the electronic aspects of those systems and does not include descriptions of the basic operation of hydraulic power steering systems.

18.1 VARIABLE-ASSIST STEERING

18.1.1 Fundamentals of Electronically Controlled Power Steering

Electronically controlled power steering improves steering feel and power-saving effectiveness, and increases steering performance. It does so with control mechanisms that reduce the steering effort. An electronic control system, for example, may be added to the hydraulic booster or the whole system may be composed of electronic and electric components.

The intent of electronic controls, initially, was to reduce the steering effort when driving at low speeds and to supply feedback for the appropriate steering reaction force when driving at high speeds. In order to achieve those goals, devices such as vehicle speed sensors were used to detect vehicle speed in order to make smooth and continuous changes in the steering assist rate under conditions ranging from steering maneuvers at zero speed to those at high speeds. However, as vehicles became equipped with electrohydraulic systems and fully electronic and electric systems, the emphasis for these systems started to include reduction in power requirements and higher performance.

The main functions required for electronically controlled power steering are listed in Table 18.1.

18.1.2 Types of Electronically Controlled Power Steering

Electronically controlled power steering systems presently available commercially can be classified according to their basic structure and basic principles into three types: hydraulic, hybrid, and full electric systems, as shown in Table 18.2. Detailed explanations of these systems are given as follows.

IPR2023-01234
Petitioner - Ex. 2017 - Page 395

TABLE 18.1 Functions Required for Electronically Controlled Power Steering

Reduction of driver's burden when turning the steering wheel and improvement in the steering feel	• Reduction in steering effort • Smoothness of steering operation • Feedback of appropriate steering reaction forces • Reduction of kickback[1] • Improvement in convergence[2] • Creation of other new functions
Power saving	
Failsafe	• Maintaining of manual steering function in the event of any malfunctions

TABLE 18.2 Classification of Electronically Controlled Power Steering System

Basic structure	Control method	Control objects	Sensors				Actuator	Major effects	
			Vehicle speed	Steering torque	Angular velocity	Current		Steering force responsive to vehicle speed	Power saving
Electronically controlled hydraulic system	Flow	Flow supply to power cylinder	O			O	Solenoid	O	O
	Cylinder bypass	Effective actuation pressure given to cylinder	O			O	Solenoid	O	
	Valve characteristics	Pressure generated at control value	O			O	Solenoid	O	
	Hydraulic reaction force control	Pressure acting on the hydraulic reaction force mechanism	O			O	Solenoid	O	
Hybrid system	Flow	Flow supply to power cylinder	O		O	O	Motor	O	O
Full electric system	Current	Motor torque	O	O		O	Motor	O	O
	Voltage	Motor power	O	O	O	O	Motor	O	O

18.1.3 Explanations of Each System

Electronically Controlled Hydraulic System. This system consists of a linear solenoid valve, a vehicle speed sensor, and other electronic devices located in part of the hydraulic circuit of the hydraulic system. The opening of the solenoid valve is controlled based on signals from the vehicle speed sensor. The flow and pressure of the hydraulic fluid is controlled by means of the opening of the solenoid valve.

The assist rate is smoothly and continuously varied in response to the vehicle speed, so that when the vehicle is stationary, the opening of the solenoid valve is small to ensure that the steering effort is appropriately light. When the vehicle is moving at high speed, the opening of the solenoid valve is large to ensure that the steering effort is appropriately heavy.

Flow Control Method. In this method, a solenoid valve is located at the pump discharge port as shown in Fig. 18.1. The electronic control device regulates the solenoid valve opening at high vehicle speeds to reduce the pump discharge volume, thus increasing the required steering effort. By reducing the resistance of the circuit between the pump and the power cylinder, power requirements are reduced. Figure 18.2 shows the position of the solenoid

IPR2023-01234
Petitioner - Ex. 2017 - Page 396

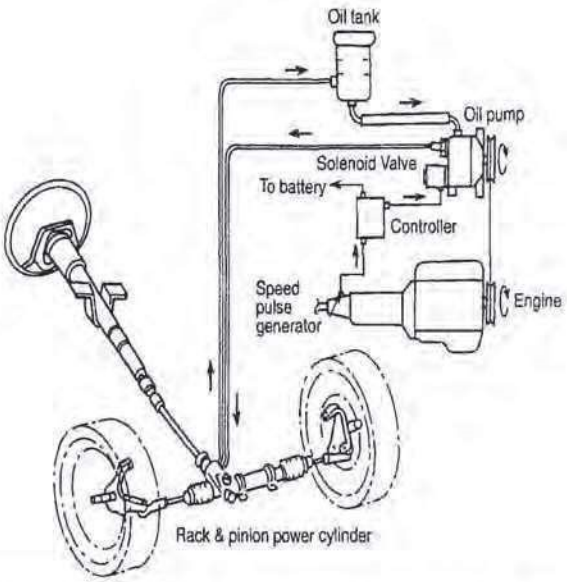
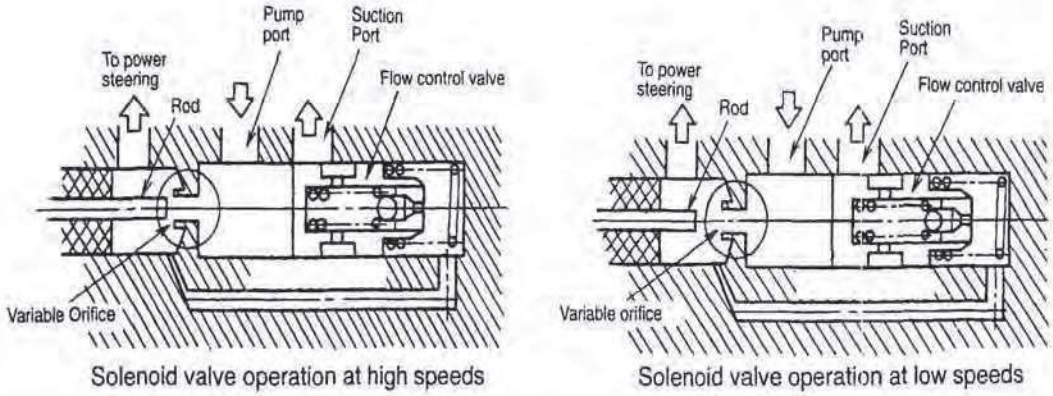


FIGURE 18.1 Vehicle speed-responsive pump discharge flow volume control type.[1]



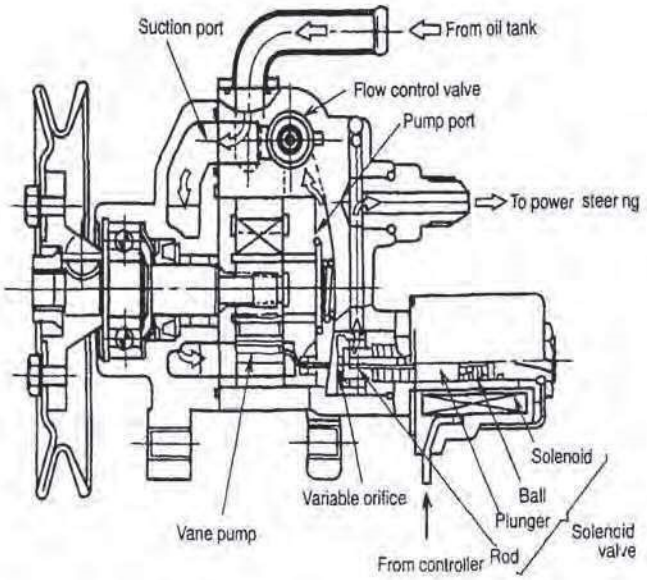


FIGURE 18.2 Structure and operation of pump with solenoid valve.[1]

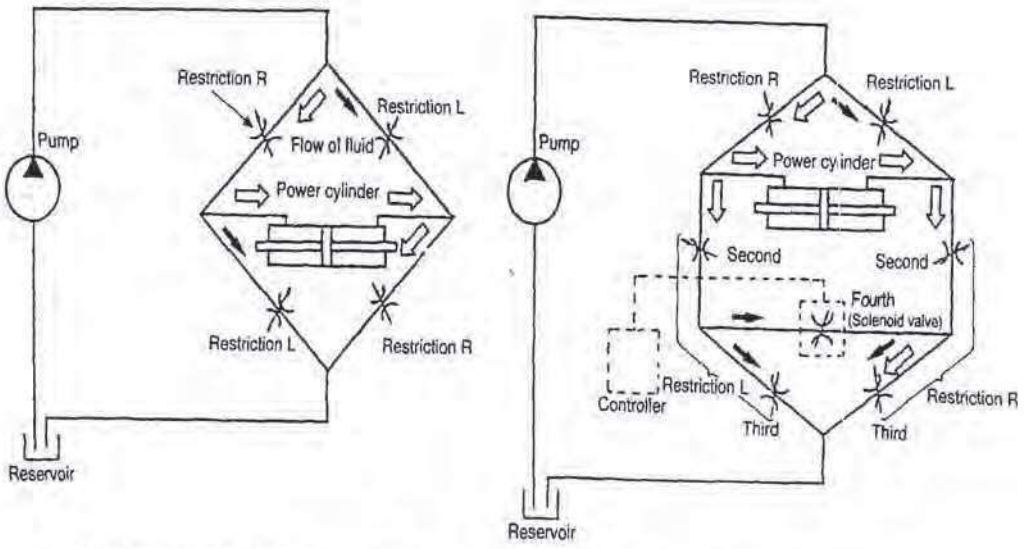
valve at the pump, with separate diagrams showing the operation at high and low vehicle speeds.

The flow of hydraulic fluid to the power cylinder is reduced when driving at high speeds, so that, for this method, the magnitude of the steering response rate and the steering reaction force are balanced at a point of equilibrium.

Cylinder Bypass Control Method. In this method, a solenoid valve and a bypass line are located between both chambers of the power cylinder.[2] The opening of the valve is extended by the electronic control equipment in accordance with increases in vehicle speed, thus reducing the hydraulic pressure in the power cylinder and increasing the steering effort. Like the flow control method, this system may also seek the equilibrium point for the steering response rate and the steering reaction force.

Valve Characteristics Control Method. In this method, the pressure control restrictions of the rotary valve (control valve) mechanism, which control the volume and pressure of the hydraulic fluid supplied to the power cylinder, are divided into second and third parts. A fourth part, controlled by means of the vehicle speed signal, is provided in the hydraulic line between the second and third parts as shown in Fig. 18.3. The structure of this system is shown in Fig. 18.4. The steering effort is controlled by carrying out variable control of the fourth part to vary the assist ratio. Because the structure is simple and the flow from the pump to the cylinder is supplied efficiently without waste, this system exhibits a good response rate. Figure 18.5 shows the hydraulic pressure characteristics in the valve characteristics control method with the driving current of the solenoid valve in accordance to the vehicle speed control signal as a parameter. When the current is 0.3 A, the valve is fully open, and this represents the high-speed driving condition.

Hydraulic Reaction Force Control Method. In this method, the steering effort is controlled by means of a hydraulic reaction force mechanism, which is located at the rotary valve (control valve). A hydraulic reaction force control valve increases the hydraulic pressure (reaction pressure) introduced into the hydraulic reaction force chamber in accordance with increases in the vehicle speed. The rigidity of the reaction force mechanism (equivalent spring constant) is variably controlled so as to directly control the steering effort.



Bridge circuit for conventional power steering

Bridge circuit for electronically-controlled power steering

FIGURE 18.3 Closing bridge circuit for control valve.[2]

IPR2023-01234
Petitioner - Ex. 2017 - Page 398

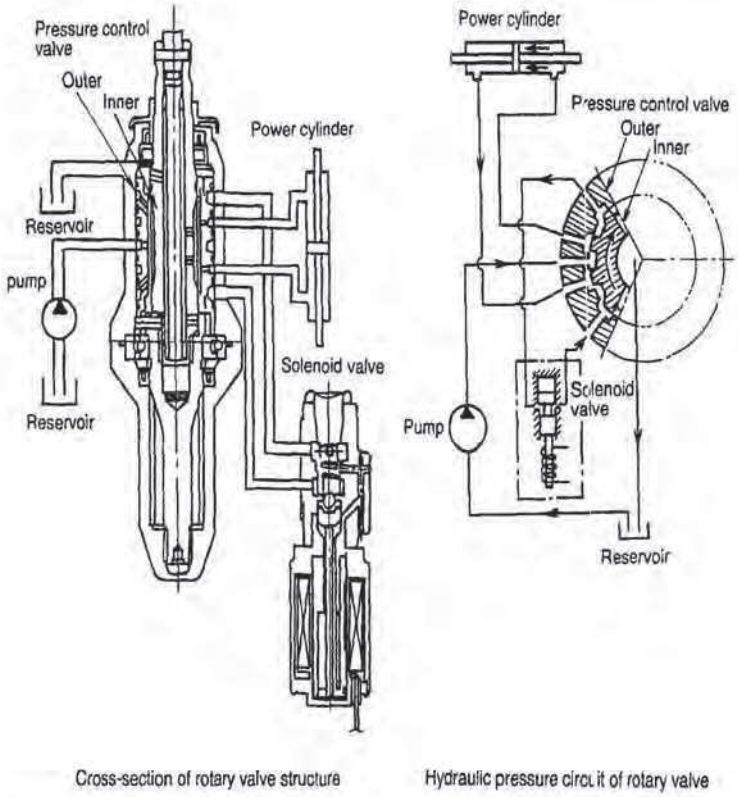


FIGURE 18.4 Valve characteristics control method.[1]

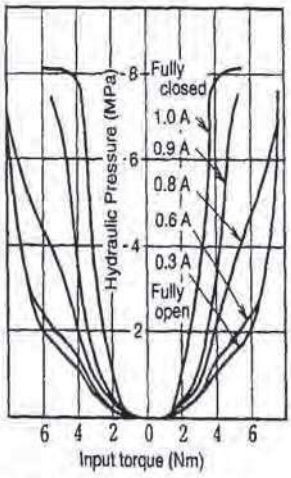


FIGURE 18.5 Valve characteristics in response to vehicle speed.[1]

This method requires the inclusion of a reaction force mechanism, which makes the structure of the control valve more complex, which in turn increases the cost. However, because the rigidity of the reaction force mechanism increases in accordance with increases in the vehicle speed, there is no vagueness in the steering feel in the area around the straightforward steering position. Because this method assigns the steering reaction force irrespective of the volume of hydraulic fluid supplied to the power cylinder, the magnitude of the steering reaction force can be set freely without the need to sacrifice any of the steering response rate.

IPR2023-01234
Petitioner - Ex. 2017 - Page 399

18.1.4 Hybrid Systems

Hybrid systems utilize a flow control method in which the hydraulic power steering pump is driven by an electric motor. The steering effort is controlled by controlling the rotating speed of the pump (discharge flow).

The drive efficiency of the generator and motor are low compared to that of the hydraulic pump, which is driven by the vehicle engine. But because any residual flow is not discharged, the power loss is lower than that of the engine pump when driving at high speeds.

Because the pump is not driven by the vehicle engine, there is also a large degree of freedom in the selection of the mounting location for the pump.

Driving Mode Responsive Method. In this method, the control system consists of a vehicle speed sensor, steering angular velocity sensor, an electronic control unit, and a motor driven hydraulic pump, as shown in Fig. 18.6.

As is shown in Fig. 18.7, the driving conditions (such as driving in urban areas, country areas, winding regions, or highways) are automatically judged, and the pump flow rate is controlled in accordance with this condition in order to provide the appropriate steering effort for the driving conditions. Fine control adjustments are achieved by means of this method as compared with vehicle speed-responsive types mentioned previously.

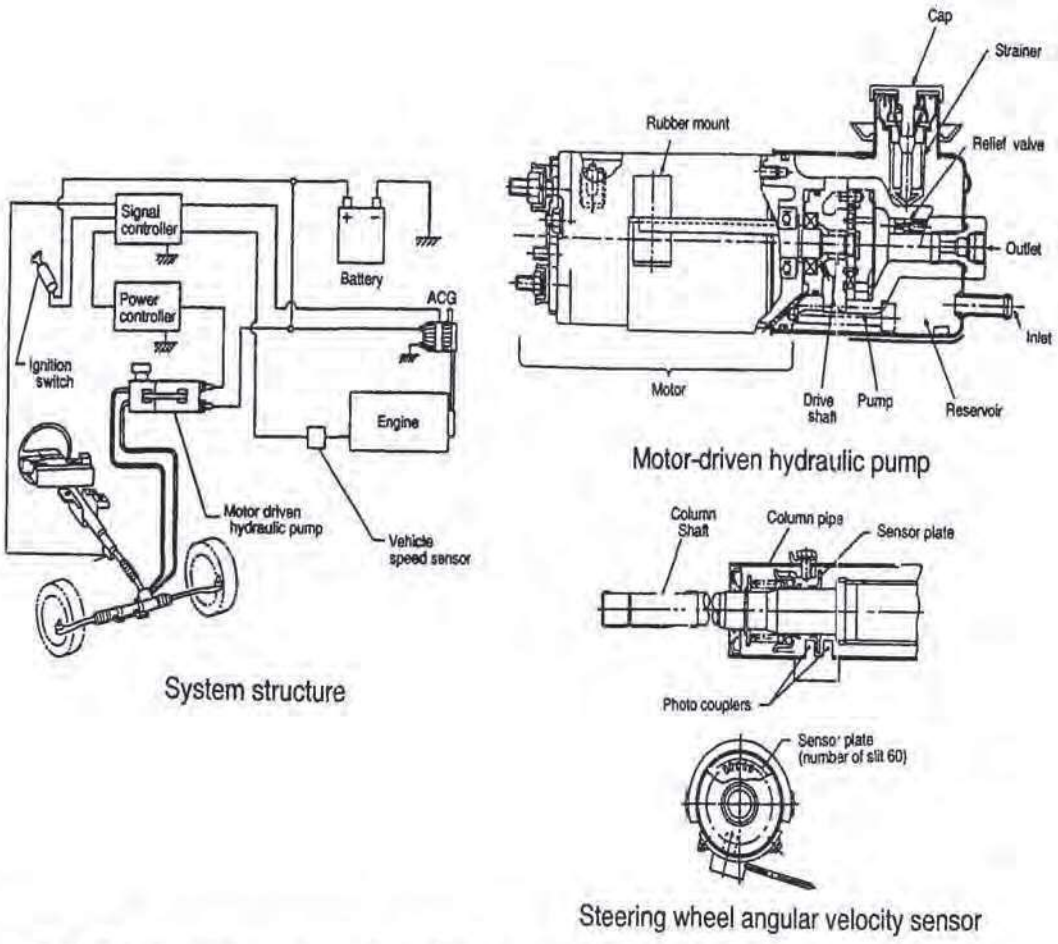


FIGURE 18.6 Driving mode responsive-type hybrid power steering.[3]

IPR2023-01234
Petitioner - Ex. 2017 - Page 400

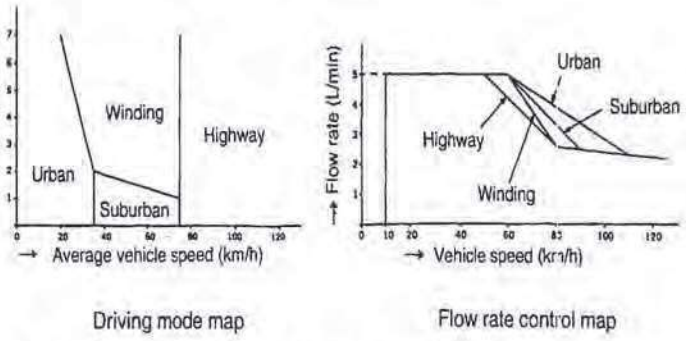


FIGURE 18.7 Driving mode and pump flow rate.[3]

Steering Wheel Speed Responsive Method. For this method, the system consists of components such as a vehicle speed sensor, steering wheel angular velocity sensor, an electronic control unit, and a motor-driven hydraulic pump, as shown in Fig. 18.8. The pump flow volume is controlled in accordance with the angular velocity of the steering wheel and the vehicle speed as shown in Fig. 18.9. As mentioned previously, the discharge flow volume of the pump is reduced and the steering response drops when the vehicle is driven at high speeds. Therefore, in this system, the speed of the motor is increased in accordance with the detected angular velocity of the steering wheel in order to increase the discharge flow volume to solve the problem. Accordingly, losses in power resulting from the circulation of residual flow within the system are kept to the minimum possible level, and the magnitude of the reaction force can be controlled freely without sacrificing any of the steering response rate.

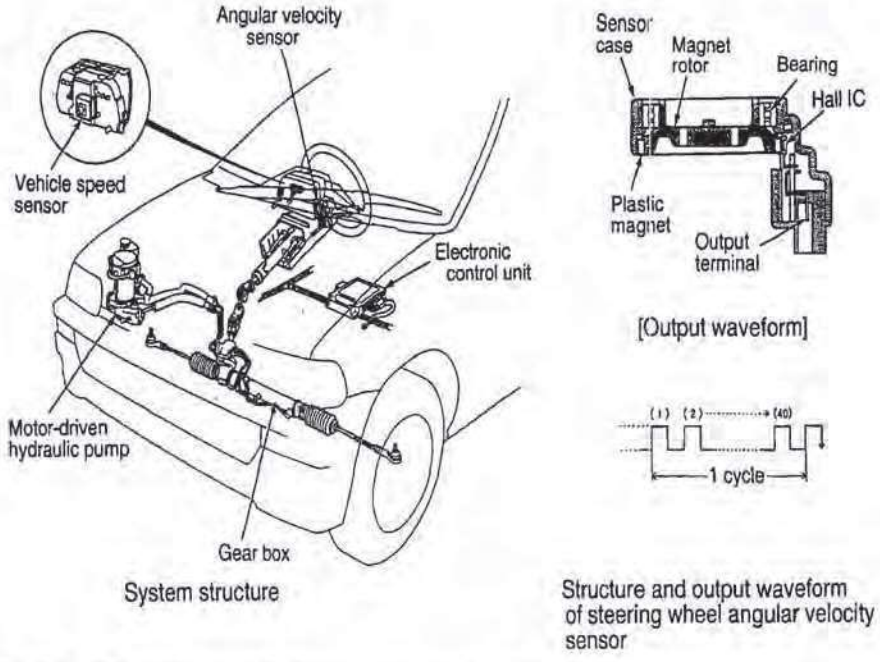


FIGURE 18.8 Steering speed-responsive-type hybrid power steering.[4]

IPR2023-01234
Petitioner - Ex. 2017 - Page 401

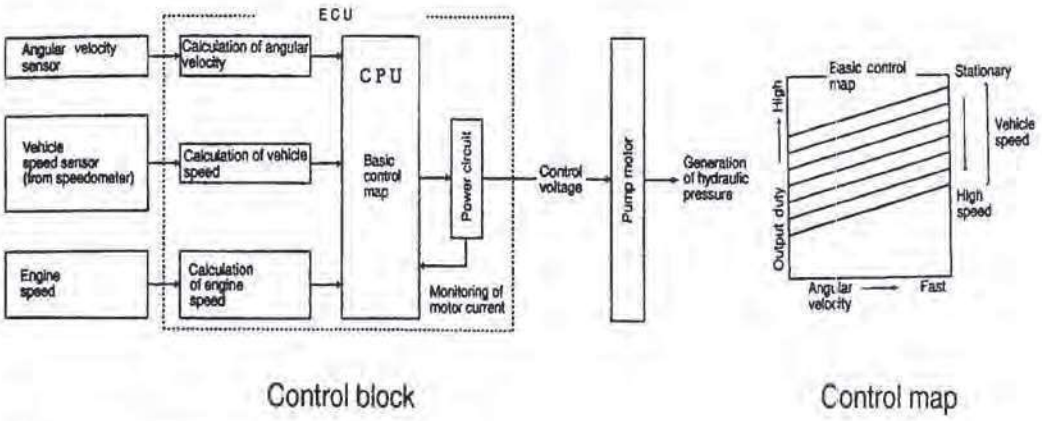


FIGURE 18.9 Basic control.[4]

18.1.5 Electric Power Steering

Electric power steering (EPS) is a fully electric system, which reduces the amount of steering effort by directly applying the output from an electric motor to the steering system. This system consists of vehicle speed sensors, a steering sensor (torque, angular velocity), an electronic control unit, a drive unit, and a motor, as shown in Fig. 18.10. Signal outputs from each sensor are input to the electronic control unit, where the necessary steering assistance is calculated and applied by the drive unit to control the operation of the motor.

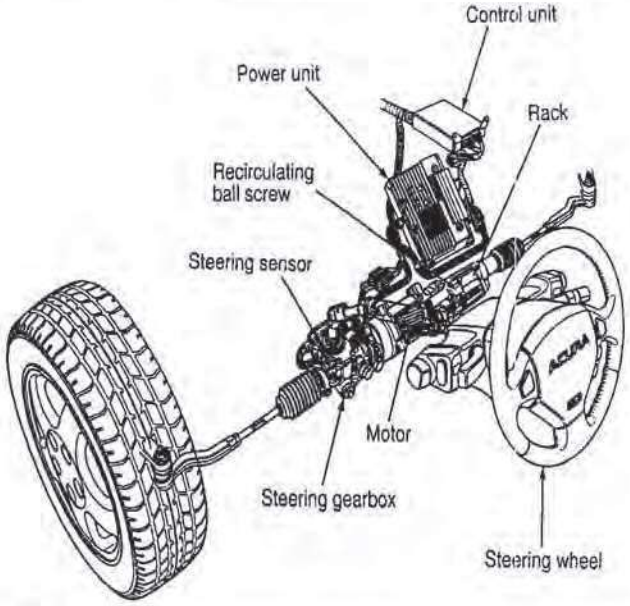


FIGURE 18.10 Structure of EPS System[5] (rack assist-type ball screw drive).

Because the motor output is controlled directly in this system, the setting range for the steering effort is large, and also because it is possible to supply only the amount of power that is necessary when the steering wheel is turned, a large reduction in power requirements can be effectively achieved with no power losses. This means, in contrast to hydraulic systems, that it is not necessary for the pump to keep operating continuously when the steering wheel is not being turned.

IPR2023-01234
Petitioner - Ex. 2017 - Page 402

TABLE 18.3 Classification of Motor Drive Mechanism in EPS

Method	Motor drive method	Power transmission mechanism	Figure
Pinion assist	Column shaft drive	Motor→worm gear→column shaft→pinion shaft	18.11
	Pinion shaft drive	Motor→gear train→pinion shaft	18.12
Rack assist	Another shaft pinion drive	Motor→planetary gear train→another shaft pinion→rack shaft	
	Ball screw drive	Motor→ball screw→rack shaft	18.10

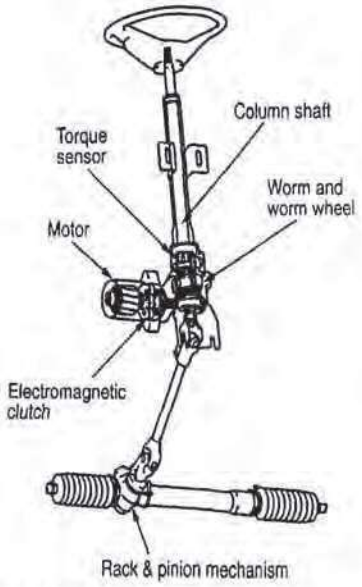


FIGURE 18.11 Column shaft drive method.[1]

In rack-and-pinion steering mechanisms, the EPS system applies the motor power to the pinion gear shaft or to the rack shaft. Several reduction gears are incorporated to amplify the torque of the motor. This system can be classified according to the drive method as given in Table 18.3 and Figs. 18.10 to 18.12. The maximum amount of assist, the smoothness of the steering feel, and the degree of noise occurring during steering are, by and large, determined by the power transmission systems in this table. In general, it is possible to obtain a greater amount of assist from the rack assist method than from the pinion assist method, and the rack assist method is optimal for vehicles in which the front axle load is high.

Details of the respective sensors, controls, and the results achieved thereby are given as follows under common headings.

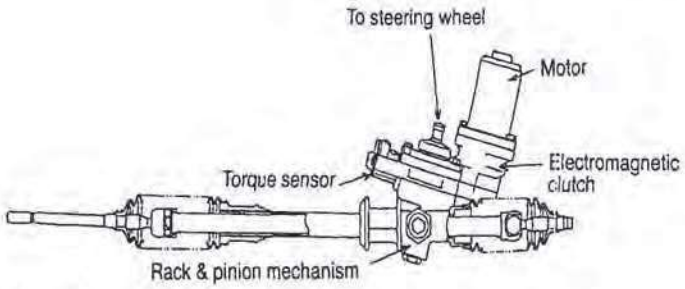


FIGURE 18.12 Pinion shaft drive method.[1]

Sensors. The EPS system utilizes a variety of sensors to control the motor. These sensors include a torque sensor, which detects the steering effort of the steering wheel; a steering wheel angular velocity sensor, which detects the angular velocity of the steering wheel; a battery sensor, which detects the battery voltage; a current sensor, which detects the motor current and the battery current; and a vehicle speed sensor. Of these sensors, the torque sensor and the steering wheel angular velocity sensor, which form the core of the EPS system, are described as follows. (Also see Chap. 3.)

Torque Sensor. The pinion shaft in the rack-and-pinion steering mechanism is divided into two sections of input shaft and pinion gear. The torque sensor comprises a torsion bar

IPR2023-01234
Petitioner - Ex. 2017 - Page 403

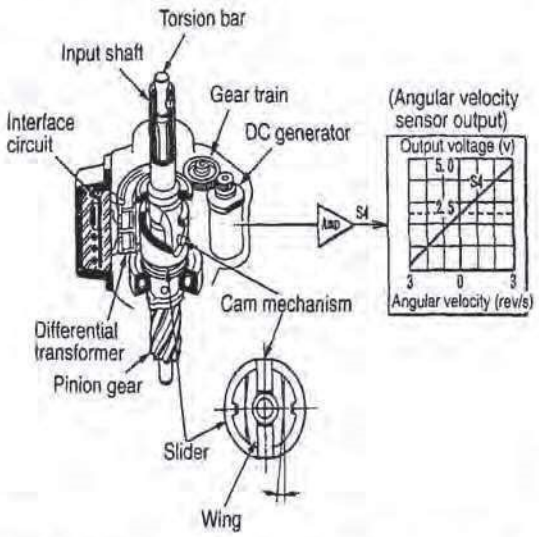


FIGURE 18.13 Torque sensor and angular velocity sensor.[5]

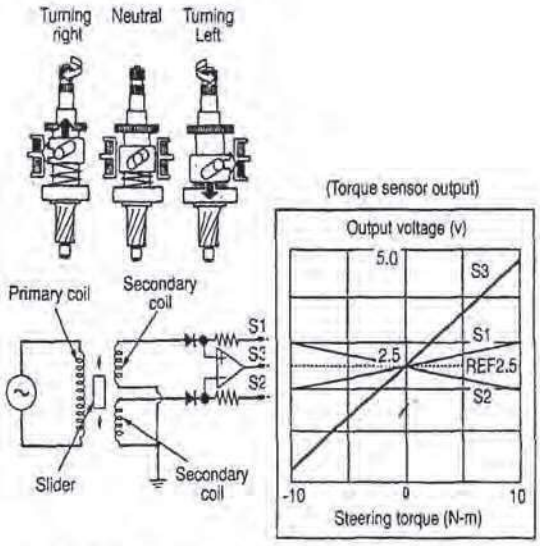


FIGURE 18.14 Diagram of torque sensor operation.[5]

that connects the two sections, a slider with a movable iron core, a cam mechanism that converts the twist torque of both sections of the shaft into an axial direction displacement, and a differential transformer that converts the axial direction displacement of the slider into an electric signal.

The structure is shown in Fig. 18.13. Figure 18.14 shows examples of the detection of the magnitude and direction of the slider displacement. Signal S3 is the output signal of torque and S1 and S2 are outputs for diagnosis use. The differential transformer-type torque sensor has a dual electric structure to provide differential outputs, so that a high sensing accuracy and good temperature characteristics can be obtained, and detection of failure can also be made accurately.

In addition to this type of torque sensor, there are other torque sensors that use a potentiometer instead of a differential transformer, and also types in which the relative displacement in the turning direction is measured in a noncontact manner using a coil, without there being a mechanically movable part such as the slider.

Angular Velocity Sensor. The angular velocity sensor consists of a gear train, which is located around the input shaft, and a dc generator, which is driven at an increase of speed by this gear train. The structure is shown in Fig. 18.13. The turning direction and angular velocity of the steering wheel are detected by the turning direction and angular velocity of this dc generator. Signal S4 indicates the output from the steering wheel angular velocity sensor.

Electronic Control Unit (ECU). The ECU consists of an interface circuit that coordinates the signals from the various sensors, an A/D converter and a PWM unit that are all built into an 8-bit one-chip microprocessor, a watchdog timer (WDT) circuit that monitors the operation of this microprocessor, and a PWM drive circuit that drives the power unit mentioned previously. The ECU conducts a search for data according to a table lookup method based on the signals input from each sensor and carries out a prescribed calculation using this data to obtain the assist force.

In addition, trouble diagnosis for the sensors and the microprocessor is also carried out. When a problem is detected, power to the motor is interrupted, an indicator lamp illuminates, and the problem condition is memorized. Then this problem mode flashes on a display as necessary.

Power Unit. The power unit comprises a power MOSFET (metal oxide semiconductor field effect transistor) bridge circuit which drives the motor in a forward or reverse direction, a drive circuit which controls the respective power MOSFET of this power MOSFET bridge circuit, a current sensor, and a relay which turns the motor current ON and OFF.

IPR2023-01234
Petitioner - Ex. 2017 - Page 404

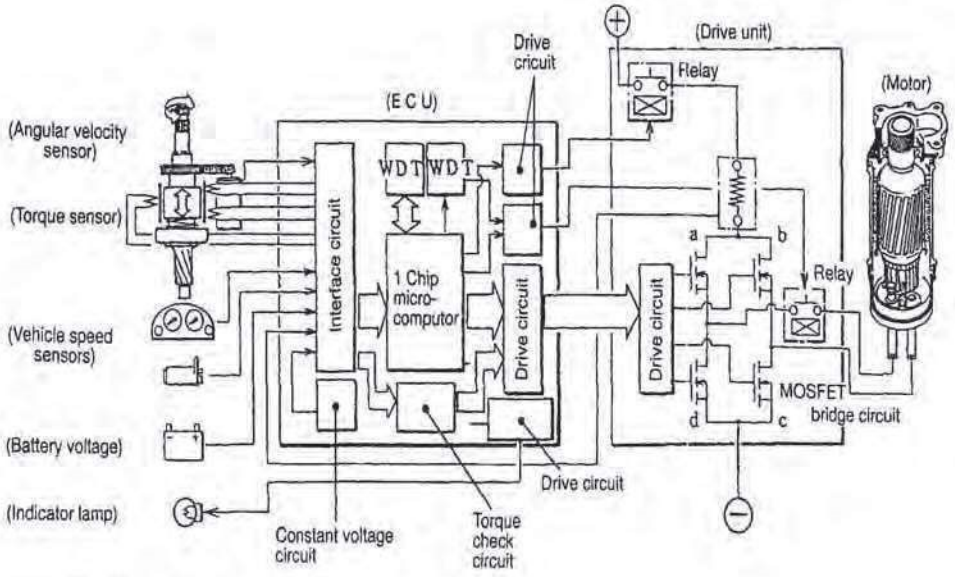


FIGURE 18.15 ECU and drive unit.[6]

The structure is shown in Fig. 18.15. The motor is driven based on instructions from the ECU. The current at this time is monitored by the ECU, and the power supplied to the motor is interrupted in the event of an abnormality.

Depending on the magnitude of the current, some systems are provided with an integrated ECU and power unit, while other systems have each section separate.

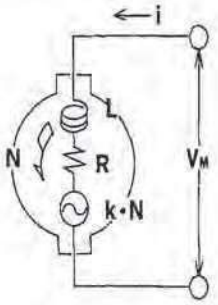


FIGURE 18.16 Motor equivalent circuit.[6]

Motor Control Methods. In the equivalent circuit of the motor, which is shown in Fig. 18.16, the relationship between the terminal voltage V_M, the impedance L, the resistance R, the induced voltage constant k, the revolution speed N, the current i, and the time t, is expressed by the following equation:

$$V_M = L(di/dt) + R \cdot i + k \cdot N \quad (18.1)$$

$$\doteqdot R \cdot i + k \cdot N \quad (18.2)$$

And it is known that the current **i** is proportional to the motor torque T_M.

As can be understood from Eq. (18.2), there are two control methods. In the motor current control method (refer to Fig. 18.17), the target motor current I_T, which is proportional to the motor assist torque T_M, is determined from the signal output T from the torque sensor, and control is performed so that there is no difference between this target current value I_T and the value detected through feedback from the current sensor I_M.

In the motor voltage control method (refer to Fig. 18.18), the motor voltage component ($V_{M1} = R \cdot i = k_T \cdot T_M$; k_T is a proportional constant) which corresponds to the motor assist torque as calculated from the output signal T from the torque sensor, and the motor voltage component ($V_{M2} = k \cdot N$) which corresponds to the motor speed as calculated from the output signal $\dot{\theta}_1$ from the steering wheel angular velocity sensor. These two voltage components are then added and output.

Current Control Method. In this method, the target value for the motor current, which corresponds to the motor assist torque, is set so that it is equal to the vehicle speed response type derived from the signal of the vehicle speed sensor.

IPR2023-01234
Petitioner - Ex. 2017 - Page 405

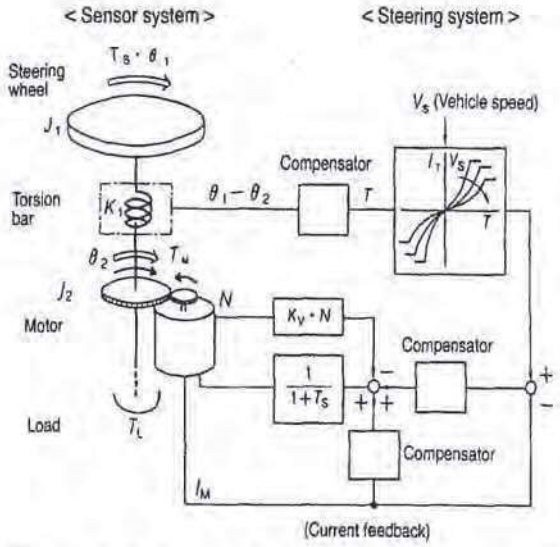


FIGURE 18.17 Diagram of principle of motor current control method.[7]

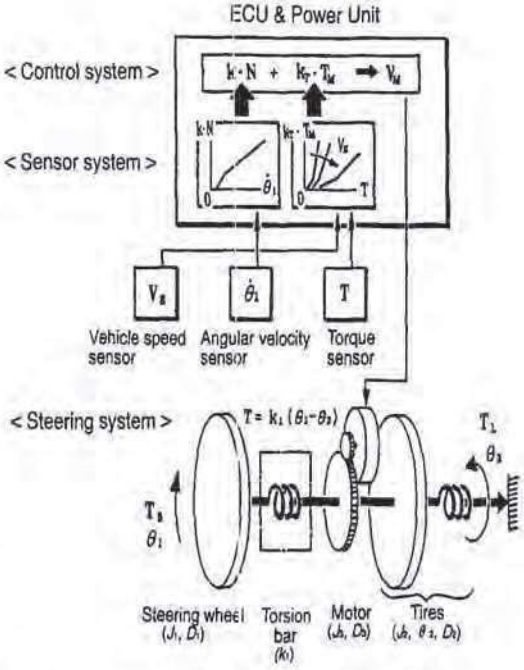


FIGURE 18.18 Diagram of principle of motor voltage control method.[8]

Voltage Control Method. In this method, both the motor torque and the motor speed can be controlled by the output from the torque sensor and the steering wheel angular velocity sensor. When the vehicle is traveling at low speeds, *normal control* is carried out. With this control, the value for $(R \cdot i + k \cdot N)$ in Eq. (18.2) is output to the motor to obtain a good motor response rate (steering response rate) and thus provide a comfortable steering performance. When the vehicle is traveling at high speeds, it is possible to carry out two types of control. In the first method, *return control,* the value for $(k \cdot N)$ is made smaller so that a damping torque which is proportional to the motor speed is generated. In the second method, *damper control,* motor torque is generated in the opposite direction of motor rotation with $V = 0$ when the steering wheel is released in turning.

Normal Control. This is a method of drive control for steering with a reduced steering effort and a good steering response rate. As is shown in Table 18.4, when the steering wheel is turned to the right, FET (a) is ON at the same time that FET (c) is carrying out PWM drive, and current flows to the FET bridge circuit as shown in Fig. 18.19 based on the value of V_M in Eq. (18.2). If the angular velocity of the steering wheel increases, the PWM duty also increases.

An example of the steering characteristics in an actual vehicle can be seen in Fig. 18.20. Figure 18.20*a* represents the assist characteristics during stationary swing, with the dotted line representing the steering characteristics when no assist force is provided. Figure 18.20*b* is the steering response rate; Fig. 18.20*c* is the steering characteristics corresponding to the vehicle speed; and Fig. 18.20*d* is the steering characteristics relative to the lateral acceleration of the vehicle.

TABLE 18.4 FET Drive During Normal Control[5]

Steering condition	FET (a)	FET (b)	FET (c)	FET (d)	Motor operation
Steering to right	ON	OFF	PWM	OFF	Operates in direction steering to the right
Straight ahead	OFF	OFF	OFF	OFF	Stops
Steering to left	OFF	ON	OFF	PWM	Operates in direction steering to the left

IPR2023-01234
Petitioner - Ex. 2017 - Page 406

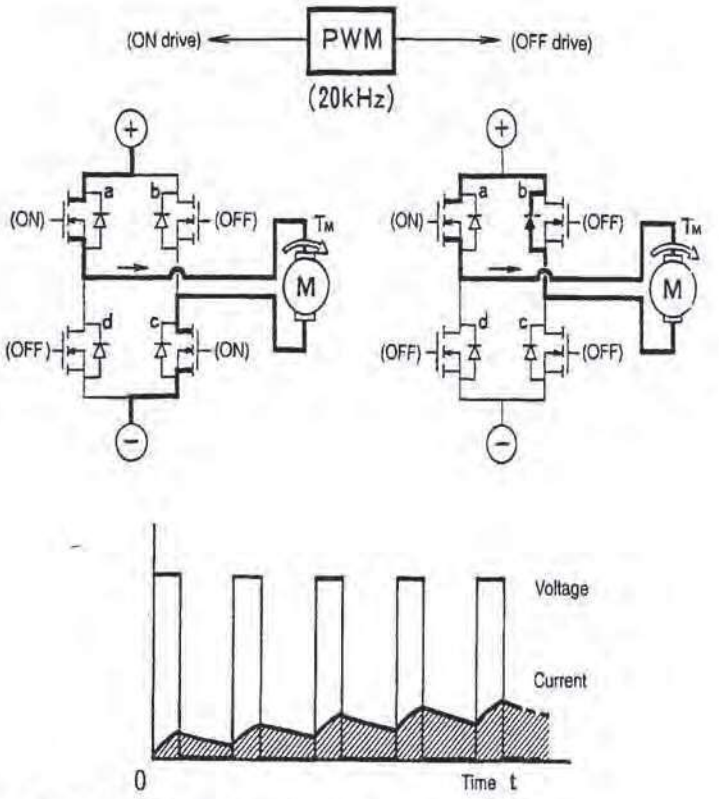


FIGURE 18.19 Diagram of bridge circuit operation.[6]

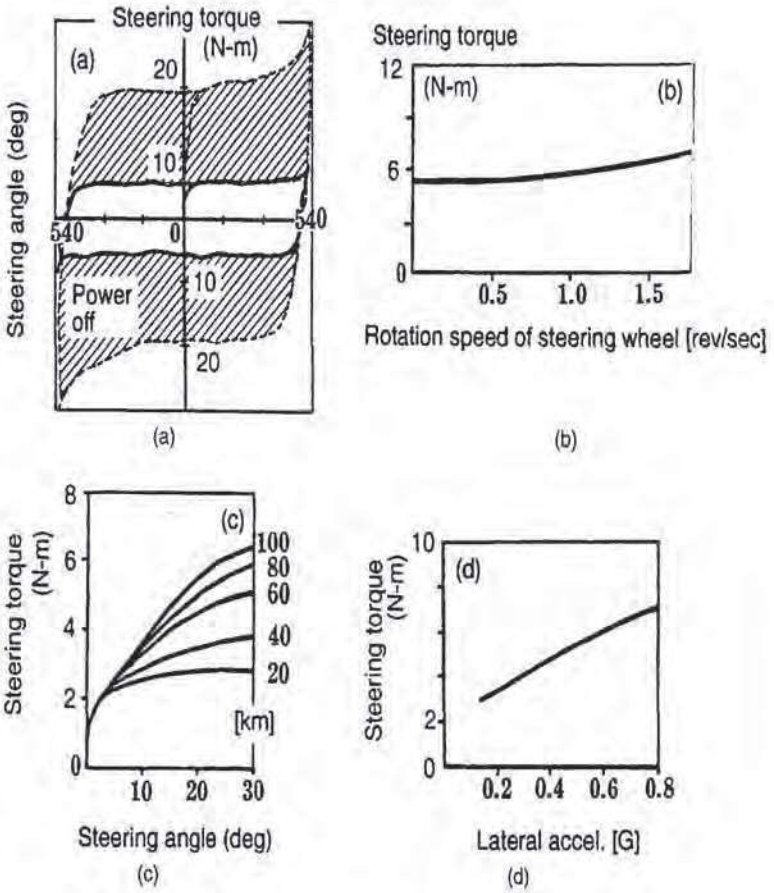


FIGURE 18.20 Steering characteristics.[8]

Return Control. This method of drive control is for varying the steering wheel return characteristics. When the driver is returning the steering wheel to the neutral position at low-speed driving, the motor current is immediately reduced in order to make the motor operate in the reverse direction to the torque generating directions. As a result, a good returnability of the steering wheel should be obtained. At high-speed driving, motor current is gradually reduced in order to suppress returnability and obtain more stable steering characteristics.

As shown in Table 18.5, when the steering wheel returns to the straightforward position after being turned to the right, FET (a) carries out PWM-r drive based on the signals from the steering wheel angular velocity sensor, and, at the same time, FET (c) also carries out PWM drive based on the signals from the torque sensor.

TABLE 18.5 FET Drive During Return Control[5]

Steering condition	FET (a)	FET (b)	FET (c)	FET (d)
Return from right steering to straight ahead	PWM-r	OFF	PWM	OFF
Return from left steering to straight ahead	OFF	PWM-r	OFF	PWM

The results obtained by means of this return control are shown in Fig. 18.21. Figure 18.21*a* represents the steering characteristics when return control is not applied, and Fig. 18.21*b* represents the steering characteristics when return control is operating. The hysteresis is greater and the returnability is weaker than in Fig. 18.21*a*.

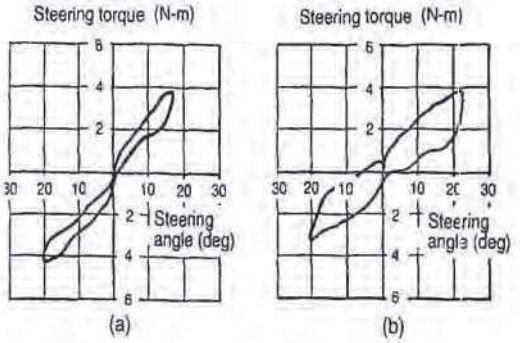


FIGURE 18.21 Comparison of steering wheel return characteristics.[6]

Damper Control. This method of drive control is for improving the convergence of the steering wheel when the vehicle is traveling at high speeds and for eliminating wandering of the steering wheel caused by the tire inputs.

As shown in Fig. 18.22, when the motor terminals are shorted, it is possible to generate motor torque in the reverse direction in proportion to the speed of the motor as is shown by the equation in Fig. 18.22, and this characteristic is utilized for control. Figure 18.23 shows the results of the application of damper control during a convergence test carried out at a vehicle speed of 120 km/h.

18.1.6 Power-Saving Effectiveness

Because the EPS system is a "power-on-demand" system, which supplies only the necessary amount of power at the necessary time, almost no power losses occur when the steering wheel is not being turned. Because of this, the system has extremely high fuel efficiency. Table 18.6 shows the results of measurements of fuel consumption during different driving modes to compare EPS with the hydraulic system. The LA-4 mode corresponds to urban road driving.

IPR2023-01234
Petitioner - Ex. 2017 - Page 408

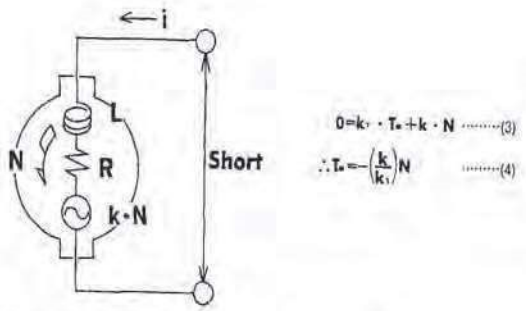


FIGURE 18.22 Principle of damper control.

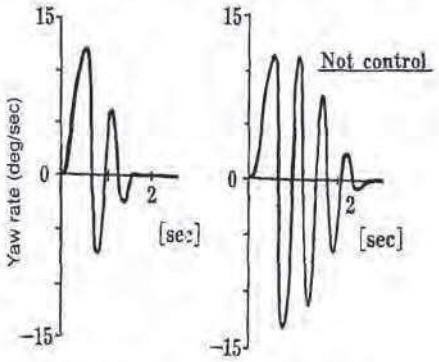


FIGURE 18.23 Effect of damper control.

18.1.7 Trends in Research and Development

The demands for faster speed, higher quality, and reduced power requirements in vehicles is continually increasing. In order to respond to these demands, research and development is under way on the application of electronic control systems with the aim of further improving functions and performance. Features that are being proposed include the introduction of fuzzy logic and the application of power steering, which responds to the driving environment by varying the assist amount in accordance with the traffic conditions or the road surface conditions in order to provide steering feel to fit the sensitivities of human operators. The most important of these is probably active reaction power steering, which provides feedback to the driver regarding the behavior of the vehicle in the form of steering reaction force. Such a system provides the driver with information regarding the operating conditions of the vehicle, for instance, the yaw velocity and/or lateral acceleration, as steering reaction forces. Not only would it improve the relationship between the driver and the vehicle to make it possible to achieve a steering feel that better suits the sensitivities of the driver, but a function that automatically compensates for irregularities in vehicle behavior caused by disturbances could also be expected.

Figure 18.24 is a system control block diagram in which the yaw rate is fed back as a steering reaction force.

Figure 18.25 shows an example of the effect of suppressing irregularities in vehicle behavior caused by side disturbances by comparing the amount of lateral removal when braking on a rut of road surface with the case for conventional power steering.

18.2 FOUR-WHEEL STEERING SYSTEMS (4WS)

For vehicles with extremely long wheel bases and vehicles which need to be operated in narrow places, the concept of a four-wheel steering system is attractive. In such systems, the rear wheels are turned in the opposite direction to the steering direction of the front wheels in

TABLE 18.6 Measurement Results on Mode Fuel Consumption[6]

			Improvement in fuel consumption	
Mode	EPS (mpg)	Hydraulic power steering (mpg)	Fuel consumption difference (mpg)	Improved rate (%)
LA-4	20.51	20.01	0.80	2.50
Highway	28.88	28.18	1.14	2.52

IPR2023-01234
Petitioner - Ex. 2017 - Page 409

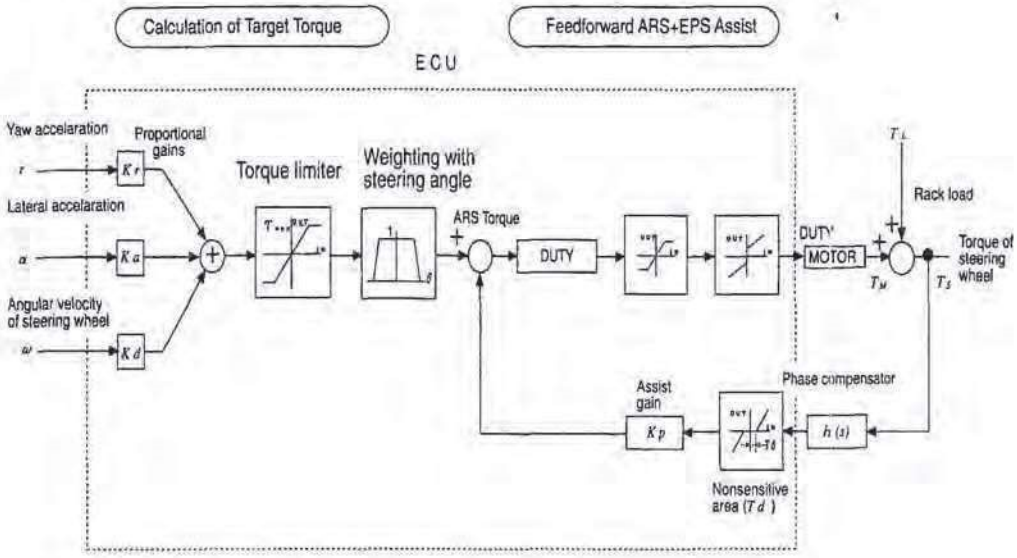


FIGURE 18.24 Block diagram of active reaction control.

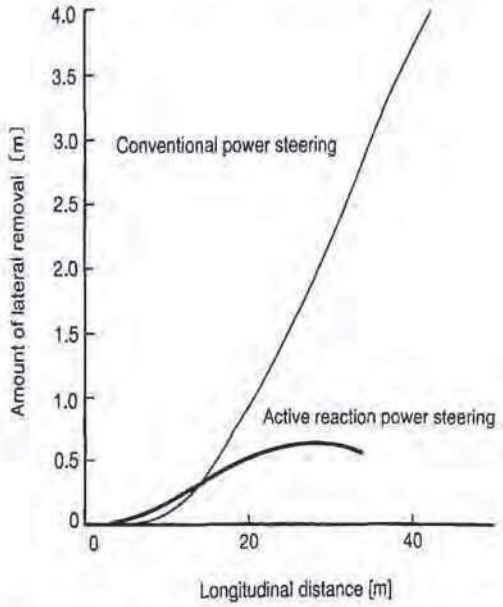


FIGURE 18.25 Effect of active reaction power steering.

order to make the turning radius as small as possible and to improve the handling ability. Such 4WS systems have been under development for some time. However, the concept of the system being used in passenger vehicles for the purpose of improving vehicle stability and steering response at medium to high speeds is relatively new.

A 4WS system for passenger cars has the following two aims:

- Reducing the turning motion (yawing) of the vehicle by steering the rear wheels in the same direction as the front wheels, thus improving the vehicle stability at high speeds
- Improving the steering response at medium speeds, while at the same time reducing the turning circle radius at low speed, by steering the rear wheels in the opposite direction to the front wheels

IPR2023-01234
Petitioner - Ex. 2017 - Page 410

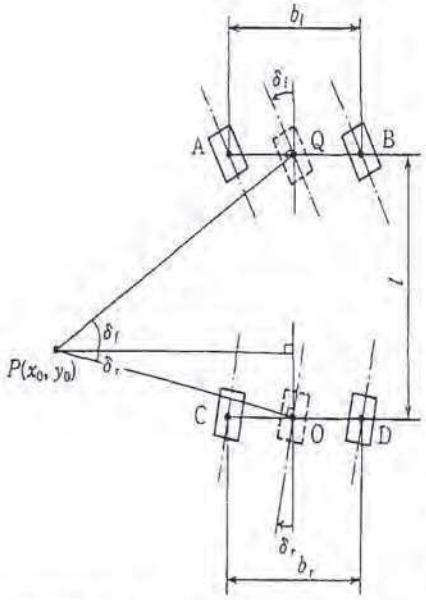


FIGURE 18.26 Half vehicle model of 4WS.[1]

18.2.1 Basic Principles of 4WS

Shortening the Minimum Turning Radius. As shown in Fig. 18.26, provided the origin point of the coordinate is set at the center of the rear tread, the coordinates of the turning center of the vehicle $P(X_0, Y_0)^v$ when the rear wheels are turned in the opposite direction from the front wheels are given in the following equations:

$$x_0 = \iota / (\tan\delta_f + \tan\delta_r) \tag{18.3}$$

$$y_0 = \iota\,(\iota \cdot \tan\delta_1) / (\tan\delta_f + \tan\delta_r) \tag{18.4}$$

And, if the turning radius for the front outer wheel is R and the difference between the turning radius of the front and rear outer wheels is ΔR, then:

$$R = \overline{BP} = \sqrt{\left(\frac{b_f}{2} + X_0\right)^2 + (\iota - y_0)^2} \cdot \sqrt{\left(\frac{b_f}{2} + \frac{\iota}{\tan\delta_f + \tan\delta_r}\right)^2 + \left(\frac{\iota \cdot \tan\delta_f}{\tan\delta_f + \tan\delta_r}\right)^2} \tag{18.5}$$

$$\Delta R = \overline{AP} - \overline{CP}$$

$$= \sqrt{\left(-\frac{b_f}{2} + X_0\right)^2 + (\iota - y_0)^2} - \sqrt{\left(-\frac{b_r}{2} + X_0\right)^2 + y_0^2}$$

$$= \sqrt{\left(-\frac{b_f}{2} + \frac{\iota}{\tan\delta_f + \tan\delta_r}\right)^2 + \left(\frac{\iota \cdot \tan\delta_f}{\tan\delta_f + \tan\delta_r}\right)^2}$$

$$- \sqrt{\left(-\frac{b_r}{2} + \frac{\iota}{\tan\delta_f + \tan\delta_r}\right)^2 + \left(\frac{\iota \cdot \tan\delta_f}{\tan\delta_f + \tan\delta_r}\right)^2} \tag{18.6}$$

In these equations, δ_f is the front wheel steering angle (average of left and right wheels), δ_r is the rear wheel steering angle (average of left and right wheels), b_f is the tread of the front wheels, b_r is the tread of the rear wheels, and ι is the wheelbase.

$$R = \overline{PQ} = \frac{\iota}{\sin\delta_f + \cos\delta_f + \tan\delta_f} \tag{18.7}$$

$$\Delta R = \overline{PQ} - \overline{PO} \tag{18.8}$$

$$= \frac{\iota}{\sin\delta_f + \cos\delta_f + \tan\delta_f}$$

$$- \frac{\iota}{\sin\delta_f + \cos\delta_f + \tan\delta_f}$$

IPR2023-01234
Petitioner - Ex. 2017 - Page 411

It can be seen from Eq. (18.7) that when the rear wheels steer in the opposite direction as the front wheels, the turning radius becomes smaller than when the rear wheels are not steered ($\delta_r = 0$). In addition, it can be seen from Eq. (18.8) that when the steering amount for the front and rear wheels is the same ($\delta_f = \delta_r$), then it becomes possible to obtain a difference of 0 between the turning radius of the front and rear wheels

Improvement in Stability and Maneuverability When Driving at Medium to High Speeds. The steering characteristics in yaw velocity and lateral acceleration of the vehicle with 4WS in which the rear wheels are steered in proportion to the front wheels steering angle in the same direction, are shown in Table 18.7, along with that for a vehicle yaw 2WS system. However, the half-car vehicle model shown in Fig. 18.26 is used as the vehicle model.

From Table 18.7, in a system in which the rear wheels are turned in the same direction as the front wheels, the stability factor K, the damping ratio ζ, and the natural oscillation of yawing ωn are not different from the values for conventional vehicles with 2WS, so that the intrinsic stability of the vehicle will not vary. On the other hand, because the lateral acceleration response delay will become smaller as the coefficients of numerators s and s^2 increase and the steady state gain in the yaw velocity will drop by the proportion to $(1 - k)$, the yawing movement which accompanies the lateral movement of the vehicle will become less and the stability within the range of practical use will be improved. If, however, the rear wheels are steered in the opposite direction to the front wheels, $k < 0$ and so $1 - k > 1$. This means that the steady state gain of the yaw velocity will increase, with the result that the steering response will be improved. The symbols used in Table 18.7 and Fig. 18.27 are explained in Table 18.8.

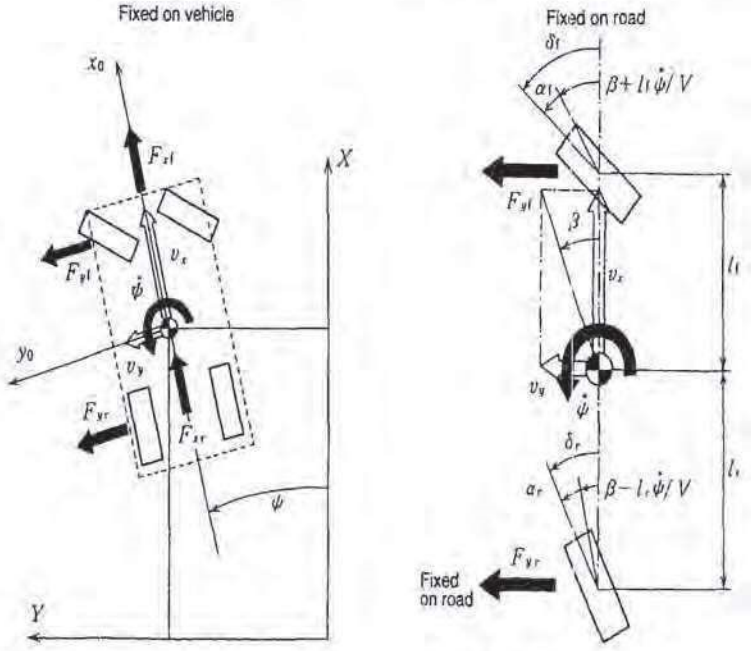


FIGURE 18.27 Coordinates fixed on road and vehicle in half vehicle model.[1]

18.2.2 Classification of 4WS

Four-wheel steering systems that are currently being implemented in vehicles are classified according to their functions and mechanisms. The aims and characteristics of each system are briefly explained in Tables 18.9 and 18.10. Because the fully mechanically controlled system shown in Table 18.10 has a low degree of control freedom, there is less tendency for it to be used. Regardless of its low cost, however, this system provides every basic function of 4WS, so that there is a possibility that it may be used in the future, primarily in smaller vehicles.

IPR2023-01234
Petitioner - Ex. 2017 - Page 412

TABLE 18.7[1]

Symbol	Name	
K	Stability factor (s^2/m^2)	
A	Steady state gain in yaw velocity	(1/s)
B_f, B_r	Steady state gain vehicle side slip angle for front and rear	(s)
T_f, T_r	Time constant for front/rear yaw velocity	(s)
τ_f, τ_r	Time constant for front/rear side slip angle	(s)
ω_n	ω_n : Response frequency	(rad/s)
	$f_n(\omega_n/2\pi)$: Natural frequency	(Hz)
$\zeta \cdot \omega_n$	$\zeta \cdot \omega_n$:	(1/s)
	$\zeta \cdot \omega_n \times V$: Steering capacity	(m/s^2)
	ζ : Damping rate	

	Vehicle with 2WS	Vehicle with 4WS in which the rear steering angle is proportional to front
Stability factor	$\frac{m(l_r K_r - l_f K_f)}{2l^2 K_f K_r} = K$	K
Steady state gain in yaw velocity	$\frac{1}{1+KV^2} \cdot \frac{V}{l}$	$\frac{1}{1+KV^2} \cdot \frac{V}{l}$
Damping rate	$\frac{1}{2} \cdot \frac{(k_f + K_r I_l + (K_f l_f + K_r l_r^2)m}{\sqrt{m I_z K_f K_r l^2 (1+KV^2)}} = \zeta$	ζ
Response frequency	$\frac{2l}{V} \cdot \sqrt{\frac{K_f K_r (1+KV^2)}{I_z m}} = \omega_n$	ω_n
Steering capacity	$\frac{1}{V}\left(\frac{K_f + K_r}{m} + \frac{K_f l_f^2 + K_r l_r^2}{l_z}\right) = \zeta \cdot \omega_x$	$\zeta \cdot \omega_n$
$\frac{\dot{\varphi}}{\delta_H}$	$\frac{1}{i_s} G_\varphi(0) \frac{1+T_f s}{1+\frac{2\zeta}{\omega_n}s+\frac{1}{\omega_n^2}s^2}$ $G\varphi(0) = \frac{1}{1+KV^2} \cdot \frac{V}{l}$	$\frac{1-k}{i_s} G\varphi(0) \frac{1+(1+\lambda\phi)T_f s}{1+\frac{2\zeta}{\omega_n}s+\frac{1}{\omega_n^2}s^2}$ $G\dot{\phi}(0) = \frac{1}{1+KV^2} \cdot \frac{V}{l}$ $\lambda\varphi = \frac{k}{1-k} \cdot \frac{T_f - T_r}{T_f}$
$\frac{\alpha_y}{\delta_H}$	$\frac{1}{i_s} G_{ay}(0) = \frac{1+T_{ay1}s+T_{ay2}s^2}{1+\frac{2\zeta}{\omega_n}s+\frac{1}{\omega_n^2}s^2}$ $G_{ay}(0) = \frac{1}{1+KV^2} \cdot \frac{V^2}{l}$ $T_{ay1} = \frac{l_r}{V}, \quad T_{ay2} = \frac{l_z}{2K_r l}$	$\frac{1-k}{i_s} G_{ay}(0) \cdot \frac{1+(1+\lambda_{ay1})T_{ay1}s+(1+\lambda_{ay2})T_{ay2}s^2}{1+\frac{2\zeta}{\omega_n}s+\frac{1}{\omega_n^2}s^2}$ $G_{ay}(0) = \frac{1}{1+KV^2} \cdot \frac{V^2}{l}$ $\lambda_{ay1} = \frac{k}{1-k} \cdot \frac{T_{ay1} + T'_{ay1}}{T_{ry1}}$ $\lambda_{ay2} = \frac{k}{1-k} \cdot \frac{T_{ay2} + T'_{ay2}}{T_{ry2}}$ $T_{ay1} = \frac{l_r}{V}, \quad T_{ay2} = \frac{l_f}{V}$ $T_{ay2} = \frac{l_z}{2K_r l}, \quad T'_{ay2} = \frac{l_z}{2K_f l}$

IPR2023-01234
Petitioner - Ex. 2017 - Page 413

TABLE 18.8[1]

Symbol	Dimension	Name
m	kg	Mass of the vehicle
I_z	kg · m^2	Moment of the inertia of vehicle
l	m	Wheel base
l_f, l_r	m	Distance between center of gravity and front/rear wheel shaft
V	m/s	Vehicle speed $V = \sqrt{v_x^2 + v_y^2}$
v_x, v_y	m/s	Longitudinal and lateral velocity of the center of gravity
a_x, a_y	m/s^2	Longitudinal and lateral acceleration of the center of gravity
ψ, ϕ	rad	Yaw angle, roll angle
$\dot{\psi}, \dot{\phi}$	rad/s	Yaw velocity roll rate
β	rad	Side slip angle of the center of gravity
δ_f, δ_r	rad	Front/rear wheel steering angle
α_f, α_r	rad	Front/rear side slip angle
K_f, K_r	N/rad	Equivalent cornering power of front/rear
δ_H	rad	Steering wheel angle
i_s	I	Steering ratio in over all

TABLE 18.9[1]

Classification by functions	Aims
Small range of rear steer angle only controlled electronically	Improvement of steering response and vehicle stability in medium to high speed
Not only small range in medium to high speed but large range in low speed of rear steering angle are controlled electronically	In addition to the above, making the minimum turning radius small

TABLE 18.10[1]

Classification by mechanism	Feature
Full mechanical system	Simple mechanism
Electronic-hydraulic system	High degree for control freedom (compact actuator)
Electronic-mechanical-hydraulic system	High degree of freedom (mechanism is not simple)
Full electric system (electronic-electric system)	High degree of control freedom simple mechanism

18.2.3 Introduction to Each System

Fully Mechanical System. This was the first 4WS system used in passenger vehicles. It was adopted in the Honda Prelude in 1987 and in the Honda Accord in 1989. This system is a front-wheel steering angle responsive-type system in which the rear-wheel steering angle is determined wholly by the steering angle of the front wheels. The structure and fabrication of this system are shown in Figs. 18.28 and 18.29.

In rack-and-pinion type steering gearboxes for the front wheels, a rear-wheel steering pinion is provided in order to transmit the steering angle of the front wheels to the rear wheels. The displacement in the steering angle is transmitted to the rear steering gearbox via the center steering shaft. As shown in the figure, the rear steering gearbox consists of a combination of an eccentric shaft and a planetary gear. The input and output characteristics that can be obtained are shown in Fig. 18.30. The result of this is that when the steering angle for the front

IPR2023-01234
Petitioner - Ex. 2017 - Page 414

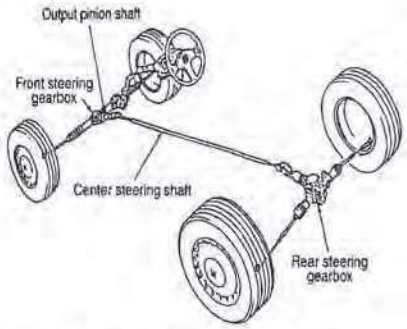


FIGURE 18.28 Fully mechanical 4WS.

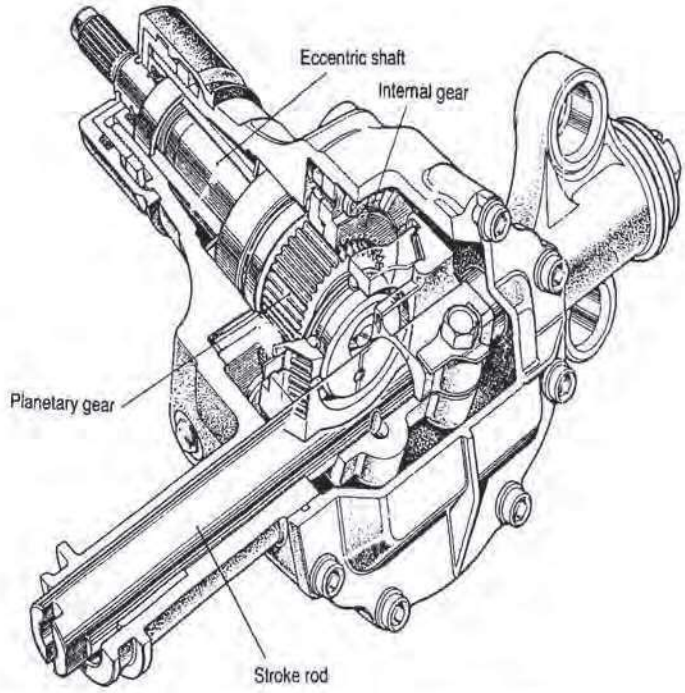


FIGURE 18.29 Rear steering actuator of full mechanical 4WS.

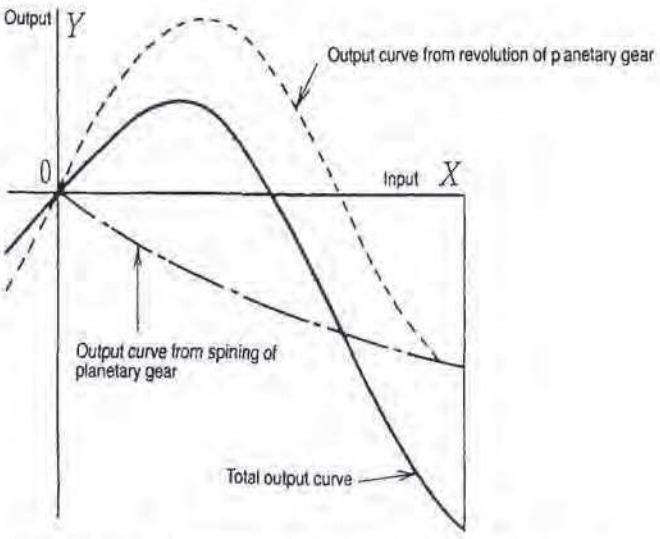


FIGURE 18.30 Input-output characteristics of rear steering gearbox.

IPR2023-01234
Petitioner - Ex. 2017 - Page 415

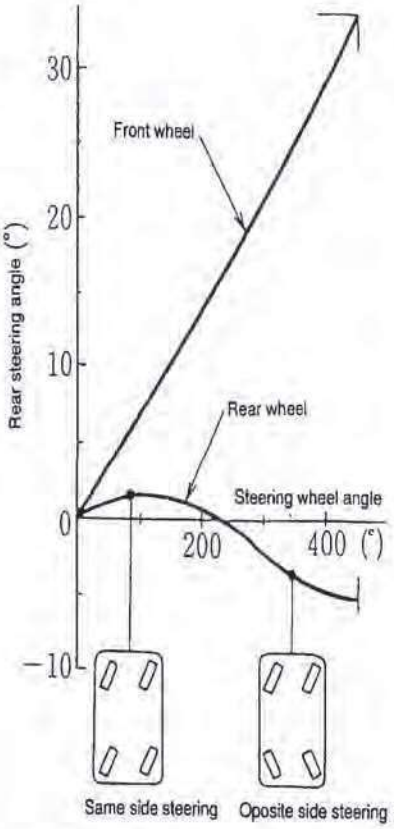


FIGURE 18.31 Characteristics of front steering speed-responsive 4WS.

wheels is small, the rear wheels turn in the same direction, but when the steering angle for the front wheels is large, the rear wheels turn in the opposite direction, as shown in Fig. 18.31. During high-speed driving, since the front wheels are only turned by very small amounts, the rear wheels thus turn in the same direction, and driving stability is improved. At extremely low speeds where the front wheels are steered through much larger angles, the rear wheels turn in the opposite direction and the turning radius becomes small, thus, the working ability should be improved.

Electronic-Hydraulic Control System

Vehicle Speed/Lateral Acceleration Responsive Type. This system was installed in vehicles like the 1986 Nissan Skyline. The structure of the system and the construction of the rear gearbox are shown in Figs. 18.32 and 18.33, respectively. In this system, a special hydraulic valve, which generates hydraulic pressure balanced with the reaction force from the front wheels in proportion to the lateral acceleration, is provided in the front-wheel power steering system, and this hydraulic pressure is transmitted to the actuator for the rear wheels. The rear-wheel actuator contains a high spring rate spring which allows displacement of the output rod to the position that balances the hydraulic pressure received. The rear wheels are steered in the same direction as the front wheels by means of the displacement of this rod. Accordingly, the relationship between the vehicle speed and the steering angle of the rear wheels varies in accordance with

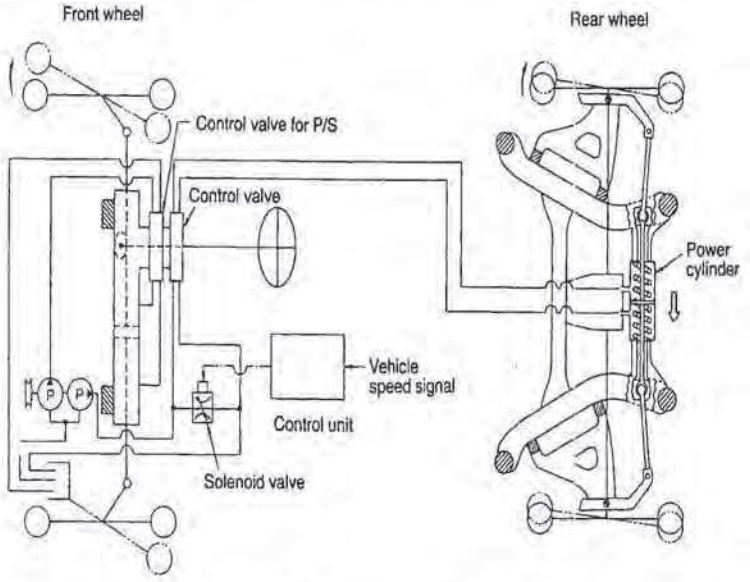


FIGURE 18.32 Lateral acceleration-responsive 4WS.[1]

IPR2023-01234
Petitioner - Ex. 2017 - Page 416

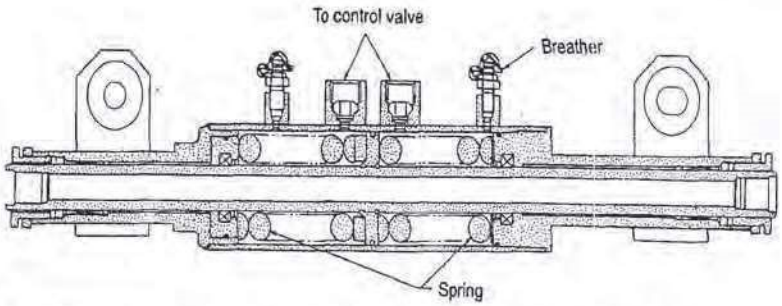


FIGURE 18.33 Rear steering actuator of lateral acceleration-responsive 4WS.[1]

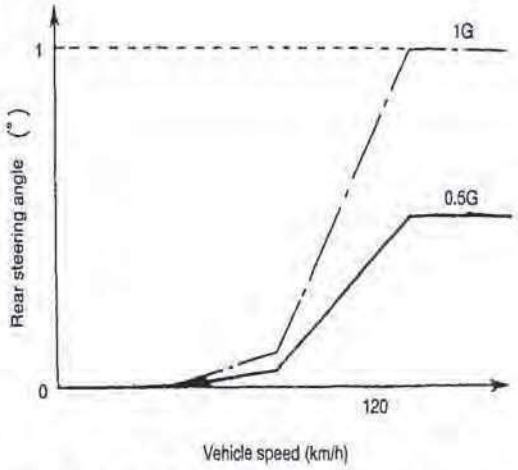


FIGURE 18.34 Characteristics of rear steering angle.[1]

the lateral acceleration as shown in Fig. 18.34. In this system, the maximum steering angle of the rear wheels is confined to a fairly low value, so that it is not intended to be a system for improving the minimum turning radius of the vehicle at very low speeds.

Vehicle Speed/Front-Wheel Steering Angle/Steering Wheel Velocity Responsive Type. This system was installed in vehicles such as the 1988 Nissan Sylvia, and was developed for the purpose of further improvement of vehicle stability and maneuverability during medium- to high-speed driving. The structure of the system and the construction of the rear-wheel actuator (solenoid servo valve) are shown in Figs. 18.35 and 18.36, respectively. In this system, the working fluid discharged from the hydraulic pump is directly introduced to the solenoid servo valve and controlled by instructions from an ECU (electronic control unit), after which it is sent to the power cylinder.

The ECU detects the front-wheel turning angle and the steering speed of the steering wheel by means of signals from the steering wheel angle sensor located in the steering wheel. The values thus calculated and the vehicle speed are used to determine the steering angle for the rear wheels. The maximum steering angle of the rear wheels is confined to a fairly low value in this system also, so that it was intended only to be a system for improving the vehicle stability and maneuverability at medium to high speeds. However, it does not improve only the stability by turning the rear wheels in the same direction, but also improves the maneuverability by momentarily turning the rear wheels in the opposite direction to the front wheels when the steering wheel is turned quickly at medium vehicle speeds. That is, the initial yawing movement (yaw velocity) of the vehicle is improved and steering response is thus improved. Figure 18.37 shows the steering angle pattern of the rear wheels with time expressed along the horizontal axis.

IPR2023-01234
Petitioner - Ex. 2017 - Page 417

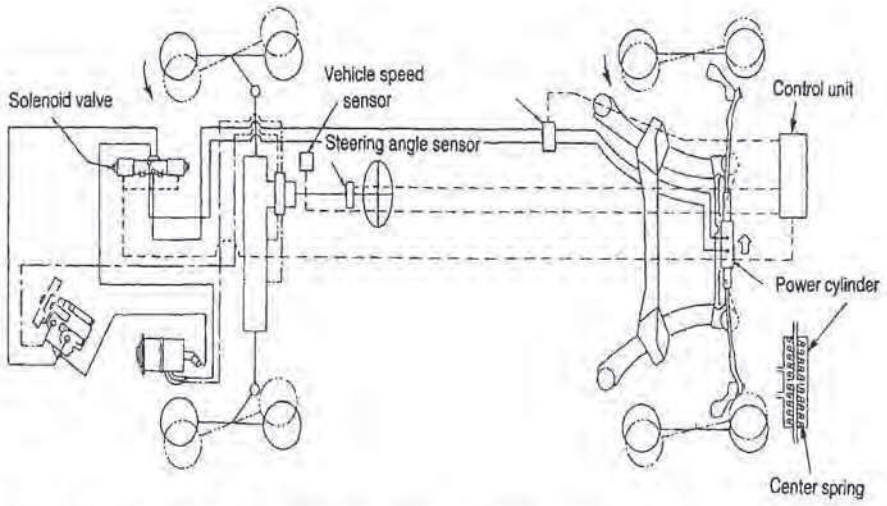


FIGURE 18.35 System construction of front-wheel-responsive 4WS.[1]

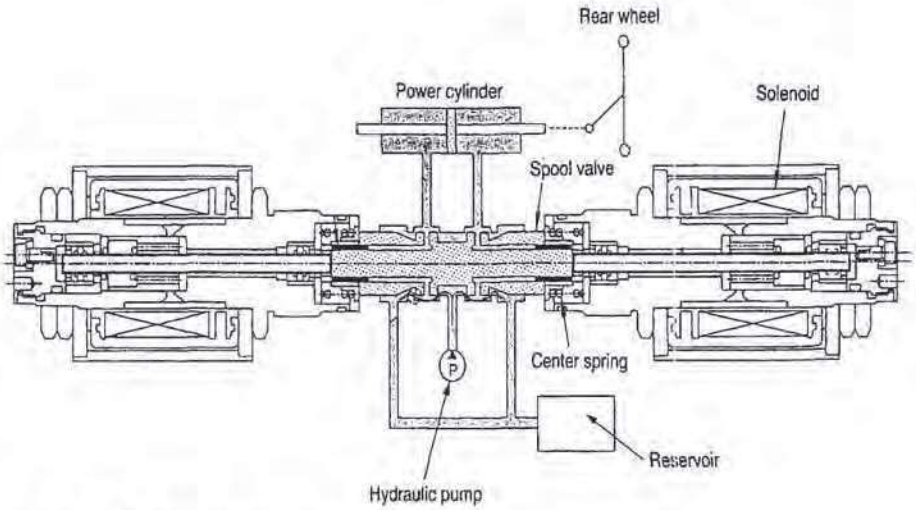


FIGURE 18.36 Solenoid servo valve of front steering angle-responsive 4WS.[1]

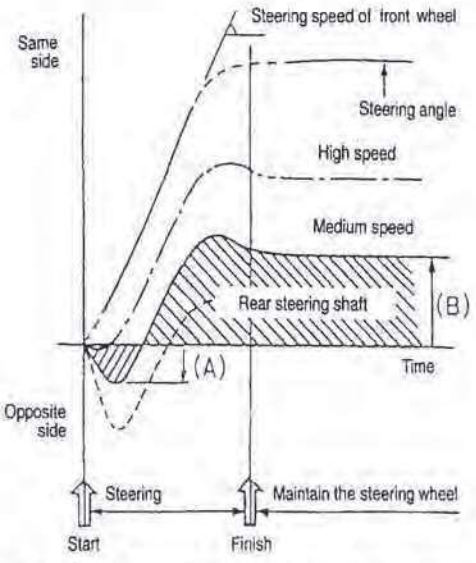


FIGURE 18.37 Characteristics of front steering angle-responsive 4WS.[1]

IPR2023-01234
Petitioner - Ex. 2017 - Page 418

Electronic-Hydraulic-Mechanical Systems

Vehicle Speed/Front-Wheel Steering Angle Responsive Type. This system was introduced in the 1987 Mazda Capella, and was designed with the aim of being a system for improving both stability when driving at high speeds, like the fully mechanical system, and vehicle minimum turning radius at low speeds. The structure of the system and the construction of the rear actuator are shown in Figs. 18.38 and 18.39, respectively. This system can be broadly divided into the power assist section and the phase control section. The power assist section consists of a linear spool valve and a power piston, and utilizes hydraulic pressure as the dynamic force. The phase control section comprises a bevel gear which engages with the input shaft, a control yoke, and a control rod which is connected to a valve. The angle of the control yoke is driven by a stepping motor via a worm gear, thus controlling the turning direction of the rear wheels so that the rear wheels can be turned, not only in the same direction, but also in the opposite direction as the front wheels.

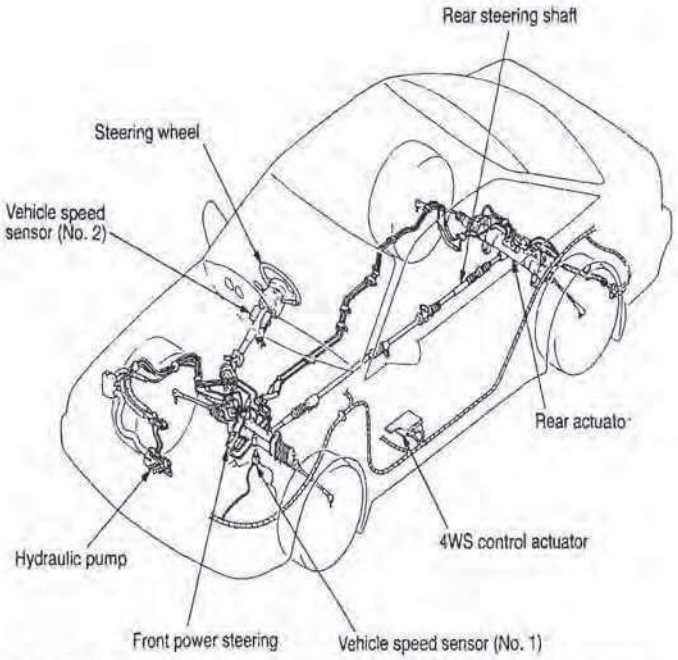


FIGURE 18.38 Front steering angle and vehicle speed-responsive 4WS.[11]

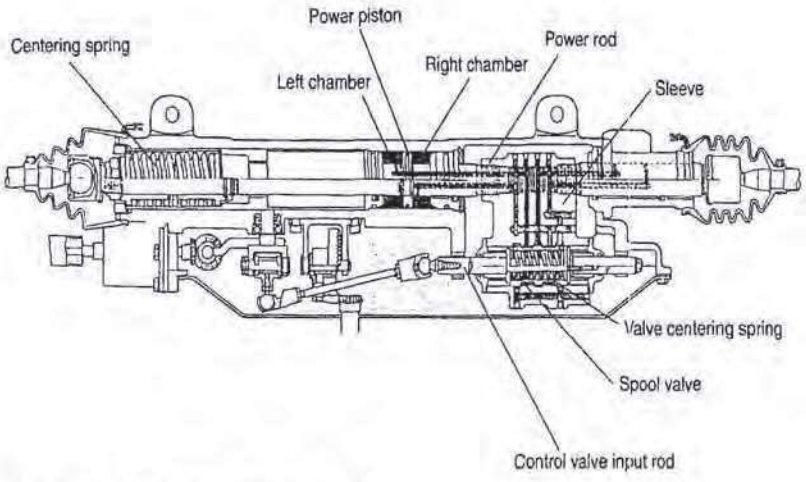


FIGURE 18.39 Rear steering actuator.[11]

IPR2023-01234
Petitioner - Ex. 2017 - Page 419

In Fig. 18.40, *a* represents the situation in which the rear wheels are turned in the same direction, and *b* represents the situation in which the rear wheels are in the opposite direction. The direction of movement of the valve spool in relation to the turning direction of the input shaft is opposite for *a* and *b* as shown. Figure 18.41 shows the situation in which the ratio of the steering angle of the rear wheels with respect to the steering angle of the front wheels is continuously changing with respect to the vehicle speed.

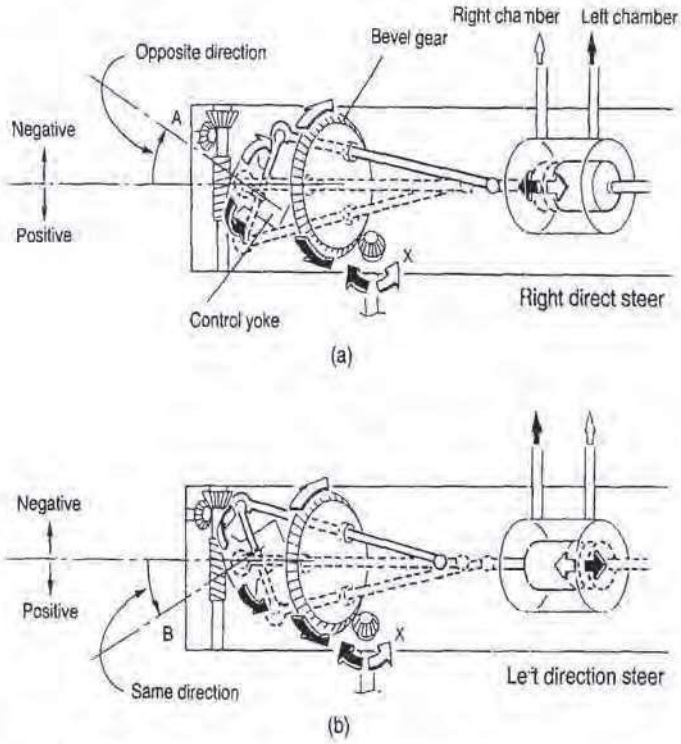


FIGURE 18.40 Explanation diagram of rear actuator.[11]

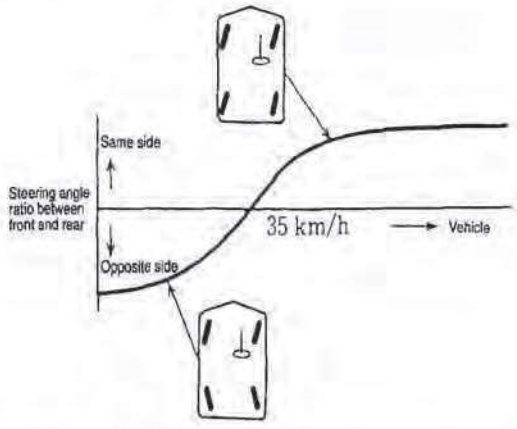


FIGURE 18.41 Characteristics of front steering angle and vehicle speed-responsive 4WS.[1]

Vehicle Speed/Front-Wheel Steering Angle/Yaw Velocity Responsive Type. This system was introduced in the 1992 Toyota Soarer. Figures 18.42 and 18.43 show the system structure and the construction of the rear-wheel steering actuator, respectively. The system consists of two sections: a *mechanical-hydraulic type* steering mechanism to steer the rear wheels by a

IPR2023-01234
Petitioner - Ex. 2017 - Page 420

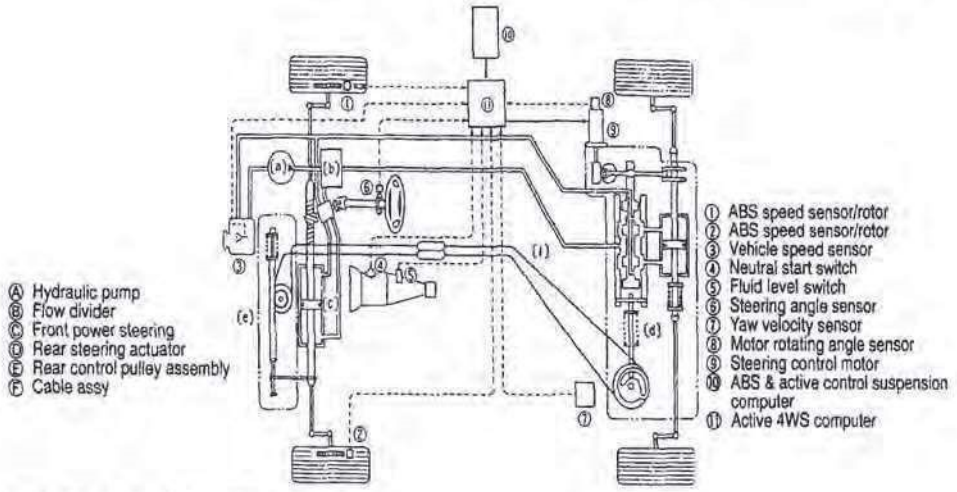


FIGURE 18.42 Active 4WS system.[10]

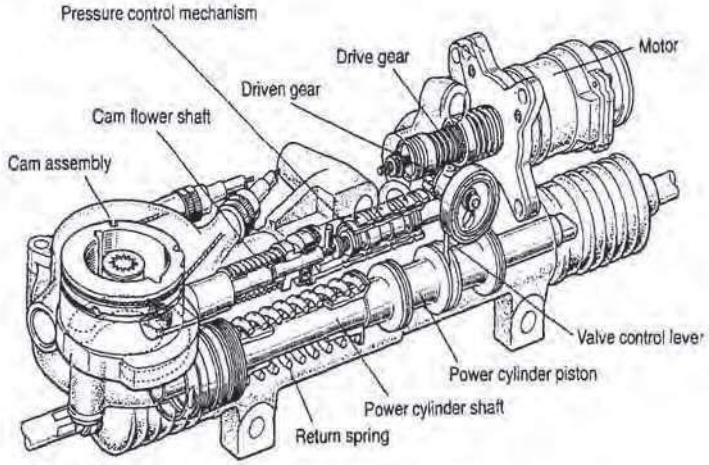


FIGURE 18.43 Rear steering actuator unit.[10]

considerably large steering angle in the opposite direction to the front wheels in order to make the turning radius small at low speeds, and an *electronic-hydraulic type* steering mechanism to steer the rear wheels by a considerably smaller value in order to not only improve the steering response and the stability during middle- to high-speed driving, but also to suppress the unexpected movements due to the outside disturbances.

Mechanical-Hydraulic Type Steering Mechanism. This mechanism consists of steering angle transmission cables, which transmit information concerning the steering angle of the front wheels to the rear-wheel steering actuator; a joint to connect the front and rear cables; a pulley assembly, which converts the displacement of the front-wheel steering rack into cable movement; a cam, which converts the movement of the cable into displacement of the sleeve valve inside the rear-wheel steering actuator; and a copy valve, which steers the rear wheels as far as the instruction given by the sleeve valve and maintains them in position. Furthermore, a dead zone is provided in the pulley assembly so that the rear wheels are not steered in the opposite direction to the front wheels when the vehicle is traveling at high speed.

Electronic-Hydraulic Type Steering Mechanism. This mechanism is designed to improve the steering response and the stability of the vehicle and to suppress the unexpected movements from outside disturbances when the vehicle is traveling at medium to high speeds. For this purpose, the system consists of five types of sensors for detecting the driving conditions and the steering situations, an ECU which determines the steering angle for the rear wheels

IPR2023-01234
Petitioner - Ex. 2017 - Page 421

based on the signals from these sensors, a pulse motor which drives the gear mechanism based on instructions from the ECU, a gear mechanism which converts the rotation of the pulse motor into a spool valve displacement, and a hydraulic copy valve which steers the rear wheels as far as the instruction given by the sleeve valve and maintains them in that position.

Control Method. The basic algorithm to determine the steering angle for the rear wheels is given in Fig. 18.44. When driving in the medium- to high-speed range, the front-wheel steering angle proportional gain for the rear wheels is set to 0; instead of that, the yaw velocity proportional gain in the direction which suppresses the yaw rate is set. Accordingly, in the medium- to high-speed range, the rear wheels are turned in the same direction as front wheels, with the same effect as that of the other system mentioned before. The feature of this system is that a yaw rate sensor is provided to detect the vehicle dynamics and utilizes its signal as a control parameter. The effect of this is the addition of a function which automatically compensates the confusion in vehicle behavior caused by outside disturbance.

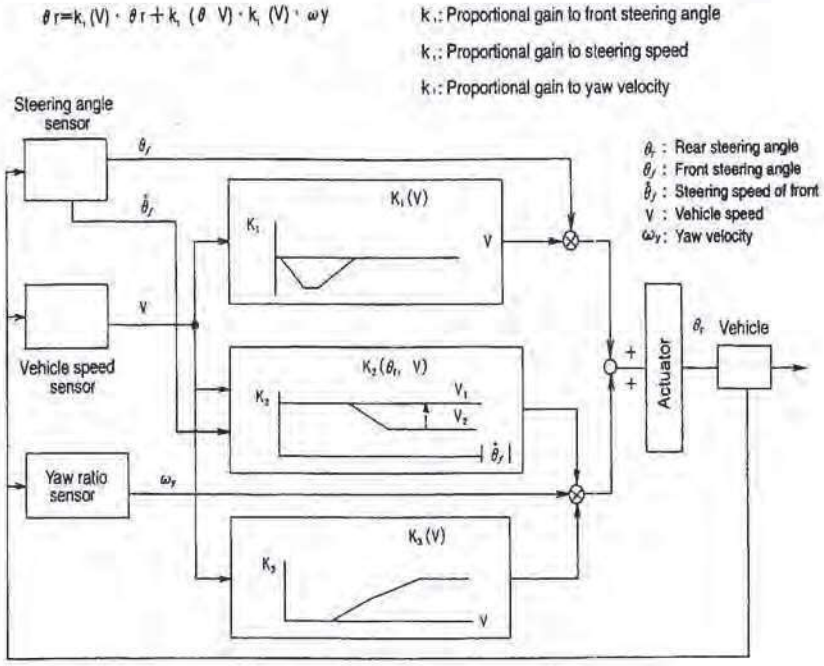


FIGURE 18.44 Control block diagram.[10]

18.2.4 Electronic-Electric Control Systems

Vehicle Speed/Front-Wheel Steering Angle/Steering Speed Responsive Type. This system was introduced in the 1991 Honda Prelude. The system structure is shown in Fig. 18.45, and the construction of the rear-wheel actuator is shown in Fig. 18.46. This system has a structure whereby the rotation of an electric motor that is controlled by the ECU is converted into linear motion by means of a ball screw to directly drive the rear wheels. The system is easy to install. Cross sections of the structures of the front-wheel steering angle sensor and the rear-wheel steering angle sensor are shown in Figs. 18.47 and Fig. 18.48, respectively.

Also in this system, the turning of the rear wheels is determined by the vehicle speed, the front steering angle, and the steering wheel velocity. The determining algorithm is similar to the system mentioned previously. In this system, improvements in the stability at high speeds, improvement in the steering response when the steering wheel is turned quickly, and improvement in the turning radius of the vehicle at low speeds have been realized simultaneously.

The most recent example of an electronic-electric system is the system[12] that has been installed in the 1993 Nissan Laurel. The approach to control in this system is the same as in the

IPR2023-01234
Petitioner - Ex. 2017 - Page 422

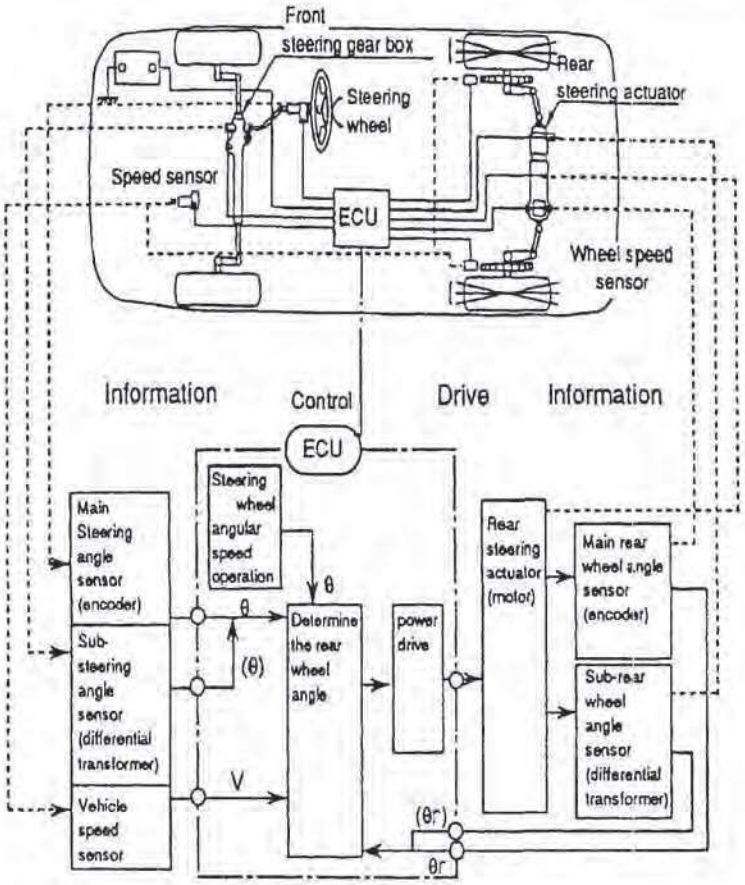


FIGURE 18.45 Block diagram of the full-electric 4WS.

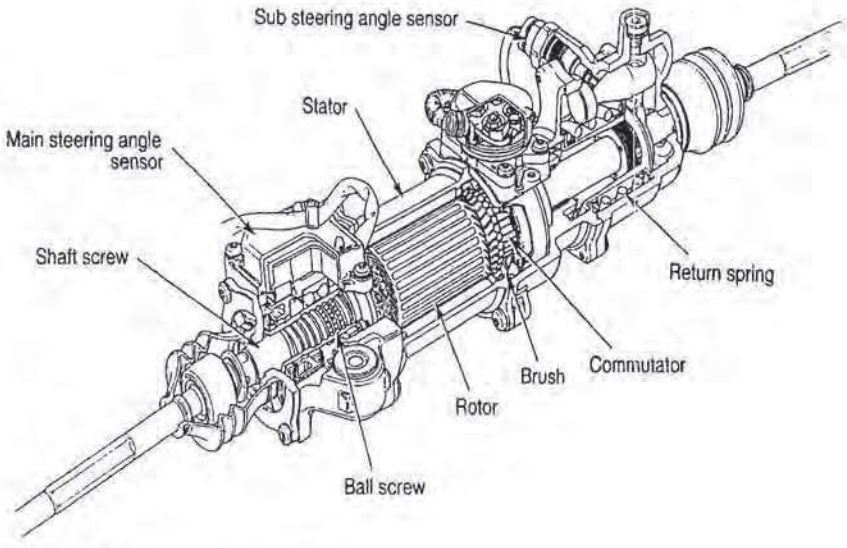


FIGURE 18.46 Rear steering actuator.

IPR2023-01234
Petitioner - Ex. 2017 - Page 423

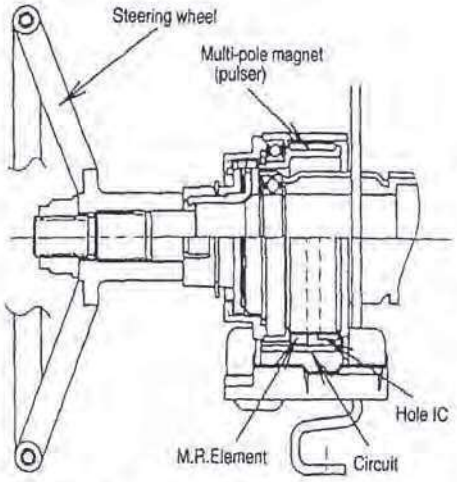


FIGURE 18.47 Main steering angle sensor.

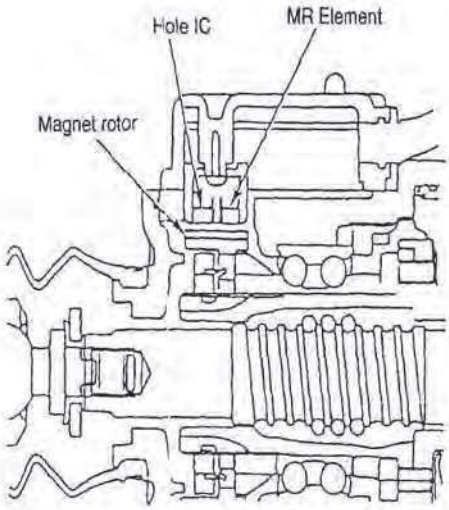


FIGURE 18.48 Rear steering angle sensor (main).

vehicle speed/front-wheel steering angle/steering wheel velocity responsive type system mentioned before, but by using an electric actuator, the space taken up by the system has been reduced and ease of installation improved.

Figure 18.49 shows the system structure, and Fig. 18.50 shows the steering angle generation modes for the rear wheels.

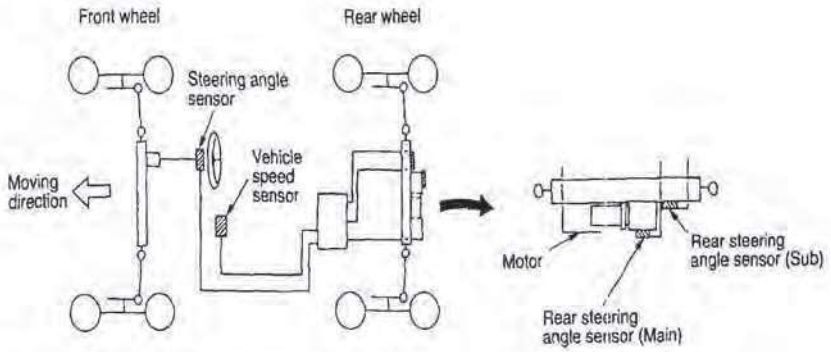


FIGURE 18.49 System construction of HICAS.[12]

18.2.5 Trends in Research and Development

Four-wheel steering systems that have been installed in current vehicles mainly adopt the program control technique in which the rear-wheel steering angle is programmably determined based on the beforehand scheduling relationship with the vehicle speed, the front steering angle, and steering wheel velocity. The aim of the system is the improvement of the insufficient performances in handling characteristics of the vehicle under special steering situations.

Recently, however, the system based on the new concept is being earnestly researched in order to drastically improve the handling characteristics in any region for practical use. Such technology is similar to that of CCV (control configured vehicle), which is used in airplanes, and named as *active control technology* in general. In this section, a basic introduction to the following two representative concepts concerning the active four-wheel steering system (A-4WS), which adopts the active control technology in the 4WS systems, will be given.

IPR2023-01234
Petitioner - Ex. 2017 - Page 424

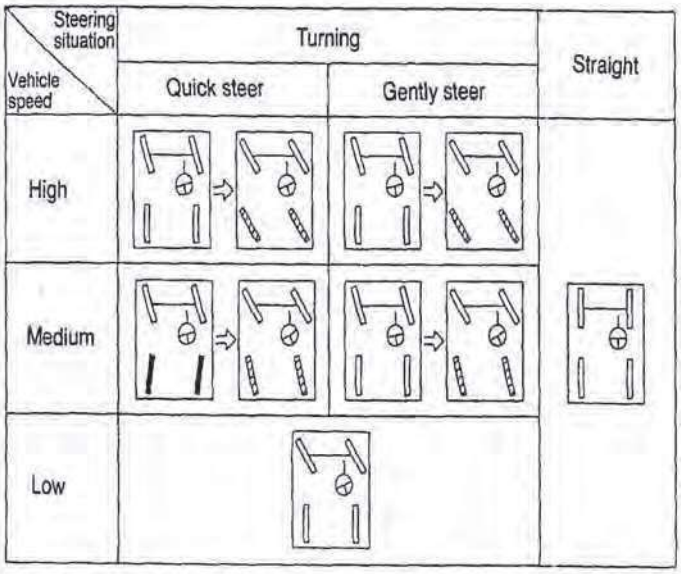


FIGURE 18.50 Rear steering angle generation mode.[12]

Vehicle's Slip Angle Control System. Generally, the moving direction of the center of gravity of the vehicle is not the same as the heading direction of the vehicle while the vehicle is turning, and the angle between these two directions is called the *side slip angle of the vehicle.* When the side slip angle of the vehicle is large, the driver is forced to drive with an oblique line of vision. This can be considered one cause of increased driving difficulties. From this point of view, the control concept has been proposed whereby the side slip angle of the vehicle while driving is always kept close to 0. In addition, the cause of the increasing of phase delay in lateral acceleration according to the vehicle speed is that the steady state gain in the sideslip angle is reduced together with the vehicle speed and becomes negative at high speed. In order to eliminate such phenomena, the concept which keeps the sideslip angle close to 0 may also be desirable.

The sideslip angle B can be expressed in general by the following equation:

$$\beta = \frac{1}{POL(s)}\{B_f(1+\tau_f \cdot s)\delta_f + B_r(1+\tau \cdot s)\delta_r\} \tag{18.9}$$

$$B_f: \frac{2l_r lk_r - l_f m v^2}{2lk_r V} \cdot A,\ B_r: \frac{2l_f lk_f - l_r m v^2}{2lk_f V} \cdot A$$

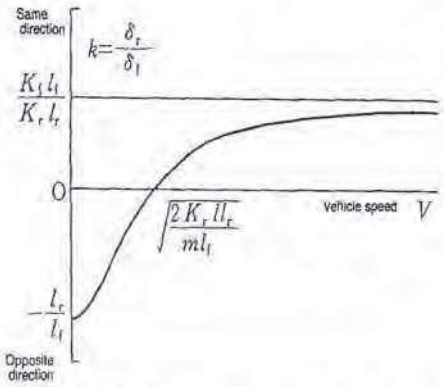


FIGURE 18.51 Steering angle ratio for making the vehicle sideslip angle equal to 0.[1]

Provided the numerator s in Eq. (18.9) = 0, the steering angle ratio between the front and rear wheels that is required for realizing a sideslip angle of 0 can be obtained from Eq. (18.10) as a function of the vehicle speed. This is shown graphically in Fig. 18.51.

$$\frac{\delta_r}{\delta f} = -\frac{B_f - B_f \tau_{fs}}{{}_B r + B_r \tau_r s} \tag{18.10}$$

$$= \frac{-\iota_{f+} + (\iota_r m/2k_f\iota)V^2 - (I_z/2K_r\iota)V \cdot s}{\iota_{f+} + (\iota_r m/2k_f\iota)V^2 - (I_z/2K_f\iota)V \cdot s}$$

If the front- and rear-wheel control principle that includes the phase proceeding func-

IPR2023-01234
Petitioner - Ex. 2017 - Page 425

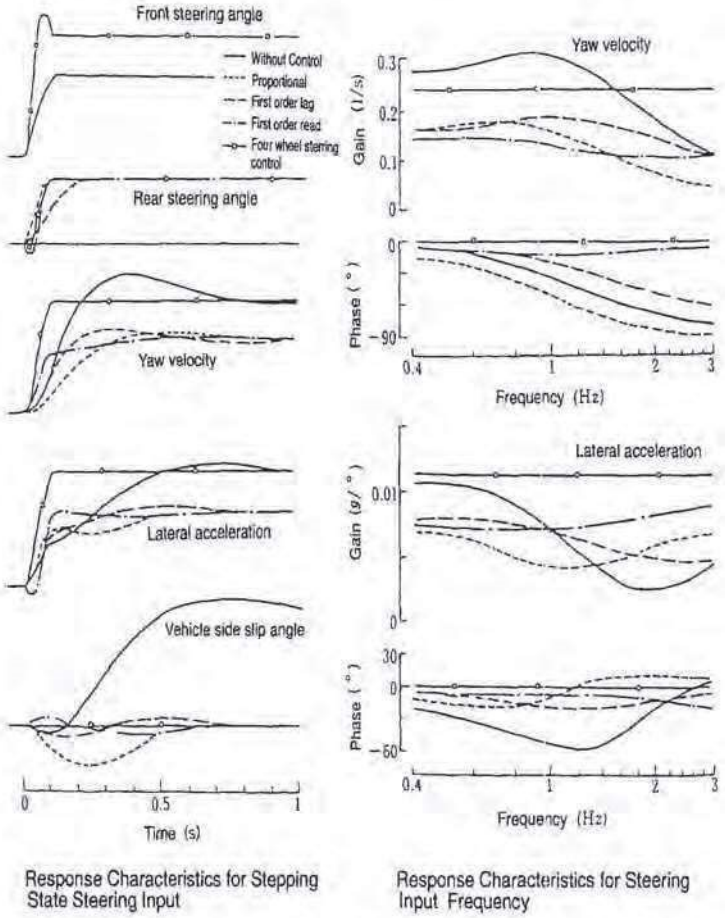


FIGURE 18.52 Affections in steering response characteristics by using the delay/advanced control means.[1]

tion for the front-wheel steering angle is employed, the vehicle characteristics can be set more freely. An example of the simulation analysis when the front and rear wheels are steered with a control principle such as the above is shown in Fig. 18.52.

Model Following Control System. In this system, the desirable vehicle behavior in accordance with the driver's steering operations is predetermined as a reference model, and the control is carried out so that the actual vehicle behavior fits this model. Generally, the lateral acceleration and the yaw velocity are used as the parameters for expressing the lateral movement of the vehicle. If the independent models are set for both of these characteristics, and make the actual vehicle behavior follow them, it is necessary to actively control both of the front and rear wheels. Research into systems such as this is currently being carried out, but in this section, a system for controlling the steering angle of the rear wheels that uses a range model for D^* which is defined by the linear combined Eq. (18.11) for the yaw velocity and the lateral acceleration will be introduced.

$$D^* = da_y + (1 - d)V\phi \tag{18.11}$$

If the weighted constant d in Eq. (18.11) equals 0, this control system becomes a yaw velocity model following control system, and if $d = 1$, then it is a lateral acceleration following control system.

IPR2023-01234
Petitioner - Ex. 2017 - Page 426

GLOSSARY

Convergence Yaw stability of the vehicle when driver inputs a rapid steering wheel movement and releases the steering wheel.

Kickback Steering torque and angle arising from inverse input through the tires from uneven concrete road or other surface.

REFERENCES

1. "Steering," chap. 8, *Handbook of Society of Automotive Engineers of Japan* vol. 2 (Design), Society of Automotive Engineers of Japan, Inc., 1991.
2. Nissan Ciema, guidebook in Japan, 1991.
3. Shigeru Iga, et al., "Motor driven power steering for the maximum steering sensation in every driving situation," SAE paper 880705, 1988.
4. *Honda Today* service manual in Japan, 1991.
5. Acura NSX service manual, 1991.
6. Yasuo Shimizu, et al., "Development of electric power steering," SAE paper 910014.
7. Syunichi Wada, et al., "Electric power steering system," Mitsubishi Denk Giho, vol. 66, no. 9, 1992.
8. Yasuo Shimizu, et al., "Control of electric power steering (EPS)," *The 68th JSME Spring Annual Meeting*, vol. C 1605, 1991.
9. Naohiro Yuhara, et al., "Improvement of vehicle handling quality through active control of steering reaction torque," *International Symposium on Advanced Vehicle Control 1992*, no. 923073.
10. *Toyota Technical Review*, vol. 41, no. 1, 1989.
11. Mazda Motor Company Introduction to Capella (new car), 89-5-NM005, 1989.
12. Nissan Motor Company Introduction to Laurel (new car), F005705, 1989.

ABOUT THE AUTHOR

Makoto Sato, executive chief engineer of Honda R&D Co., Ltd., was graduated from Nagoya Institute of Technology in 1960 and began his career with Kokusan Electric Co. He moved to Honda R&D Co., Ltd. in 1968 and began working on vehicle dynamics control systems with electronic technologies. He is now researching new safety technologies with intelligent electronics, especially in the area of crash avoidance.

IPR2023-01234
Petitioner - Ex. 2017 - Page 427

CHAPTER 19
LIGHTING, WIPERS, AIR CONDITIONING/HEATING

Richard Valentine
Motorola Inc.

19.1 LIGHTING CONTROLS

Controlling lamps with power electronics offers many advantages and a few disadvantages over conventional switches or relays. An important advantage includes easier diagnostics compared to the classical mechanical switch or relay approach, while a significant disadvantage includes the higher cost of the electronics. Because some lights, such as headlamps, turn signals, and brake lamps are safety related, a method to test the integrity of these lamps is an advantageous feature. The power electronic design can not only turn lights on or off, but it can vary the light's intensity and detect abnormal conditions such as open or shorted lamps. The cost tradeoff issue becomes more interesting when the power electronics load control is connected onto a data bus or multiplexed network (see Chap. 26).

The typical automotive lamp can range from small-wattage panel lamps to large 60-W or higher headlamps (refer to SAE ref HS-34/93 for auto lamp standards). Tungsten and halogen types prevail for many vehicular lamp designs. The prime difference between standard tungsten nonhalogen and halogen lamps is in light efficiency. Halogen types produce about 20 percent more light for each watt of energy consumed. Other types of lamps, such as light-emitting diodes (LEDs), fluorescents, or gas discharge, are somewhat adaptable for vehicular applications. The power electronics operating requirements vary for each lamp technology category.

19.1.1 Incandescent/Halogen

The single most important rule when switching normal incandescent lamps is to select a power transistor that can sustain a 10 to 15 times inrush current level. For example, a 2-A-rated stop lamp requires a 20- to 30-A-rated power transistor for an electronic switch design. When designing a lamp-driven circuit, other considerations besides inrush currents must be taken into account: maximum power transistor operating temperatures, shorted load protection, voltage supply transients, reverse voltage supply condition, open load detection, high or low side design topology, MCU interface, switching edge speed limits, and variable brightness control. In addition, the electronic lamp switch should not drop more than 0.3 V to ensure that the lamp's intensity is not degraded. Incandescent lamp light output is very sensitive to the lamp's operating voltage. A 20 percent drop in an incandescent lamp's nominal operating voltage can reduce its light output by 50 percent.

IPR2023-01234
Petitioner - Ex. 2017 - Page 429

Inrush Current Effects. Lamp loads behave like high positive temperature coefficient resistors. When the lamp is cold, the resistance value of its filament is about 1/10 of its normal operating resistance. Lab tests show a definite relationship between the lamp's peak inrush current level and light output intensity with respect to time. If the lamp current is limited to its nominal value, it takes longer—one-half second or more—for the filament to reach its nominal temperature, but if the current supply is unlimited, the lamp heats up very quickly. The lamp response time and the available supply current must be considered for applications when an instantaneous light output is desired, such as with turn signals or brake lights in a vehicle. A 1-s delay at 89 km/h (55m/h) equals 24.6 m (81 ft). Four seconds of time is about how long some vehicles take to stop at a vehicle speed of 89 km/h. If the driver has exerted maximum braking, and his stop lamp waits for 1 s to convey this action to trailing vehicles, the driver will almost be halfway stopped before the trailing vehicle has a stop light indication. This is not acceptable, and the delay time in stop or possibly in turn signal indicators must be minimized to benefit the reaction time for other drivers.

Limiting the lamp's inrush current will probably increase the lamp's longevity in high duty cycle applications, such as a flasher, because the mechanical stress on the filament is reduced. A limited inrush current design should decrease the chances of the lamp failing during the initial turn on. In vehicular applications when external induced filament vibration is high, the lamp reliability may not be improved enough to justify a current limiting design. A current limiting design does increase the power transistor's peak heat dissipation, and when operating with an energy source that is capable of supplying high peak currents, such as an automotive battery, the rationale to include current limiting would be to use a smaller, less expensive transistor or to minimize voltage sags in the wire bus when several lamps are switched on at the same time. A current limiting design may include a network to control the switching transition times from OFF to ON to OFF.

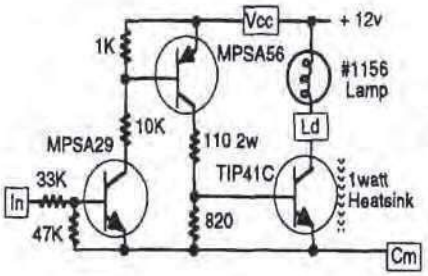
Setting the switching times to over 0.001 s would help minimize EMI effects. Most power transistors can switch in less than 1 μs, with some power FETs able to switch in 50 ns. These RF switching speeds are undesirable and will be detectable by other electronic systems in the vehicle, such as the AM radio.

Lamp Driver Design. The power electronics can drive the lamp in one of two simple ways. One is *low side switching* (Fig. 19.1) with the lamp connected between the power supply and the transistor, or *high side switching* (Fig. 19.2) with the lamp connected between the transistor and common. The main drawback to low side switching is that one side of the lamp is always connected directly to the battery supply, and if this lead is shorted to common, very high currents will occur. A high side switch disconnects the power supply from the load, so if the switch is off, the chances of an accidental power supply short when replacing or troubleshooting the lamp are minimal. On the other hand, in the high side switch design, a switch ON condition will cause very high current levels to flow through the power transistor in the event of a short. The selection between high or low side switching is affected by the lamp's environment.

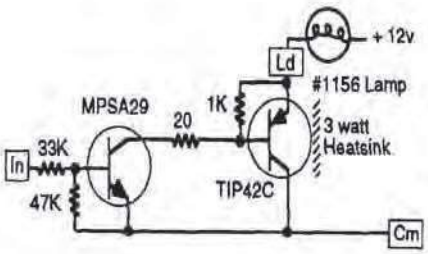
In a low side design, leakage currents that may flow from the lamp's socket or connectors can be a concern. This is especially true if the lamp is operated in a salt-laden, high-moisture atmosphere. This problem occurs because of the constant voltage potential at the socket and is one reason why most exterior vehicular lighting systems use high side switching. Other applications, such as instrument backlighting or signal indicators that are usually located inside the vehicle, can be a low side design to take advantage of lower-cost NPN transistors or N-channel power FETs. N-channel power FETs can be used for high side switching by adding a charge pump as shown in Fig. 19.2*a*. Special power linear devices are also available that incorporate a charge pump for high side switching of small lamps. These power linear IC devices (MC3399, MC33091, or equivalent) will find more usage as their pricing and reliability become more attractive for automotive application.

Power Control Device Selection. When the drive topology has been decided upon, a power device can be chosen. There are numerous tradeoffs between bipolar and power FET transistors. The N-channel power FET device requires minimal drive power for a low side switch and

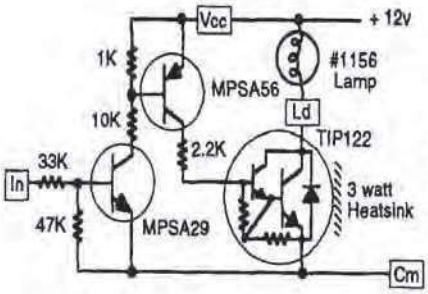
IPR2023-01234
Petitioner - Ex. 2017 - Page 430



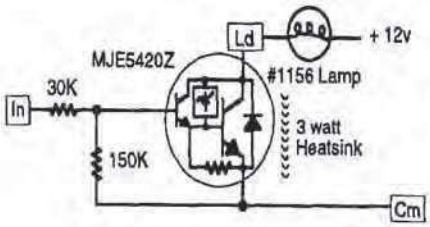
The NPN transistor runs in full saturation mode, but requires 1.5 watt base drive resistor.



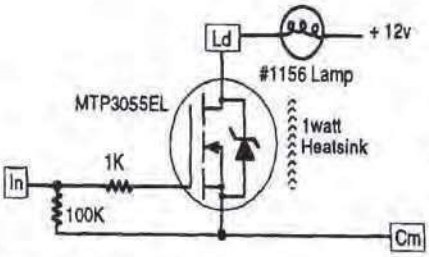
The PNP transistor dissipates about 3 watts since it does not operate in saturation mode.



NPN Darlington transistor dissipates about 3 watts since it does not operate in saturation mode.



NPN Darlington trans stor has internal active zener element to clamp over voltage transients in forward SOA mode. Device dissipates about 3 watts since it does not operate in saturation mode.



N Channel MOSFET transistor dissipates about .8 watts, and can sustain low energy voltage spikes.

FIGURE 19.1 Low side switching.

IPR2023-01234
Petitioner - Ex. 2017 - Page 431

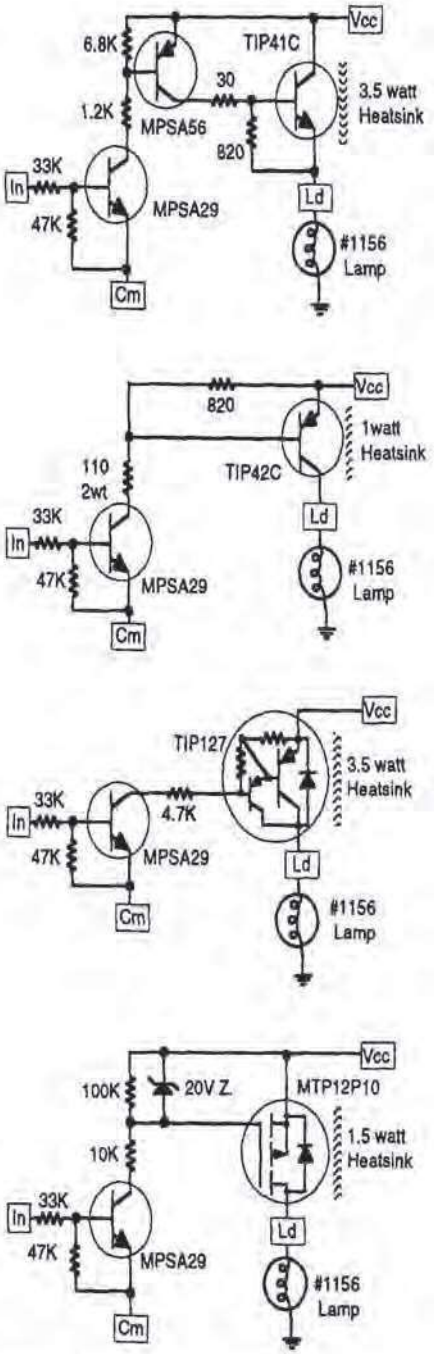
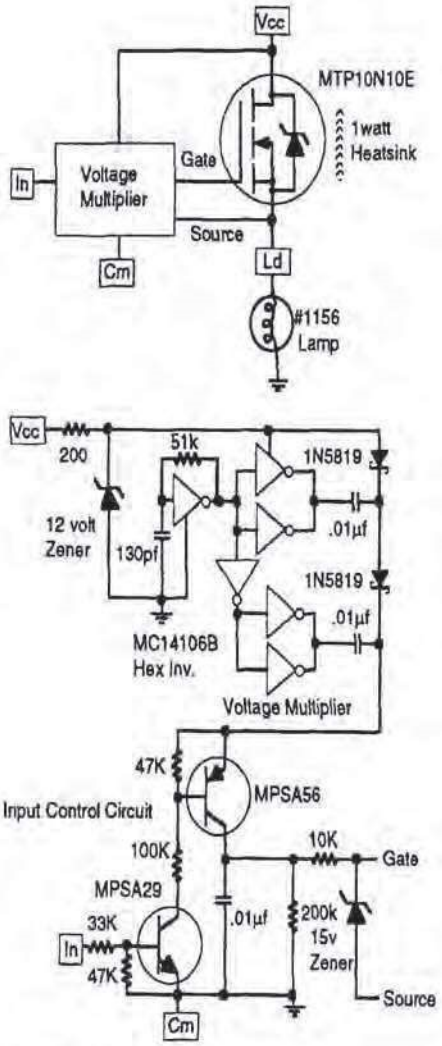


FIGURE 19.2 High side switching.

is cost-competitive with similar rated bipolars. Low side switching can easily use N-power FETs, whereas a high side switch would need more expensive P power FETs. Power FET transistors will usually be able to conduct the high peak inrush currents much more readily than bipolar transistors. This is because power FETs have higher transconductance than bipolars. Bipolars are usually biased for operation at the lamp's average load current and will therefore operate in a linear mode during the lamp's initial turn on, thereby offering some current-limiting at the expense of increased peak junction temperature. The power FET will usually con-

IPR2023-01234
Petitioner - Ex. 2017 - Page 432



The N-Channel MOSFET requires a gate voltage bias above the source voltage. This voltage can be supplied from a separate power supply or from a voltage multiplier.

Voltage multiplier allows N-Channel gate to be biased above source voltage. A Schmidt Invertor is used as an oscillator to generate a square wave that charges capacitors with 180° out of phase signals. The capacitor charging voltage adds to the rectifier DC voltage, and totals up to 3x the Vcc bus minus rectifier drops and switching losses. Several N-Channel MOSFETs could be driven with additional input control circuits from one charge pump circuit.

FIGURE 19.2*a* N FET high side design.

duct many times its average current without going into a linear mode, provided the overcurrent condition time period is fairly short, less than 100 ms.

Lamp driver long-term reliability is determined mainly by the power transistor's heat dissipation and somewhat by the solder joint totals. Selecting P-power FET devices for the high side configuration because of the low number of parts, ease of drive interface, and low power dissipation appears best, but P-channel FET devices are usually 50 percent more costly. The N-channel devices win both for cost and reliability in a low side switch design. Table 19.1 summarizes the various lamp driver designs.

Short-Circuit Protection. Another consideration is shorted circuits. The bipolar transistor is typically biased for minimum base drive power loss. During a shorted load condition, the bipolar will pull out of saturation, enter into a linear operation mode, and may fail due to excessive junction temperatures, ordinarily before a fuse will blow. A properly sized power FET may be able to safely conduct enough shorted load current to blow the fusing element. Power FET devices of 50 V are available that exhibit less than 0.0[illegible] ohm forward ON resistance in a fingernail-sized surface-mount package such as a MTB75N05HD or the equivalent.

IPR2023-01234
Petitioner - Ex. 2017 - Page 433

TABLE 19.1 Lamp Switch Design Comparison

Device type	Driver stage loss, W	Output device loss, W	Pwr. eff. in/out, %	Relative system cost	Parts count total, pcs	Solder joints total, pts	Relative reliability
High side switch configurations for 2.1-A lamp load							
NPN	0.2	2.7	89	high	9	25	low
PNP	1.31	0.8	92	medium	6	18	medium
Darlington PNP	0.03	2.7	89	high	5	13	low
P-channel MOSFET	0.01	0.9	96	high	7	19	medium
N-channel MOSFET	0.05	0.7	97	highest	19	54	low
Low side switch configurations for 2.1-A lamp load							
NPN	1.32	0.8	91	medium	9	23	medium
PNP	0.13	3.2	88	high	5	15	low
NPN Darlington	0.08	2.7	90	high	8	23	low
NPN Darlington w/Zener	0.0004	2.7	90	low	3	10	medium
N-channel MOSFET	0.0002	0.7	97	low	3	10	high

Power supply voltage = 12 V

This type of device could safely conduct 14 A continuously (assuming a 50 °C ambient temperature and 2 W constant power dissipation, $[I = (P/R)^{1/2}]$.

Another way of protecting a transistor against excessive current levels is to monitor the current value by the insertion of a low-value power resistor in series with the load. A comparator is used to detect the current sense resistor's voltage drop and will toggle if this voltage drop exceeds the comparator's reference voltage. The comparator output is tied to an R-S flip-flop logic network that latches off the input signal. Some power FET devices are now manufactured with an internal current mirror element and eliminate the need for an external large power resistor. A basic circuit is shown in Fig. 19.3 for an internal current-sensing power

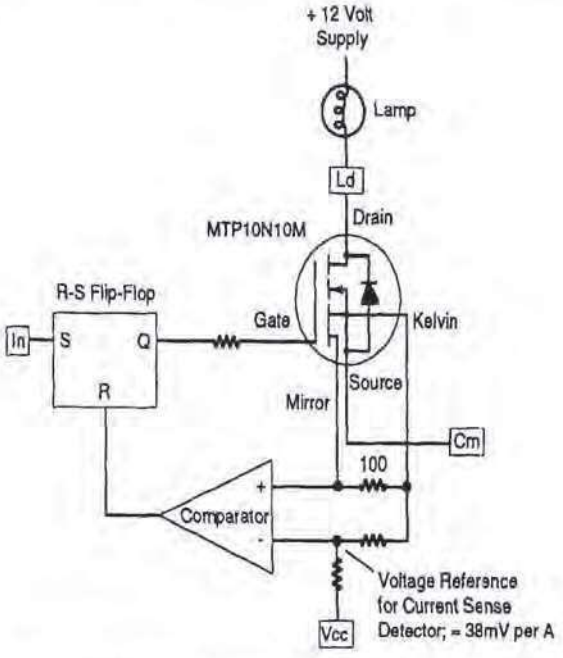


FIGURE 19.3 Internal current-sensing FET lamp drive.

IPR2023-01234
Petitioner - Ex. 2017 - Page 434

FET lamp driver. This circuit uses an RS flip-flop that will shut off the gate voltage. When the RS flip-flop has been toggled by the comparator, the RS input (set line) has to be retoggled to turn on the current-sensing power FET again. When an overcurrent condition occurs, the current-sensing power FET is latched off until the input is retoggled.

The transistor's voltage rating will be determined by the maximum voltage transients on the power supply line. In vehicular battery-charging systems, the normal 12-V supply can reach over 85 V due to intermittent battery connections when the alternator is operating. If the transistor is not avalanche-rated and enters a second breakdown due to excessive power supply voltages, it will fail shorted. Higher-voltage systems require much higher-voltage-rated devices.

MCU-based Lamp Driver. The current-sensing power FET can be directly interfaced to a single-chip microcomputer. The use of a single-chip microcomputer can allow the switch control circuit to perform many tasks: open load detection, shorted load protection, variable intensity, and diagnostics. The MCU concept is especially attractive when several lamps are clustered together and driven from the same module. Figure 19.4 shows the use of a single-

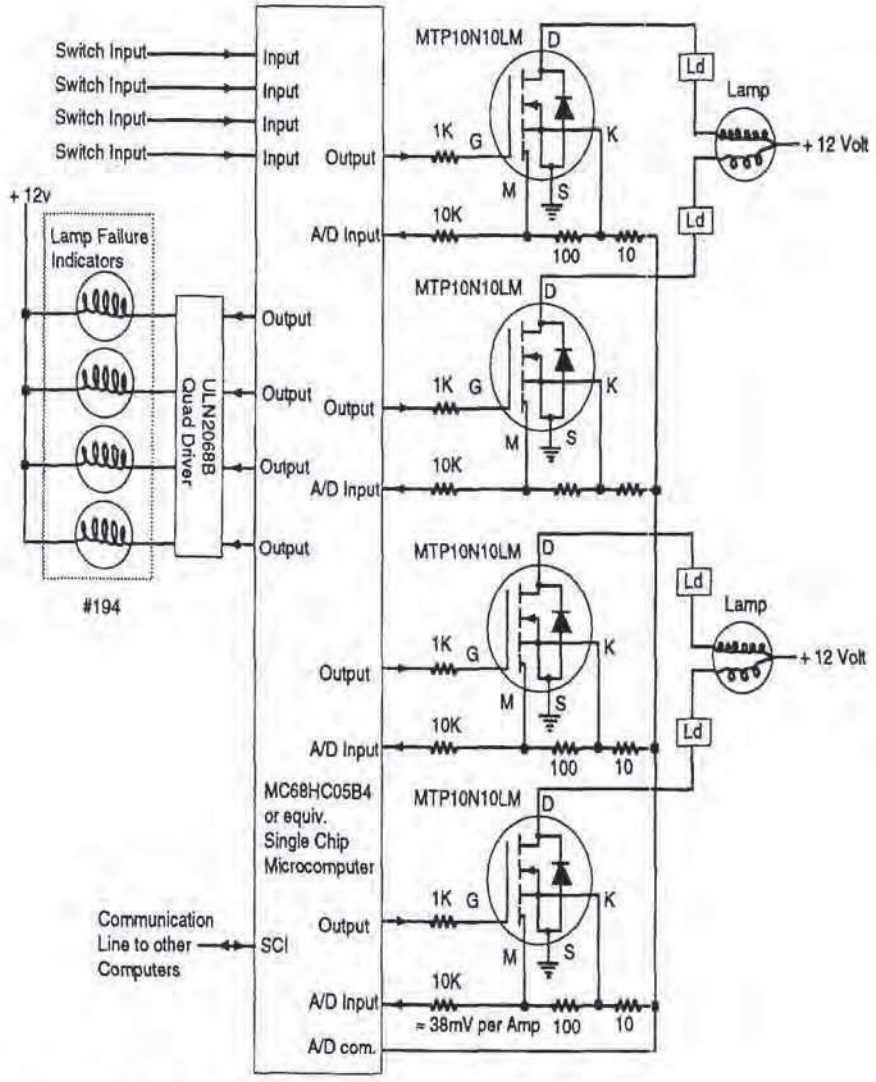


FIGURE 19.4 MCU lamp control.

IPR2023-01234
Petitioner - Ex. 2017 - Page 435

chip MCU for controlling four lamp filaments. Many more lamps could easily be added to this design. Low side switching is used to accommodate the use of logic level N-channel current-sensing power FETs. The MCU's program is set to sustain a shorted load condition for less than 50 ms; this allows a cold lamp turn-on condition to be tolerated. If a shorted load occurs after the initial turn on, the program can shut off the load in less than 1 ms, wait for 1 s, and then try to renenergize the lamp. A diagnostic fault lamp is energized to alert the user that a fault has occurred. An open load can be detected when the lamp is energized by having the program monitor the A/D inputs for a zero value. An 8-bit A/D converter will resolve to about 0.02 V when referenced from a 5-V supply. Therefore, a normal load current of 2 A will generate about a 0.084-V level, which will be read as a 04-hex number by the program. A value of 00 to 01 H would be considered an open, and a value of greater than 06 H would constitute a shorted load. A distinction could be made in the lamp failure indicator between an open and shorted load by turning the failure indicator full on for an open, and then flashing it at a 1-Hz rate for a shorted condition. The failure indicators are 3-W lamps for bright visibility, such as is required in vehicular dashboards. High-efficiency LEDs could be used when the 3-W lamp's brilliance is not required, and the LEDs may be directly driven from the MCU's output ports when connected in a low side switch configuration.

Variable light intensity can be obtained by programming a 100-Hz frequency with 0 to 100 percent pulse-width modulation. The 8-bit MCU can vary the pulse width by 256 steps, which would appear as an infinite intensity control to the human observer. One difficulty with PWM is when its duty cycle is producing very narrow pulses, such as at 1 percent or 99 percent. These narrow pulses may not allow the power stage to completely switch on or off. One method to minimize narrow PWM pulses is to force the PWM to jump from 0 percent to about 5 percent, and from 95 to 100 percent. This can easily be accomplished in the software design.

An external communication link can be established via the MCU's serial data port. This would allow the light control functions to be remotely accessible by another computer.

In summary, standard discrete power FET or bipolar transistors can effectively control incandescent lamp loads. Power FETs are preferred because of their low drive power requirement and high transconductance. The addition of an MCU enables the lamp control design to include many desirable features, such as shorted load protection, and minimizes the need for more advanced lamp driver semiconductors such as smartpower or power IC devices. MCUs are available with a built-in MUX port to communicate with other load control modules for remote operation of several lamps or other loads.

19.1.2 Fluorescent Lamps

A fluorescent lamp is commonly defined as a light source that produces light by the interaction of an arc with the gas mixture inside a glass vacuum tube. When this gas mixture is ionized by means of a high-voltage pulse from the tube's end terminals, its internal resistance decreases from megohms to several hundreds of ohms. Fluorescent lamps are typically 2 to 3 times more power efficient than standard incandescent lamps. The automotive lamp applications for fluorescents may include inside lighting, instrument back panel lighting, and other areas where an unfocused and discontinuous light spectrum, but highly efficient light source, can be utilized. The main drawback to fluorescent lamps is that they require a fairly high voltage to initiate the arc and a means to limit the lamp current once the arc is established. In other words, the fluorescent design will cost much more than a similar incandescent-sized light. This is an important consideration when operating the fluorescent lamp from a 12-V supply.

A 12-V powered fluorescent driver design requires an 8- to 16-V input to about 300-V output convertor with current limiting. These types of circuits usually operate at high frequencies (20 to 100 kHz) to minimize the size of passive components, such as transformers and capacitors, and to minimize audible noise. This type of circuit can generate significant EMI and RFI if not properly shielded and filtered. Figure 19.5 shows a block diagram of a 12-V fluorescent driver.

IPR2023-01234
Petitioner - Ex. 2017 - Page 436

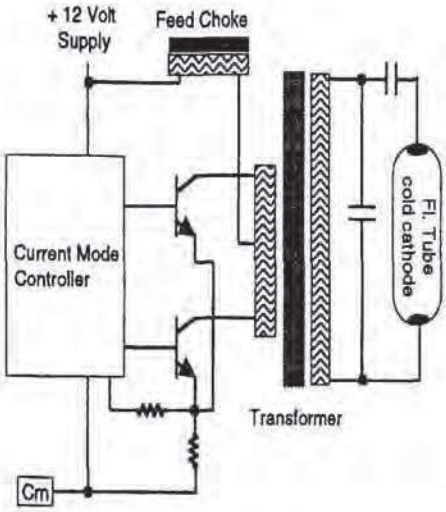


FIGURE 19.5 12-V fluorescent driver.

19.1.3 High-Intensity Gas Discharge Lamps

This class of lights includes mercury vapor, metal halide, and low- or high-pressure sodium. Some progress has been made to incorporate HID (high-intensity discharge) lamps in automotive applications. The HID metal halide type lamp offers high efficiency, up to four times more lumens per watt than incandescent, and high light output in a small package that can be utilized for headlamps. Again, the main drawback is the cost of the necessary power driver electronics. HID lamps require a circuit design similar to fluorescent drivers but at much higher power levels. The cost of the HID driver electronics limits their widespread use for automotive usage.

19.1.4 Electroluminescent (EL)

These low-intensity blue-green color light sources are used for decorative night lighting purposes and as backlighting for liquid crystal displays (LCD). EL lighting generally requires a low-current 100-V ac source. A 12-V dc to 100-V ac invertor is required for vehicular systems.

19.1.5 Light Emitting Diodes (LEDs)

Red LEDs may be adapted for stop light indicators. The LED produces a true red and does not require colored lenses. By combining several series LED strings together in one assembly, a stop light indicator is possible. A constant current source can be utilized to maintain a constant LED illumination level as shown in Fig. 19.6.

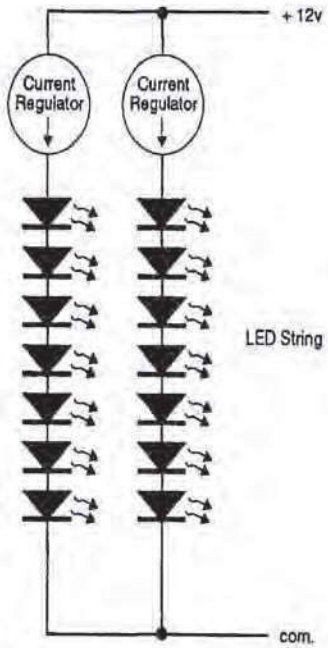


FIGURE 19.6 Constant LED illumination level design.

19.2 WINDSHIELD WIPER CONTROL

Windshield wiper (WW) systems are required by government regulations and therefore should be designed for high reliability. The motor control usually allows for low- and high-speed operation, or variable speed. The mechanical wiping motion is accomplished by a worm-gear design which gives torque multiplication and connects to the windshield wiper mechanical arm assembly. The key design specification is that the motor must sustain a "stalled" wiper condition without damage. The motor must also provide sufficient torque to run the wiper

IPR2023-01234
Petitioner - Ex. 2017 - Page 437

mechanism under worst-case conditions, such as blades frozen to the windshield. Electronic controls are used with WW systems, usually for intermittent operation plus variable speed. The driver adjusts a time interval control potentiometer for a one- to several-seconds wiper rate. The electronic circuit activates the motor with the appropriate time interval. A travel limit switch is normally used to insure that the wipe cycle is completed, and that the blades are returned to their nominal position.

Automatic windshield wiper designs are possible with today's technology that utilize a moisture detector to determine the degree of WW action required.

19.2.1 PM Motor Speed Control

The auto industry uses dc PM motors because they are economical to produce and ensure good performance. The motor's speed can be varied by either a simple voltage dropping passive resistor or an active linear voltage regulator. This simplistic method is widely used for vehicular motors requiring variable speed control. It does have a serious drawback in terms of power efficiency. For example, to control the speed of a motor that draws 20 A at full speed requires about 10 A at half speed. At full speed, the overall motor control system's efficiency will be around 80 percent. If the speed is reduced to half, the system's efficiency drops to 40 percent. This is because there is a heat loss of 70 W in the series voltage dropping element, in addition to the 14 W lost in the motor. A more efficient speed control system is therefore a desirable goal and can be accomplished by interrupting the motor's voltage at a variable duty cycle or by using a switching power supply. A switching power supply to control up to 300 W would cost more than the motor because of its high-frequency transformers and other components.

PWM Speed Control Design. Electronic permanent magnet motor speed designs can range from a single power transistor to turn the motor on or off to an "H" bridge microcontroller-based system with closed-loop speed control. The design of a unidirectional 280-W 20-A motor speed control will be examined that uses power FET semiconductor technologies.

Since the PM motor is a dynamic machine with the armature acting as a flywheel, the voltage interruption or chopping rate could be 1000 Hz or slower, before the motor's speed actually pulsates. A problem at 1000 Hz or other audible rates is noise generated from within the motor. This audible motor sound may not be tolerable for drivers or passengers. At higher frequencies—16 kHz or greater—the audible noise is minimized. Another noise issue is the significant electronic radio frequency interference (RFI) that radiates into the electrical system, including the vehicle's radio equipment. This RFI is generated by the fast switching edges of the PWM signal. The drawing in Fig. 19.7 illustrates slow and fast switching speeds and the resultant power transistor dissipation relationships. Slowing down the switching edges minimizes the radio frequency interference (RFI), but the switching speed parameters also play a crucial role in the overall controller system. High transitional speeds are desirable to minimize switching losses and to improve reliability, but very fast switching speeds become impractical beyond a certain point due to the inherent inductance in the wire and component leads. A compromise has to be made between the edge speeds and power device heat loss.

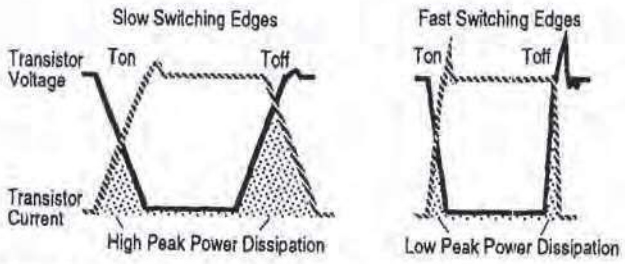


FIGURE 19.7 Slow vs. fast power loss.

IPR2023-01234
Petitioner - Ex. 2017 - Page 438

Switching Speed Effects. Figure 19.8 graphs the switching edge speed effects upon the power transistor's power dissipation when switching a 20-A motor load from a 14.4-V power supply. Three different operating frequencies are plotted, one at 20 kHz, one at 16 kHz, and the last at 2 kHz. Note how the 2-kHz switching times are less critical than the higher 16-kHz and 20-kHz frequencies. In order to minimize audible noise, the 16- or 20-kHz frequency can be used, but, unfortunately, the 200- to 500-ns switching speeds required to minimize switching losses cause the intrinsic inductance in the hookup wiring, components, and motor to become critical. These faster edge speeds will generate significant voltage spikes across the hookup wiring and may lead to reliability problems unless precautions are made to minimize stray inductance in this wiring.

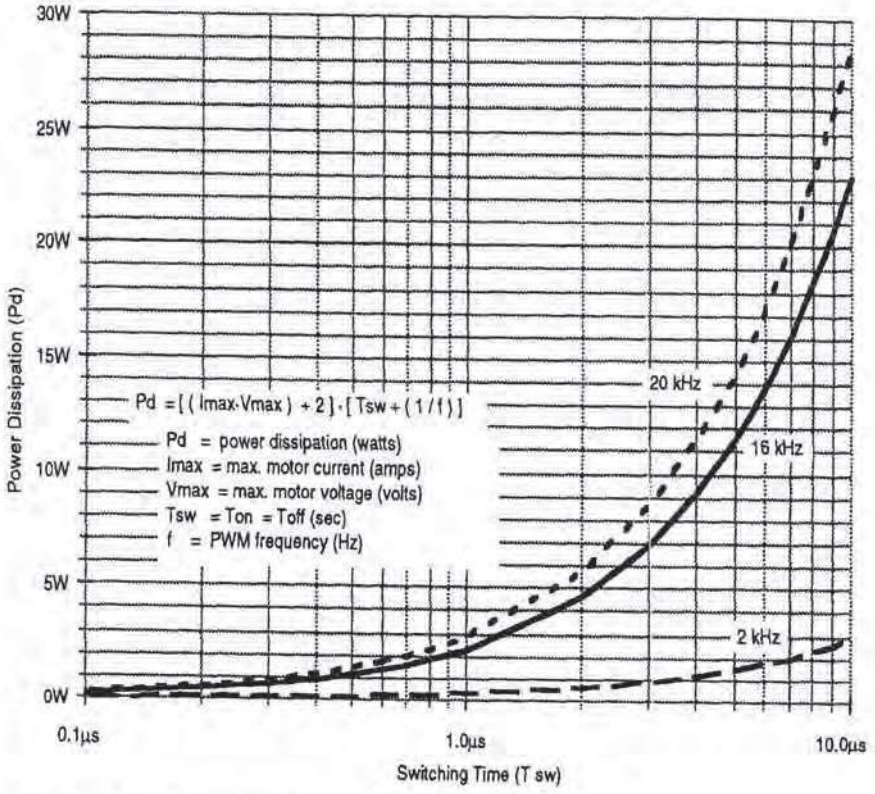


FIGURE 19.8 Power loss vs. switching speeds.

If the motor controller design has lead lengths that exceed 25 mm (1 in), their inductance values must be considered. An inductance value of 0.12 µH can be obtained in about 127 mm (5 in) of wire length with a #12 wire size, as shown in Fig. 19.9. This 0.12-µH value may not sound like much, but a plot (Fig. 19.10) of power line inductance versus switching transition times shows that just 0.1 µH of lead inductance can generate a 10-V voltage spike (at 20-A motor current) when switching edges are about 0.2 µs. Therefore, if fast switching edges are to be used, as with a 20-kHz operating frequency, a capacitor filter network is mandatory near the motor's power lead and controller. This filter network actually has to smooth out both the 20-kHz, and the much higher frequencies associated with the 200- to 1000-ns switching edges. To summarize, when fast switching edges are generated, filter networks are mandatory, or the hookup wiring will act as an antenna.

Motor Inductance Clamping. The kickback voltage from the motor's inductance also has to be contained, as the motor's inductance value will be dominant over the hookup wiring. This high-energy-laden voltage spike must be dealt with or the power transistor will enter an

IPR2023-01234
Petitioner - Ex. 2017 - Page 439

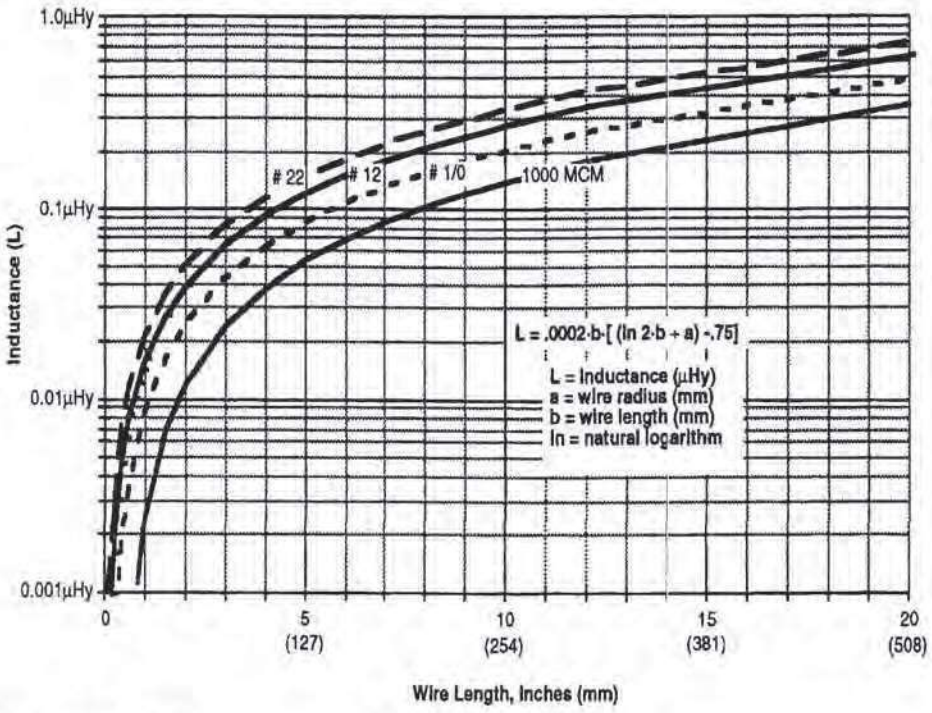


FIGURE 19.9 Line Z.

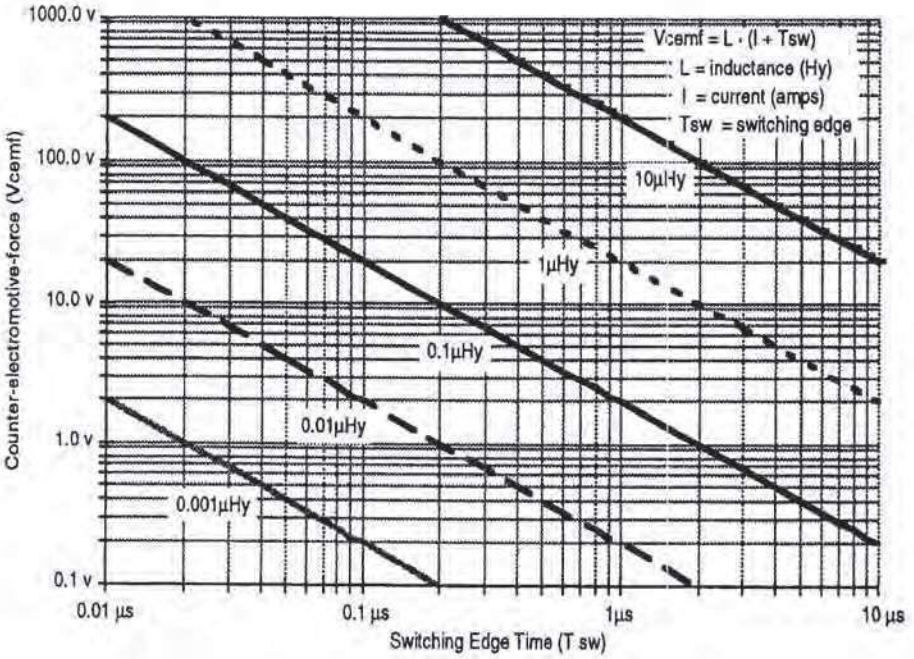


FIGURE 19.10 L di/dt effects.

avalanche or second breakdown mode, which is something to be avoided. The energy content of the motor's inductive kickback voltage is mainly determined by the motor's current, the motor's internal and external wire inductance value, and the rate at which the current is switched off. A high-current-rated freewheeling rectifier network can be connected across the controller's battery and motor terminals to clamp the motor's inductive kickback voltage spike. The reverse recovery times of these freewheeling rectifiers do affect the power transistor's switching performance.

IPR2023-01234
Petitioner - Ex. 2017 - Page 440

When operating at a frequency of 20 kHz or a 50-μs repetition rate, the motor's inductance value is large enough to keep the freewheeling rectifier in a forward conduction mode until the next 50-μs cycle occurs. For example, if the PWM is set to a 25 percent duty cycle, the power transistor is on for the first 12.5 μs, and the freewheeling rectifier is in conduction for the remaining 37.5 μs. This means that when the next cycle occurs, the power transistor is switching on while the freewheeling rectifier is still in conduction. The result is that the power transistor and freewheeling rectifier conduct a high level "shoot-through" current spike. The magnitude and duration of this current spike are directly related to the rectifier's reverse recovery time rating, lead inductances, and the battery supply source impedance at the rectifier and power transistor location. Selecting freewheeling rectifiers with a "soft" reverse recovery characteristic will help minimize the shoot-through current problem.

The motor's back-emf, is produced from the rotating armature in a magnetic flux from the permanent magnets (PM). The PM motor's back-emf with a fixed mechanical load is normally lower than its power supply voltage and should therefore not exceed the voltage ratings of the power transistor.

Motor Current. When the motor's inductive generated transients are safely contained, one needs to deal with stalled and shorted motor conditions. Note that the motor's copper windings exhibit a positive temperature coefficient of 0.00393 per °C. Therefore, a 0.25-ohm motor resistance value at 25 °C room temperature would be about 0.18 ohm at –40 °C. Using the 20-A motor as the load, the maximum stalled or locked rotor current can be calculated as shown below.

$$I_{max} = E_{max} \div R_{mtr} = 14.4 \div 0.18 = 77 \text{ A}$$

where E_{max} = maximum power supply voltage
R_{mtr} = minimum motor resistance*

Power Transistor Specifications. When the maximum motor current has been established, the power transistor device specifications can be determined. In this case, the device needs an average current rating of at least 77 A, but the prime consideration for reliable power transistor operation is its worst-case heat dissipation.

The worst case scenario would include maximum values for the supply voltage, ambient temperature, and motor current. A maximum junction temperature of 150 °C for the power transistors is used as a maximum point. It should be noted that the reliability will increase by about one order of magnitude for each 10 °C drop in the power transistor's junction temperature. The following equations calculate the power transistor's maximum allowable heat dissipation for use in an 85 °C environment using a 2.7 °C/W heatsink unit and a 1 °C/W junction to case power FET thermal resistance.

$$PD_{max} = (TJ_{max} - TA_{max}) \div (R\text{ø}JC + R\text{ø}CS + R\text{ø}SA)$$

$$= (150 - 85) \div (1 + .1 + 2.7)$$

$$= 17.1 \text{ W}$$

where TJ_{max} = maximum allowable junction temperature
TA_{max} = maximum ambient temperature
$R\text{ø}JC$ = junction to case thermal resistance
$R\text{ø}CS$ = case to heatsink interface thermal resistance
$R\text{ø}SA$ = heatsink to ambient thermal resistance

* Formula for calculating the motor's cold resistance value is $R_{mtrcold}$ = [(delta temp. × R_{coef}) R_{mtr}] + R_{mtr} = [(–65 × 0.00393) × 0.25] + 0.25 = 0.18.

IPR2023-01234
Petitioner - Ex. 2017 - Page 441

After the maximum transistor power dissipation is known, the maximum forward voltage drop, VDS_{on}, and ON resistance can be calculated as shown:

$$VDS_{on} = PD_{max} \div I_{max}$$
$$= 17.1 \div 77$$
$$= 0.22 \text{ V at } 150 \text{ °C Tj}$$
$$RDS_{on} = VdS_{on} \div I_{max}$$
$$= 0.22 \div 77$$
$$= 0.003 \text{ ohm at } 150 \text{ °C Tj}$$

In order to obtain a 0.003-ohm power FET ON resistance value at 150 °C Tj, several power FET devices will need to be paralleled. Bipolar devices were not even considered because of their high-current base drive requirements. Power FETs exhibit about a 75 percent ON resistance increase from a 25 to 150 °C rise in junction temperature. Therefore, six MTB75N05HD or equivalent devices in parallel would be required to achieve 0.003-ohm total ON resistance value when operating in an 85 °C ambient with a 2.7 °C/W heatsink. Six devices may not be economically attractive, so a larger heatsink may be more desirable. If the heatsink's thermal resistance is lowered to 1 °C/W, an ON resistance of 0.005 ohm would be required, which is three MTB75N05HD or equivalent paralleled devices. This is an example of the cost tradeoff between heatsink size and power FET ON resistance. It also points out that the power FETs ON resistance must be considered at the actual worst-case operating temperatures.

Short Current Protection. Some form of overcurrent protection would minimize power transistor failures in the event of a shorted motor, as might happen if the motor leads touched each other. Assuming motor's internal resistance will always present at least 90 percent of its nominal value, the shorted motor leads is the worst possible overcurrent condition. If three 75-A-rated power FETs are used in parallel, they would be capable of conducting well over 200 A. This current level may clear a 30-A fuse or activate a circuit breaker before the power FETs start to seriously overheat. In some wiring systems a *fuse link* is used to protect against a catastrophic wiring harness fire. The fuse link is usually just a short piece of copper wire that is encased in flame resistant insulation and is one wire-size smaller than the motor harness wire. The fuse link would probably not clear before the failed power transistors had shorted and blown open. If a fuse is selected that is slightly larger than the motor's normal run current, the power transistors may be capable of sustaining the shorted load current levels long enough to blow out the fuse before the transistors fail. A more reliable shorted load protective concept may still be necessary.

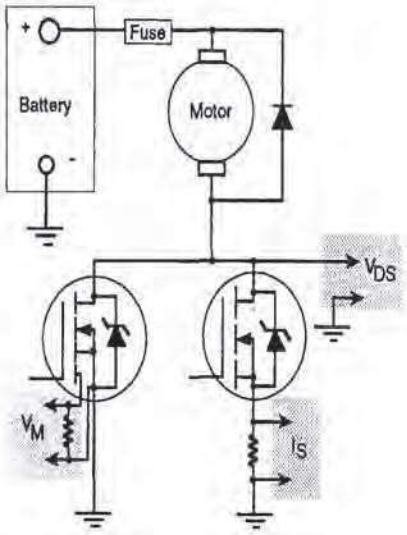


FIGURE 19.11 Load current sensing.

It may be desirable to latch off the power transistor during shorted load conditions. Load current sensing can be accomplished in three ways, as shown in Fig. 19.11. The voltage drop across the power transistor can be monitored, and, when a certain threshold is reached, the gate drive is latched off until the next operating cycle. Another method is to insert a series resistor in the source's path and monitor the voltage drop across the resistor. An internal current-sensing power FET device can also be substituted for one of the power FETs, with its current mirror voltage representing a portion of the total load current.

The method of measuring the transistor's forward ON voltage does have some inher-

IPR2023-01234
Petitioner - Ex. 2017 - Page 442

ent drawbacks. The drain-to-source measurement circuit has to be synchronized with the gate drive voltage, and the forward voltage will change by at least 2 to 1 at a nominal current level over a –40 to +175 °C junction temperature range. The temperature drift of 2 to 1 means that, at 175 °C, a 60-A overcurrent would read the same as 120 A at –40 °C. Therefore, at high temperatures, the overcurrent detector may falsely shut down with a stalled motor, and, at cold temperatures, the overcurrent may not shut down at all. The most accurate current measurement method is to use a series resistor added in the high current path.

A single-chip microcontroller could greatly enhance the operation of this design by allowing more functionality. For example, a stalled motor condition could be detected and a preset shutdown mode invoked to protect the motor against burnout. The MCU would include internal A/D for current detection directly from the current-sensing resistor or from the internal current-sensing power FET. The PWM signal would also be generated from the MCU. Figure 19.12 shows an MCU-based speed control conceptual design that uses an 8-bit single-chip microcomputer.

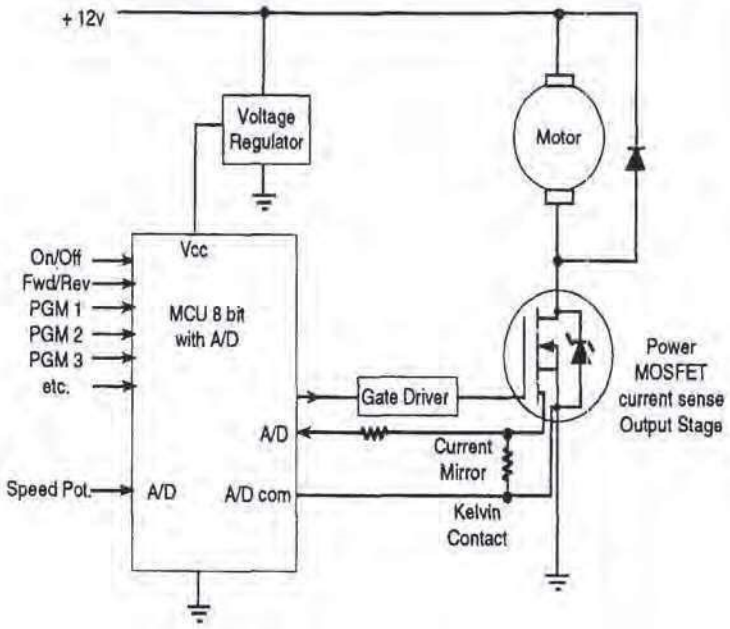


FIGURE 19.12 MCU motor control.

19.3 AIR CONDITIONER/HEATER CONTROL

Electronic controls allow an automatic climate control system to be designed for the comfort of the driver and passengers. An upscale automatic HVAC (heater and air conditioning) system, Fig. 19.13, may utilize an MCU to compute the most effective heat and ac flow rates. The heater and ac evaporator fan motor speed control designs can be similar to the WW variable speed design previously discussed if PM motors are selected. Brushless motors (BLMs) offer several features for this application. The BLM offers no brush-to-commutator noise. This feature alone is desirable in luxury vehicles, and, when one considers the increased mechanical reliability gained by the elimination of the brush-commutator assembly, the BLM cost-to-performance ratio seems more reasonable.

19.3.1 BLM System

If a motor-driven load requires closed-loop speed and direction control, the cost disadvantage of a BLM system becomes less significant. Figure 19.14 shows a typical permanent magnet brush motor compared with a BLM with both motors utilizing speed and directional control

IPR2023-01234
Petitioner - Ex. 2017 - Page 443

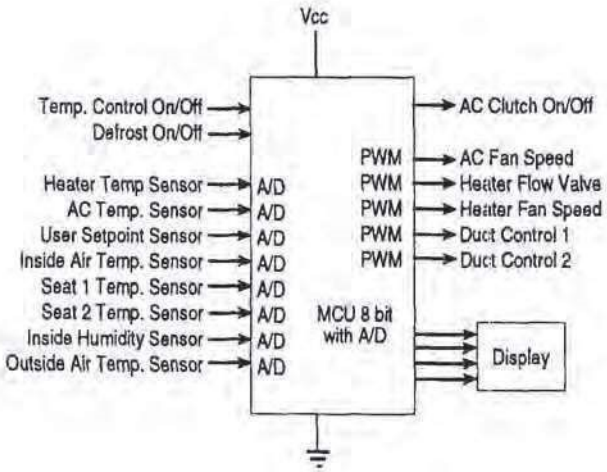


FIGURE 19.13 Climate control system.

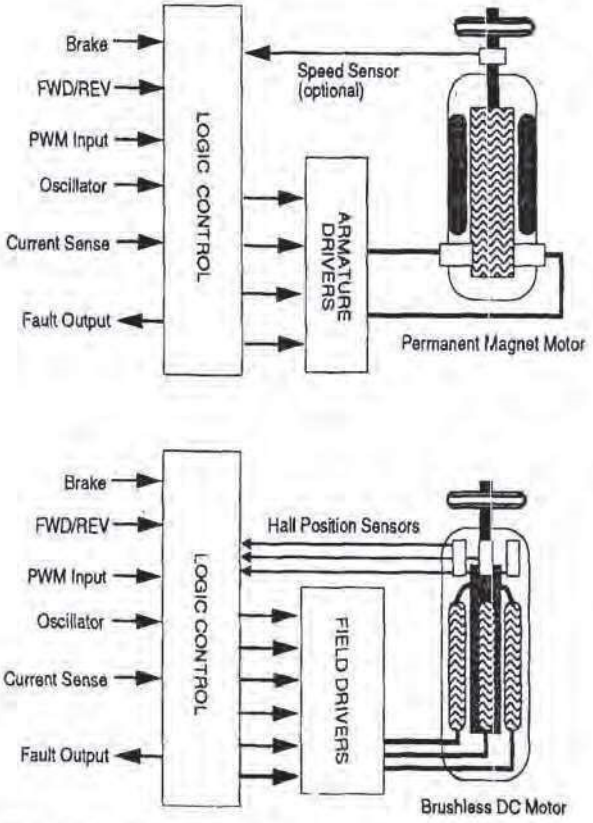


FIGURE 19.14 PM vs. BLM.

networks. Note that the BLM system uses only about one-third more drive electronics than the PM motor.

The BLM drive electronics may consist of a BLM linear bipolar integrated circuit, such as an MC33035 or similar device, that not only contains logic gates for commutation timing, but also includes internal driver stages capable of driving either power bipolar or power FET output transistors, or the MCU itself can be used to generate the necessary BLM control signals. One possible system may include the MC33035 linear bipolar IC and six power FETs. Three of the power FETs are internal current-sensing types. These current-sensing FET signals are conditioned and fed back to the MCU and to the linear IC as signals representing a motor

IPR2023-01234
Petitioner - Ex. 2017 - Page 444

normal condition or a motor overload condition. When the MCU detects a motor overload condition, a predetermined course of action takes place. First, the overload is counted as an event. The MCU timer allows the overload to continue for a length of time depending on how much time has elapsed from the previous overload. This is done to allow for the thermal heat buildup that will occur when the motor is overloaded or stalled on a repetitive basis, enabling the motor to have a high starting torque when cold, but to protect the windings, bearings, and drive electronics when the motor's temperature has become dangerously high due to repeated starts with a faulty load. The MCU's EEROM is used to remember user settings such as temperature preferences, as well as for interfacing into a multiplex data network.

19.3.2 Clutch Coil Control

The HVAC system also controls the ac clutch coil, plus other small duct motors or solenoids. Care must be taken when switching these highly inductive loads with power transistors. Figure 19.15 shows several possible voltage clamping networks to prevent damage to the power module when the inductive loads are switched off. The following formula should always be on hand and used when designing power-switching circuits that drive coils or solenoids.

$$V_{pk} = L\,(Di/Dt)$$

where V_{pk} = maximum inductive generated voltage
Di = coil's peak current level when switched off
Dt = switching time of the coil's current level

A typical air-conditioner clutch coil may exhibit 15 mH of inductance and 3 ohms resistance (or 4.8 A of current), and, when operating from a 14.4-V battery, would generate about 720 V when switched off in 100 μs (V_{pk} = 0.015 × (4.8/.0001). Needless to say, this would severely stress or destroy a typical 50-V-rated power transistor. Some form of voltage clamping is required.

A fully automatic HVAC system can monitor the inside and outside air temperatures. The MCU program can monitor these inputs plus the user's temperature setpoint and then compute the heater and/or ac fan motor's speed plus heater core flow rate and/or ac clutch to achieve the desired inside temperature. The HVAC MCU software design can be implemented using fuzzy logic rules rather than standard control algorithms or massive lookup tables.

19.3.3 Fuzzy HVAC Control

Fuzzy logic design can be used to develop an HVAC control program. In general terms, a fuzzy logic design allows the software programming of an MCU-based controller to be simplified and is especially useful for complex nonlinear control dynamics. At this time, standard MCU devices can be used for fuzzy programming. Future MCU devices will probably be available that will enhance a fuzzy program. Programmers who can easily understand how to compose assembly language programs for converting various input signal conditions into the required output signals may not contemplate a fuzzy logic design, but, for many system designers, the fuzzy program method will shorten the software design and can allow the program design to be evaluated with the use of fuzzy development tools even before the hardware has been constructed.

A fuzzy logic implementation using an 8-, 16-, or 32-bit single-chip microcontroller (MC68HC11, MC68HC16, MC68332, etc.) requires the control system's behavior to be well defined from an intuitive sense. The designer defines the input conditions and desired output in a subjective manner. For example, if the auto's inside temperature is 25 °C, most people would probably find that value comfortable. In fuzzy terms, 25 would be 100 percent true for an input

IPR2023-01234
Petitioner - Ex. 2017 - Page 445

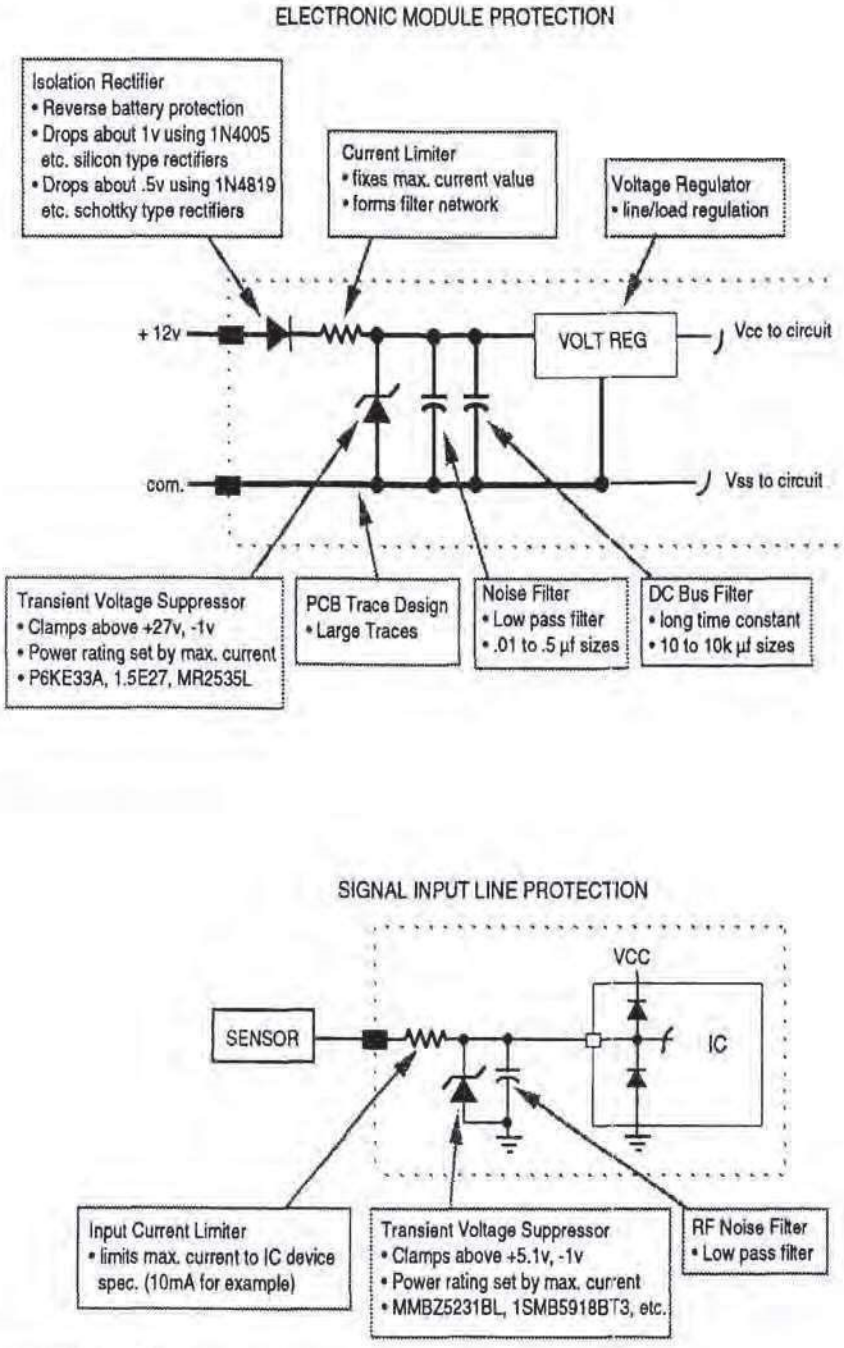


FIGURE 19.15 Voltage clamping networks.

membership called "comfortable," whereas 20 °C might be 0 percent and 30 °C might be 0 percent. Memberships could include "icycold," "cold," "cool," "comf.," "warm," and "hot." This thinking process fuzzifies the input temperature analog signal into numerical values that are attached to each membership. The user setpoint temperature is also divided into membership functions. The user setpoint temperature input is also fuzzified. Figure 19.16 shows the ambient and user setpoint memberships graphically. Other inputs, such as outside temperature, humidity, solar radiation, etc., could also be incorporated to produce a high-performance HVAC system. Once the input signals have been fuzzified, the first of three parts of a fuzzy design has been completed.

A second part of the fuzzy design is to assign membership functions as shown in Fig. 19.17 to the output control signals. In this example, only the heater side is shown. The output mem-

IPR2023-01234
Petitioner - Ex. 2017 - Page 446

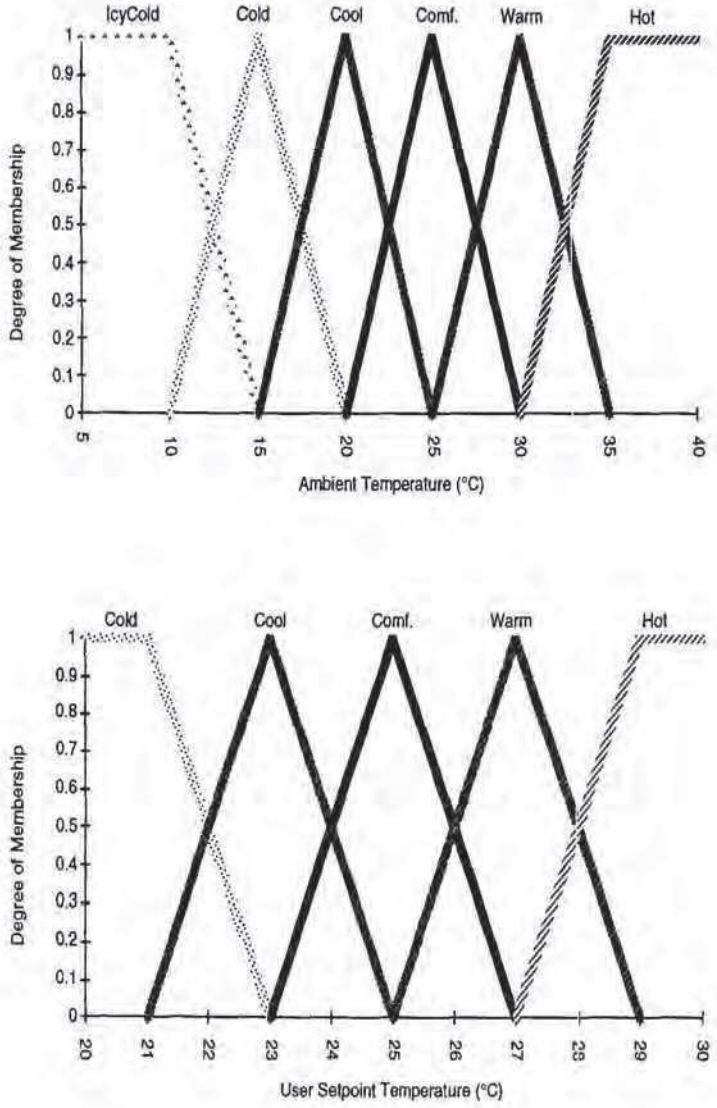


FIGURE 19.16 Fuzzy input memberships.

bership functions are classified as singletons, which only gives one value per membership. This approach trades precision for memory size.

The third part of a fuzzy design uses the min-max inference method to establish rules. A matrix representation of the input and output memberships and rules is helpful as shown in Fig. 19.18. The matrix size is determined by the input membership quantity, which is 5 for the user setpoint and 6 for the ambient temperature. This means a total of 30 rules are possible ($5 \times 6 = 30$). The designer selects which output membership function occurs for each input membership function.

Fuzzy logic development tools are available that can simulate the fuzzy design. These programming design tools simplify testing the program's performance before production. A 3-D interactive graphic display allows the designer to visually examine the input to output relationships. Irregularities can be traced back and corrected before the first prototype is built. The availability of integrated fuzzy design software for personal computers allows the system engineer to evaluate the fuzzy design approach.

In summary, the fuzzy design method requires: the input data to be applied to the input membership functions or fuzzified, invoking the rule set to the fuzzified data, and, finally, generating an output or defuzzification based upon the rules and output function type. The fuzzy

IPR2023-01234
Petitioner - Ex. 2017 - Page 447

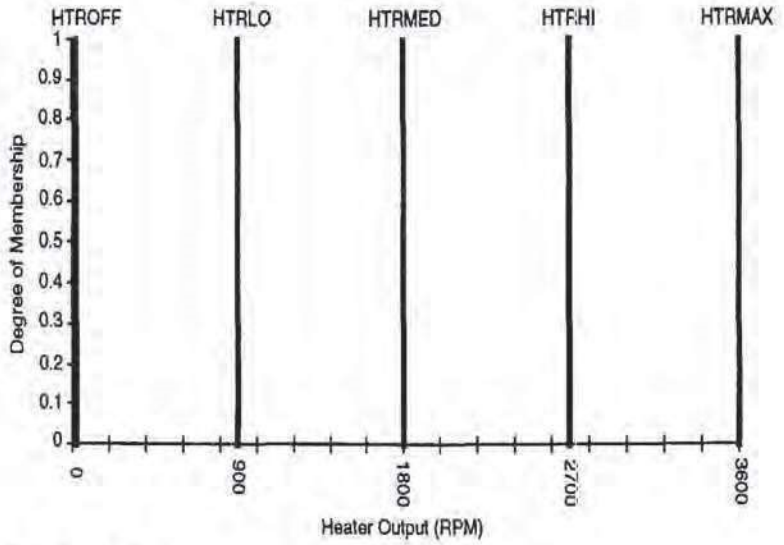


FIGURE 19.17 Fuzzy output memberships.

design can be modified with common-sense rules and rule strengths, whereas the conventional algorithm design method may require modifications at the most basic assembly code levels.

19.4 MISCELLANEOUS LOAD CONTROL REFERENCE

19.4.1 Current-Sensing Power FETs

Internal current-sensing power FETs can be used for current sensing, but their implementation may require some additional considerations. The current-sensing power FET device is a

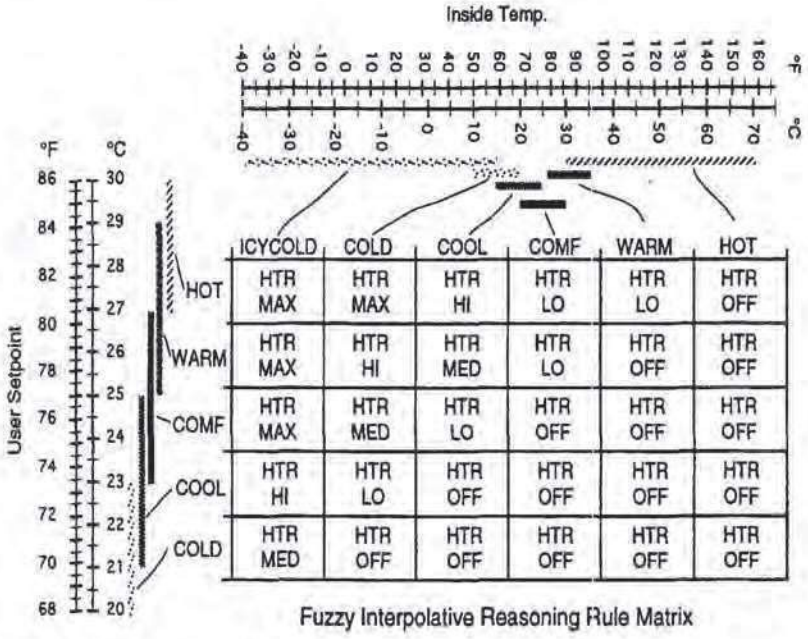


FIGURE 19.18 Fuzzy rules.

IPR2023-01234
Petitioner - Ex. 2017 - Page 448

normal power FET transistor with a very small portion of its active die area set aside for a current mirror. To use its current-sensing ability, an external resistor is connected between the current mirror output and the Kelvin output. The voltage drop across this resistor will be directly proportional to the device's current level when the device is operated in the active region. Choosing the correct value of the sense resistor is important to maintain an accurate drain current-to-sense voltage ratio over wide temperature ranges and when the unit is operated in the full ON or ohmic region.

When operating in the full ON region, the current mirror network changes from a constant current mode to a voltage source mode. This mode change occurs because the forward transconductance of the current mirror FET cells is decreasing due to the lower drain-to-source voltage. The result lowers the mirror current level to the sense resistor during full ON conditions when the load is connected between the drain and Vcc.

By selecting a sense resistance value that is less than 10 percent of the ohmic or rM(ON) value, the current mirror accuracy can be maintained. For example, if the current-sensing power FET device's rDS(ON) is 0.16 ohm and the current mirror ratio is 1800, the rM(ON) will be about 288 ohms ($0.16 \times 1800 = 288$). Therefore, a sense resistor value of less than 28 ohms is required. If a lower rDS(ON) current-sensing power FET device is used, for example, 0.026 ohm, and the current mirror ratio is 950, a sense resistor of less than 2.5 ohms should be used.

The use of an amplifier stage is still required to boost the current mirror's output signal level, which is similar to a traditional current-sensing network that uses very low resistance values (0.005 to 0.1 ohm). A low-cost operational amplifier (op-amp), LM324A, for example, will give fair performance over wide temperature ranges. The input offset voltage range of the op-amp will be a determining factor in the overall accuracy of the current-sensing power FET circuit design because of the low-millivolt current mirror signals. Instrument-grade op-amps can be used when higher accuracy is required. The op-amp circuit layout should be connected in close proximity to the current-sensing power FET's Kelvin and mirror output pins to minimize external noise pickup.

19.4.2 Overvoltage, "Load Dump," Reverse Battery

A hazard to any automotive electronics is reversed power supply connections. The power FET's internal rectifier will become forward-biased and will turn on the motor or lamp load. The FET's power dissipation will increase about 5 times normal since its voltage drop is now about 1 volt instead of the nominal 0.2 V. A standard bipolar transistor does not have the internal collector-to-emitter rectifier, but it still will suffer from a reversed power supply condition. The emitter-base junction avalanches at around 6 to 8 V, and the base-collector forms a rectifier. Therefore, the typical bipolar transistor is cooking itself into oblivion with about an 8-V drop while conducting about 1 A of lamp current. Most auto manufacturers specify that any electronic or electrical device must be able to withstand a reverse battery connection. The exact magnitude of the reverse voltage requirement varies per manufacturer, but the worst case seems to be –24 V for 10 min. This requirement is especially troublesome when the load requires an inductive kickback clamp rectifier, and either a power FET or bipolar transistor is used as the load driver. The power transistor's intrinsic rectifier and the load rectifier become forward-biased as shown in Fig. 19.19. The result? The clamp rectifier fails by shorting, the transistor shorts, and then the fuse may blow unless the rectifier or power transistor blows open first. A simple reverse battery isolator relay can be used to guard against incorrect battery polarity connections. This simple relay has been incorporated in the power supply line, which will open the line in the event of a power supply voltage reversal or if the power supply should exceed 32 V.

There are several other hazards for 12-V vehicular electronics that have to be considered. These can be divided into two groups: minimum/maximum operational voltages and voltage transients.

IPR2023-01234
Petitioner - Ex. 2017 - Page 449

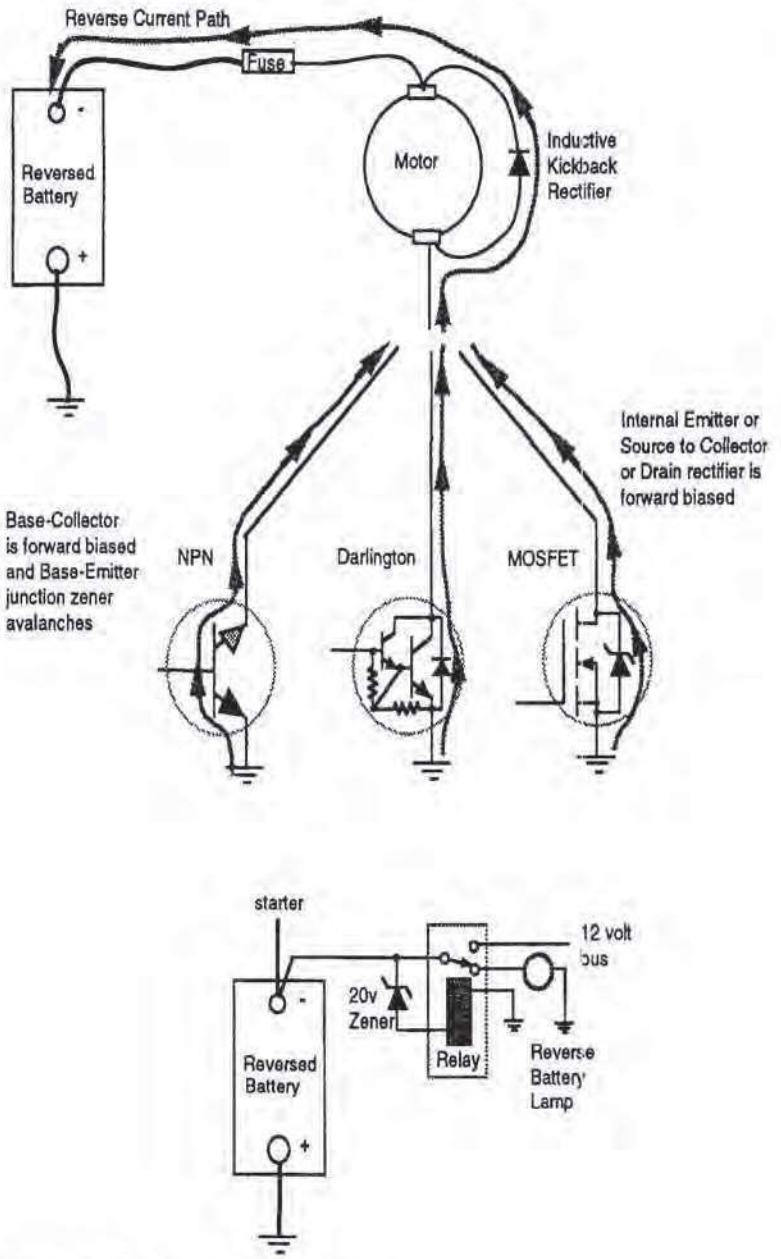


FIGURE 19.19 Reverse battery rectifier path.

The typical power supply voltage operating range for nonengine functions is 8 to 16 V. Most nonengine vehicular loads are either lamps or motors, and these types of loads will function in some proportion all the way down to near zero voltage when controlled by simple switches. When electronic control circuits are used with these loads, a power supply voltage threshold level occurs, and the load abruptly stops functioning. This threshold level normally takes place between 3 to 8 V and is dependent upon the control circuit's biasing networks and internal transistor technologies. The important criterion is that the electronic control should behave in a stable fashion when the power supply voltage varies between nominal levels and zero. A smooth transition during power supply on/off conditions in the electronic designs can be implemented with some form of hysteresis element for the analog portions and a low-voltage interrupt/reset for MCU/digital circuits.

IPR2023-01234
Petitioner - Ex. 2017 - Page 450

Voltage transients tend to be either high-energy, up to 125-V levels, or low-energy, high-voltage spikes. The alternator "load dump" voltage spike ranges from about 85 to 125 V for a duration of approximately ½ second. This voltage spike is of a high-energy nature because of the alternator's low source impedance. By using Zener-type rectifiers in the alternator in place of the alternator's normal rectifiers, the load dump voltage can be clamped to under 40 V.

High-voltage transients are generated by the fast turnoff of high-current inductive loads, such as air-conditioning compressor clutches. The polarity of high-voltage inductive kickback spikes depends upon the control switch configuration. Adding a rectifier across the inductive load to clamp the turnoff voltage spike will affect the mechanical performance of some solenoids, actuators, or relays. The mechanical turnoff will slow down. As the solenoid's magnetic field collapses, a countervoltage is generated that, in turn, causes the magnetic field to reverse, which speeds up the solenoid's turnoff action. The insertion of a back-emf rectifier clamps or shunts the counter voltage, and therefore minimizes any significant reversal of the magnetic field. Using back-to-back Zener rectifiers across the inductive load that are selected will allow satisfactory mechanical turnoff action, and yet will protect the power electronics.

Another form of electrical stress that the motor control system has to sustain is ESD or electrostatic discharge. The ESD is normally encountered in the manufacturing cycle, but can occur in the application. To minimize ESD, the control shafts, switch handles, user faceplate, etc., should be designed to dissipate ESD through a ground path away from the electronic module.

19.4.3 Microcomputer I/O Line Protection

Voltage transients on MCU input or output (I/O) lines can cause the MCU to fail. Figure 19.20 shows three different methods to contain excessive MCU input or output line voltage spikes.

Single input line protection is accomplished by a 5.1-V Zener clamp to contain positive-going transients and a Schottky rectifier for the negative-going transients. The Schottky rectifier does have temperature problems at both ends. At 125 °C, its leakage current may reach 50 μA when the input line is at a 5-V level. Therefore, the input signal may lose 50 μA of current to the Schottky which may reduce its voltage level too much for the MCU input port to respond properly. Another problem occurs at cold temperatures. At –40 °C, the forward voltage rises to about 0.47 V, which is getting close to the –0.50-V maximum level specification for most HCMOS-type microcomputer chips. A simple RF low pass filter network is also a good idea to incorporate on each input line. The RC network will minimize problems from high-energy RF fields and will limit excessive current levels from flowing through the MCU's internal substrate.

Multiple input line protection uses two Schottky rectifiers per line for clamping positive- and negative-going voltage transients. A single 4.7-V Zener is used as a common clamp to all input lines.

MCU output line protection uses a resistor, capacitor, Zener, and Schottky rectifiers. The resistor is connected in series to the load, and will therefore have to be sized to drop about 5 to 10 percent of the nominal load voltage. The resistor's main function is to limit reverse current into the MCU in case the output line is raised above Vdd or below Vss, and no other protective devices are used. Adding a small value capacitor at the load output will help minimize RFI, at the expense of reducing switching time from the MCU. Adding a Schottky and Zener rectifier to the MCU output line will protect against both negative- and positive-going transients.

Adding program traps in the MCU software will help to restart the MCU in the advent of a software crash. Experiments have shown MCU-based electronic modules that fail (program crashes, and MCU locks up until hardware restarts it) due to high bursts EMI or RFI, will still perform, but at reduced throughput, when software traps are used. One method uses a trap consisting of three NOP instructions followed by a JMP to RESET instruction. These traps

IPR2023-01234
Petitioner - Ex. 2017 - Page 451

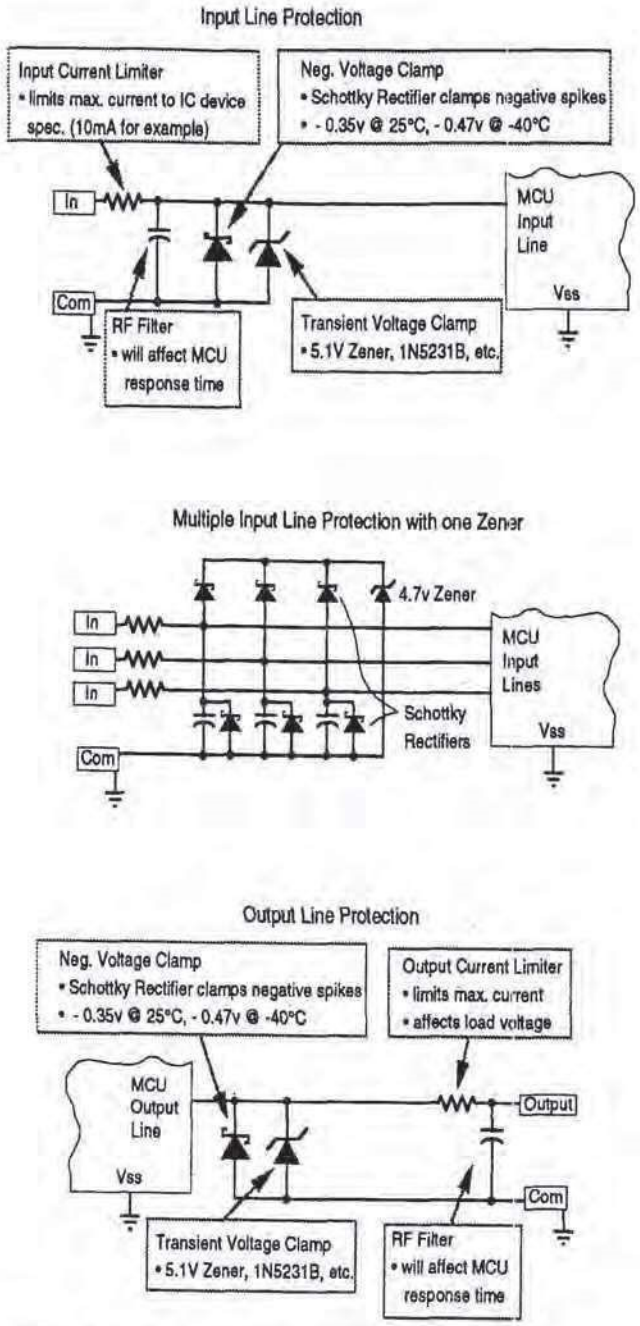


FIGURE 19.20 MCU I/O voltage spike clamping.

are used after loops or subroutines. These software traps, in addition to a watchdog timer if the MCU has this feature, will help in catching an out-of-control program.

The location of the watchdog timer reset instruction code is also important. If the watchdog timer is reset from within an interrupt routine, there is a possibility that the program could still be out of control, but that the interrupt vectors could still be working, and will therefore not reset. A good place to locate the watchdog update code is in a main program path rather than in an interrupt routine.

The PCB or thick-film design layout affects the MPU's reliability in terms of overvoltage transients. The clamping networks should be located physically close to the input socket pins

IPR2023-01234
Petitioner - Ex. 2017 - Page 452

and common. The MPU common traces should not be in the path of any voltage-clamping networks. It may also be a good idea to place an inexpensive metal shield around the MPU PCB area to protect against RFI and ESD problems.

19.4.4 Wire Size Reference

Most wire tables only give basic weight, dimensions, and dc resistance. A more complete version would include straight-line inductance as shown in Table 19.2. Unlike resistance which adds in a linear proportion to its length, inductance adds up on a logarithmic scale.

19.5 FUTURE LOAD CONTROL CONCEPTS

Higher integrated or more complex semiconductor power devices are available for specific load controls that can justify the extra cost of these smarter power types. The tradeoff is that the extra internal circuitry in the device usually limits its application to specific loads.

TABLE 19.2 Wire Gage Resistance and Inductance

Wire #	Dia., mm	Dia., in	Ohms per 305 mm (ft)	L of 25 mm (1 in), μH	L of 305 mm (1 ft), μH	L of 914 mm (1 yd), μH
1000 MCM	29.261	1.1520	0.000008	.003	.182	.746
500 MCM	20.650	0.8130	0.000016	.004	.203	.810
250 MCM	14.605	0.5750	0.000031	.006	.224	.873
0000	11.684	0.4600	0.000049	.007	.238	.914
000	10.404	0.4096	0.000062	.008	.245	.935
00	09.266	0.3648	0.000078	.008	.252	.956
0	08.252	0.3249	0.000098	.009	.259	.977
1	07.348	0.2893	0.000124	.010	.266	.999
2	06.553	0.2580	0.000156	.010	.273	1.019
4	05.189	0.2043	0.000248	.011	.287	1.062
6	04.115	0.1620	0.000395	.012	.301	1.105
8	03.264	0.1285	0.000628	.014	.315	1.147
10	02.588	0.1019	0.000999	.015	.329	1.189
12	02.052	0.0808	0.001589	.016	.344	1.232
14	01.628	0.0641	0.002526	.017	.358	1.274
16	01.291	0.0508	0.004016	.018	.372	1.317
18	01.024	0.0403	0.006386	.020	.386	1.359
20	00.812	0.0320	0.010154	.021	.400	1.401
22	00.644	0.0254	0.016139	.022	.414	1.444
24	00.511	0.0201	0.025671	.023	.428	1.486
26	00.405	0.0159	0.040818	.024	.443	1.529
28	00.321	0.0126	0.064914	.025	.457	1.571
30	00.255	0.0100	0.103093	.027	.471	1.613
32	00.202	0.0080	0.164095	.028	.485	1.656
34	00.160	0.0063	0.260891	.029	.499	1.698
36	00.127	0.0050	0.414849	.030	.513	1.741
38	00.101	0.0040	0.659695	.031	.527	1.783
40	00.080	0.0031	1.048548	.033	.542	1.825

$R_{ohm} = 4\,Lp/\pi D^2$. L = length in meters, D = length in mm, p = resistivity .017241Ω per μΩm (= Ω mm²/m). (Ref: *Automotive Handbook*, 2d ed, Bosch, 1986, pp. 176–177.)

$L\mu H = (0.0002\,L)*[(IN(2*L/(D/2)) - 0.75)]$. L = length in mm, IN = nat. log., D = dia. in mm. (Ref: *ARRL Handbook*, 1988, pp. 2–18.)

IPR2023-01234
Petitioner - Ex. 2017 - Page 453

Some form of more intelligent brake indicator system may help minimize the classic chain vehicle crashes that occur in poor driving conditions. One possible method using electronic switched stop lamps would involve a rate of closure detector system to determine if the vehicle's speed is safe for objects ahead of it. If the closure rate is unsafe, the stop lights could be activated to alert trailing (or tailgating) drivers to a pending accident.

19.5.1 Fully Integrated Power Devices

The concept of putting the MCU and power drivers on one piece of silicon is viable at limited power levels and breakdown voltages. The MC68HC05V8 MCU is but one of several semiconductor industry examples of this technology.

GLOSSARY

Charge pump A circuit that usually consists of an oscillator driving logic gates that yield out-of-phase signals that are applied to a rectifier voltage doubler network. The charge pump circuit can be integrated into MCUs and other power analog integrated circuits.

Current mirror A design that generates a signal whose level is directly proportional to another current level. The current mirror concept is used in current-sensing power MOSFETs.

Electromagnetic interference (EMI) Unwanted magnetically coupled voltages that affect the normal operation of electronic systems. EMI is a problem when high-energy circuits are in close proximity to high-impedance sensors, or any low-energy electronic control circuit. EMI also occurs in a wiring harness. One wire conducting a high-energy pulse in this harness will couple the pulse into the other harness wires. Twisted wire pairs are often used to minimize EMI susceptibility.

Freewheeling rectifier A rectifier that is connected across an inductive load or transistor switching device to suppress the voltage spike generated when the load is turned off.

H-bridge A design utilizing four power devices that are connected to reverse the voltage across both terminals of a load. H-bridges are used for bidirectional motor controls.

Half H-bridge A design using two power devices that are connected in series from the positive power supply bus to common, and a load terminal connected to the transistor's middle-connection. Two half H-bridges can make a full H-bridge. Three half H-bridges are commonly used in three-phase motor controls.

Intrinsic rectifier A rectifier that is inherently part of a semiconductor design. Most power MOSFET transistors have a drain-to-source rectifier that is formed by the nature of the MOSFET design structure. In battery-powered designs, the intrinsic rectifier is a concern during reversed battery hookups.

Load dump The effect of disconnecting the load from an alternator running at full power. In automotive equipment this condition can be caused by intermittent battery connections when the alternator is applying maximum current to the battery. When the load is abruptly disconnected, the alternator control circuitry shuts off the field current, but this current takes up to ¼ s to decay, and allows the alternator to produce a voltage much higher than its nominal value, up to 125 V in some cases. This abnormal voltage tracks the field current decay.

Pulse-width modulation A common control signal modulation method used in dc speed controls. The signal's frequency is fixed at a rate of 100 Hz to 20 kHz, but its pulse width is var-

IPR2023-01234
Petitioner - Ex. 2017 - Page 454

ied from 0 to 100 percent. The variable pulse width, in effect, acts like a variable voltage source when driving most automotive type loads.

P-channel MOSFET Usually a power transistor that requires a negative gate-to-source control voltage of 3 to 10 V. P-channel MOSFETs are normally connected between power supply positive bus and the load, and can operate from a positive voltage bus.

N-channel MOSFET Usually a power transistor that requires a positive gate-to-source control voltage of 3 to 10 V. N-channel MOSFETs are normally connected between common and the load, and operate from a positive voltage bus. The gate input characteristics are capacitive with gate power loss occurring during the switching edge transition period.

Radio frequency interference (RFI) High-frequency signals of sufficient magnitude to influence the normal operation of electronic systems. RFI sources from automotive equipment include spark plug arcing, dc motor brush arcing, electrical contact switching, and fast transitional voltage pulses from power electronic circuits.

Saturation A power transistor's forward ON region normally defined as when an increase in drive input voltage or current has little effect upon further reducing the transistors forward ON voltage. Saturation regions vary from less than 0.1 to over 3 V depending on the transistor technology and design.

Zener rectifier A semiconductor rectifier device that is designed to operate in a reverse bias mode. When the reverse voltage reaches the Zener voltage, the device abruptly starts conducting current. Zener rectifiers are used for shunt voltage regulators, overvoltage protection, and voltage level detectors. Zener rectifiers are also designed specifically for high-power voltage transient suppression. These devices are constructed to handle very high momentary current levels.

Note

Based in part on the article by Richard Valentine, "Don't underestimate transistor-based lamp driver design," *EDN*, June 7, 1990, pp. 119–124.

BIBLIOGRAPHY

Aptronix Inc., *FIDE Users Manual,* 1992.

Bairanzade, M., "The electronic control of fluorescent lamps," Motorola Semiconductor Application Note, AN1049, 1990.

Bannatyne, R., "Using fuzzy logic in practical applications," *Motorola Semiconductor Engineering Bulletin,* EB412, 1993.

Bacelis, O. W., et al., "The automotive primary power supply system," SAE Technical Paper 741208, 1974.

Berringer, Ken, "High-current DC motor drive uses low on-resistance surface mount MOSFETs," Motorola Semiconductor Application Note, AN1317, 1992.

Catherwood, M., "Designing for EMC compatibility with HCMOS MCUs," Motorola Semiconductor Application Note, AN1050, 1989.

Davis, B., et al., "The impact of higher system voltage on automotive semiconductors," SAE technical paper 911658, 1991.

Gauen, K., and J. Alberkrack, "Three piece solution for brushless motor controller design," Motorola Semiconductor Application Note, AN1046, 1989.

Graham, D., and J. Savage, "Brushless DC motor technology," *Second IAVD Congress on Vehicle Design & Components,* Mar. 1985, pp. c1–23.

IPR2023-01234
Petitioner - Ex. 2017 - Page 455

Hollander, D., "The hidden dangers of electrostatic discharge," Motorola Semiconductor Application Note, AR300, 1987.

Huettl, T., and R. Valentine, "Simplified control for brushless motors," *Machine Design,* Feb. 21, 1985, pp. 236–241.

Mihin, M., and R. Valentine, "New rectifiers clamp alternator voltage levels," SAE technical paper 872002, 1987.

Motorola Inc., "Reducing A/D errors in microcontroller applications," Motorola Semiconductor Application Note, AN1058, 1990.

Motorola Inc., TMOS power MOSFET transistor data, Chap. 2, DL135 Rev. 4, 1992.

Schultz, W., "New components simplify brush DC motor drives," Motorola Semiconductor Application Note, AN1078, 1989.

Society of Automotive Engineers, *SAE Ground Vehicle Lighting Standards Manual,* SAE HS-34, 1993.

Tal, J., "Design and analysis of pulsewidth-modulated amplifiers for DC servo systems," *IEEE Transactions on IECI,* vol. 23, no. 1, Feb. 1976, pp. 47–55.

Valentine, Richard, "Brushless DC motor control," *Control Engineering,* July 1985, pp. 134–140.

Valentine, Richard, "Don't underestimate transistor-based lamp-driver design," *EDN,* June 7, 1990, pp. 119–124.

Zhang, W., "Temperature control 2," FIDE Application Note 005-920903, Aptronix Inc., 1992.

ABOUT THE AUTHOR

Richard J. Valentine is a principal staff engineer at Motorola SPS in Phoenix, Ariz. His present assignments include engineering evaluation of advanced semiconductor products for emerging automotive systems. He holds two patents and has published 29 technical articles during his 24 years at Motorola.

IPR2023-01234
Petitioner - Ex. 2017 - Page 456

P · A · R · T · 4

DISPLAYS AND INFORMATION SYSTEMS

IPR2023-01234
Petitioner - Ex. 2017 - Page 457

CHAPTER 20
INSTRUMENT PANEL DISPLAYS

Ronald K. Jurgen, Editor

20.1 THE EVOLUTION TO ELECTRONIC DISPLAYS

In the early automobile years, cars had analog displays that contained minimal information, usually just car speed and oil pressure. As the use of electronics increased in cars dramatically from the late 1970s on, however, the traditional mechanical or electromechanical analog displays with a circular dial face and a pointer began to be challenged by newer technologies. The major ones included gas discharge or plasma displays, vacuum fluorescent displays (VFDs), liquid crystal displays (LCDs), cathode-ray tubes (CRTs), and more recently, head-up displays (HUDs). These newer technologies made it possible for car makers to give drivers a broad spectrum of information, including sophisticated graphics.

In 1978, the first production electronic digital display, a gas plasma device, was used in the Cadillac Seville; in 1984, the first standard equipment production LCD cluster was used in the Chevrolet Corvette; and in 1985, the first full-color CRT was used in a production vehicle, the Toyota Soarer.[1]

The initial rush by car makers to use electronic displays has now abated somewhat. Drivers, in many instances, did not take kindly to overkill with electronic displays—any more than they did to electronically generated voice messages—and today's use of displays tends to be more conservative. In fact, one approach fast gaining popularity is electronic analog displays rather than strictly digital ones.

This chapter will describe typical electronic displays used in cars. It is not intended to be all-inclusive. That would be beyond the scope of this handbook. But the display examples given are representative of what can be found in cars today.

20.2 VACUUM FLUORESCENT DISPLAYS

One of the most widely used electronic displays is the vacuum fluorescent display. It was first used in automotive clocks and has since been applied in other ways including audio systems, air conditioning/heating, message centers, and head-up displays. Its popularity stems from features that include availability of a variety of colors, high luminance, low voltage operation, reliability, and long life.

The basic structure of a modern VFD, Fig. 20.1, consists of a cathode, grid, and anode.[2] The tungsten-wire cathode emits thermal electrons that are accelerated when a positive voltage is applied to the anode and grid. The phosphor-coated anode emits a blue-green light when

IPR2023-01234
Petitioner - Ex. 2017 - Page 459

struck by the emitted electrons. Other colors such as yellow-green, green-yellow, yellow-orange, orange, and red-orange colors, obtained through the use of optical filters, can be used independently within the same display. Thick- or thin-film screens are used to shape the phosphor pattern in any desired manner. VFDs produce maximum perceived brightness at low input power.

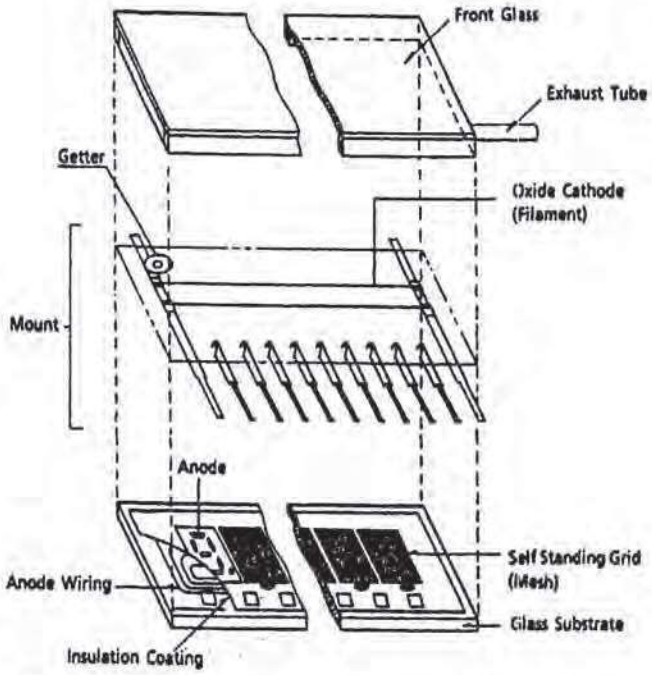


FIGURE 20.1 The basic structure of a vacuum fluorescent display. *(Reprinted with permission from SAE SP-858 ©1991 Society of Automotive Engineers, Inc.)*

Initial VFDs were single-digit displays. Multiple-digit displays followed and now single large-scale VFDs contain multiple functions such as speedometer, fuel and temperature gages, trip odometer, turn indicators, and warning signals.

A typical application of VFDs was in the electronic instrument panel on the 1985 Chrysler LeBaron.[3] The VFDs are controlled (Fig. 20.2) by a Motorola MC6805R3 8-bit, HMOS, single-chip microprocessor with internal analog-to-digital converters. Another microprocessor, a 4-bit device, is used to generate a high switching rate for the center display in the instrument panel.

20.3 LIQUID CRYSTAL DISPLAYS

LCDs are fluids consisting of organic compounds whose molecular orientation rotates polarized light by 90 degrees as light passes through the material.[4] When an electric field is applied to the fluid, its molecular orientation is altered as is its polarizing ability. The change is visible in reflected or transmitted light and can be used to form predetermined patterns or characters.

IPR2023-01234
Petitioner - Ex. 2017 - Page 460